The Development and Characterization of Aluminum Fueled Power Systems and a Liquid Aluminum Fuel

by

Jason Zachary Fischman

Submitted to the
Department of Mechanical Engineering
in Partial Fulfillment of the Requirements for the Degree of

Master of Science in Mechanical Engineering
at the
MASSACHUSETTS INSTITUTE OF TECHNOLOGY
February 2019

Author: _____

Department of Mechanical Engineering
February 1, 2019

Certified by: _____

Douglas P. Hart
Professor of Mechanical Engineering
Thesis Supervisor

Accepted by: _____

Nicolas Hadjiconstantinou
Chairman, Committee on Graduate Students

The Development and Characterization of Aluminum Fueled Power Systems and a Liquid Aluminum Fuel

by

Jason Zachary Fischman

Submitted to the Department of Mechanical Engineering
On February 1st, 2019 in Partial Fulfillment of the
Requirements for the Degree of
Master of Science in Mechanical Engineering

ABSTRACT

Various aluminum-water reactions were thermodynamically analyzed across a wide range of temperatures and pressures to determine the most favorable reaction under each condition. Results show that under most achievable temperatures and pressures the reaction will produce AlOOH, however at low temperatures and high pressures, this will transition to a reaction producing $Al(OH)_3$. This model was then corroborated experimentally using XRD and FTIR to identify the aluminum-water reaction products created at varying temperatures and pressures.

A new Ga In eutectic-limited surface coating method was developed to produce effective, consistent, aluminum fuel. This coating method also allowed for the study of the effects of increased eutectic concentration on aluminum reaction yield. These reaction yield results showed a minimum threshold concentration of 1.9% eutectic was needed to create reactive fuel, and that adding concentrations beyond that would increase the reaction yield with diminishing returns.

Using this aluminum technology, the world's first aluminum fueled car was built. A 10 kW power system fueled by an aluminum-water reaction was successfully integrated into a BMW i3 to replace its range extender and to power the vehicle. With a vision towards creating simpler power systems in the future, a liquid aluminum fuel was also developed. This fuel works by suspending 65% aluminum particles by mass into a mixture of mineral oil and fumed silica. This newly developed liquid fuel can be pumped easily, stay in suspension for months, and retains full levels of reaction completion.

Finally, a joint hydrogen-steam IC engine concept was presented and analyzed. This engine utilizes both the thermal and hydrogen energy created by an aluminum-water reaction and shows ideal system efficiencies of as high as 33% while still operating at practical system pressures.

Thesis Supervisor: Douglas P. Hart
Title: Professor of Mechanical Engineering

ACKNOWLEDGEMENTS

TABLE OF CONTENTS

LIST OF FIGURES

1. INTRODUCTION

As global energy consumption continues to climb, and the environmental concerns of consuming fossil fuels becomes more apparent, the search for viable alternative fuels and energy storage methods is becoming increasingly critical. For decades, people have held hope that the transition to a hydrogen economy would be the future of a sustainable, and high efficiency electrical grid. The development of high efficiency hydrogen fuel cells has increased the prospects of such a system, however the outstanding logistical challenges of hydrogen storage and safety have kept it from becoming a reality [1].

In recent years, aluminum fuel technologies have also been developed that can be used as an alternative, highly energy dense, power source. Methods involving ball milling [2], alloying [3], or surface treating [4] aluminum with other metals have been shown to allow aluminum to react with water, releasing its internal energy as a mix of heat and hydrogen gas. Aluminum has an energy density of 83.8 MJ/l which is 2x gasoline, 8x liquid hydrogen, and 20x li-ion batteries, making it an extremely viable energy source when reacted. Additionally, the reaction of aluminum with water produces hydrogen at a ratio of 2:3 moles of aluminum to moles of hydrogen, meaning that when reacted, it can effectively produce large quantities of hydrogen on demand. This would allow for a system where aluminum fuel can be stored and transported safely and easily, and then used to produce hydrogen when needed on site.

In this thesis, aluminum fuel is further characterized analytically and experimentally. This fuel is then used in the development of a large-scale aluminum fueled power system. Finally, looking forward towards future aluminum fueled systems, a liquid aluminum fuel was developed to allow for simpler handling and system operation, and an alternative

hydrogen-steam engine concept is explored to more efficiently utilize the reaction byproducts. It is the hope of the author that the work done here poses a significant step forward in the development and implementation of aluminum fueled power systems.

1.1   Hydrogen as a Fuel Source

Hydrogen, the most abundant element in the universe, is a compelling fuel source for several reasons. The first is that it can significantly reduce production of greenhouse gases. This is because the two primary methods for generating electricity from hydrogen are to burn it, or to feed it into a hydrogen fuel cell. Burning hydrogen is simply the combination of hydrogen with oxygen which produces water as a byproduct rather than CO or CO_2 as is the case with gasoline. Hydrogen fuel cells operate via a more controlled electrochemical reaction of hydrogen with oxygen, which again produces only water as a byproduct. The wide scale implementation of hydrogen generators could see a drastic decrease in greenhouse emissions, replaced instead by harmless water vapor.

Another advantage of using hydrogen as a fuel source is that it can be produced through electrolysis, which is the process of using electricity to split water into hydrogen and oxygen. While currently the most widely used method for hydrogen production is steam reforming, which does require the use of methane and procures CO_2, the potential for being made without the use of fossil fuels is considerable. This would allow for future renewable sources of electricity, such as solar or wind energy, to produce hydrogen in a clean manner from water. Hydrogen produced in this way can then be thought of as an energy storage system, for a later point in time when the hydrogen is then recombined with oxygen to produce electricity. This would allow for a fully closed electrical storage loop, without the use of fossil fuels or the production of greenhouse gasses along the way.

Perhaps most importantly, hydrogen fuel cells are among the most efficient fuel-to-electricity generators ever made. Hydrogen fuel cells can regularly operate within the range of 40-60% efficiency and can be designed to operate at levels as high as 85%

efficiency [5]. This can be compared to gasoline engines, which after centuries of optimization operate at efficiencies close to 20%. Even in an engine, the use of hydrogen can greatly increase efficiency, with recorded hydrogen engines operating at efficiencies up to 40% [6].

Unfortunately, the logistical challenges surrounding the storage and transportation of hydrogen have largely kept the dreams of a hydrogen economy from becoming a reality. While hydrogen has an incredibly high specific energy, it has a low energy density, meaning that it requires a relatively large volume of hydrogen to store a given amount of energy when compared to other fuels. For this reason, large volumes of hydrogen are often stored and transported compactly in pressurized containers or cooled to its liquid state. Pressurizing or cooling the hydrogen gives it a higher energy density, although even in its liquid form hydrogen still has an energy density 3x lower than gasoline. Additionally, the use and transportation of pressurized hydrogen is fairly dangerous. This is not only because pressure vessels can burst if not handled properly, but also because hydrogen is incredibly flammable. For instance, many municipalities within the United States do not even allow the transport of compressed hydrogen through tunnels [7].

Aluminum fuel technologies may pose a solution to this challenge and can help further the development of a hydrogen economy. In recent years, various methods have been developed to allow aluminum to react with water to produce hydrogen. Aluminum can be stored and transported safely and easily, and then reacted with water on site to produce hydrogen as needed. Using these aluminum fuels to produce hydrogen can help solve the energy density and safety challenges that have kept the hydrogen economy from succeeding thus far.

1.2   Aluminum as a Fuel Source

Aluminum, the most abundant metal in the earth's crust, has an incredibly high energy density, of 83.8 MJ/l. This energy density is over double that of gasoline and over an order

of magnitude higher than lithium ion batteries, as shown in Figure 1. Unfortunately, however, the internal chemical energy of aluminum is difficult to release, as an oxide layer will naturally form on its surface when in contact with air or water [8]. This oxide layer protects the aluminum and prevents it from reacting any further. Certain methods, such as grinding aluminum into a fine powder, have been developed to allow aluminum to release its energy through combustion. Unfortunately, aluminum powder is incredibly dangerous to work with and poses both an inhalation risk and combustion hazard. Despite this, aluminum powder combustion is still used in extreme situations where high energy density is critical, such as rocket fuel [9]. Several other methods have also been developed in recent years to allow aluminum to react with water, releasing its energy as heat and hydrogen as shown in the following chemical reaction:

$$2Al + 4H_2O \rightarrow 3H_2 + 2AlOOH \tag{1}$$

When fully reacted in this manner, a single kilogram of aluminum will release 15.7 MJ of heat energy per kilogram, and 1245 L of hydrogen gas.
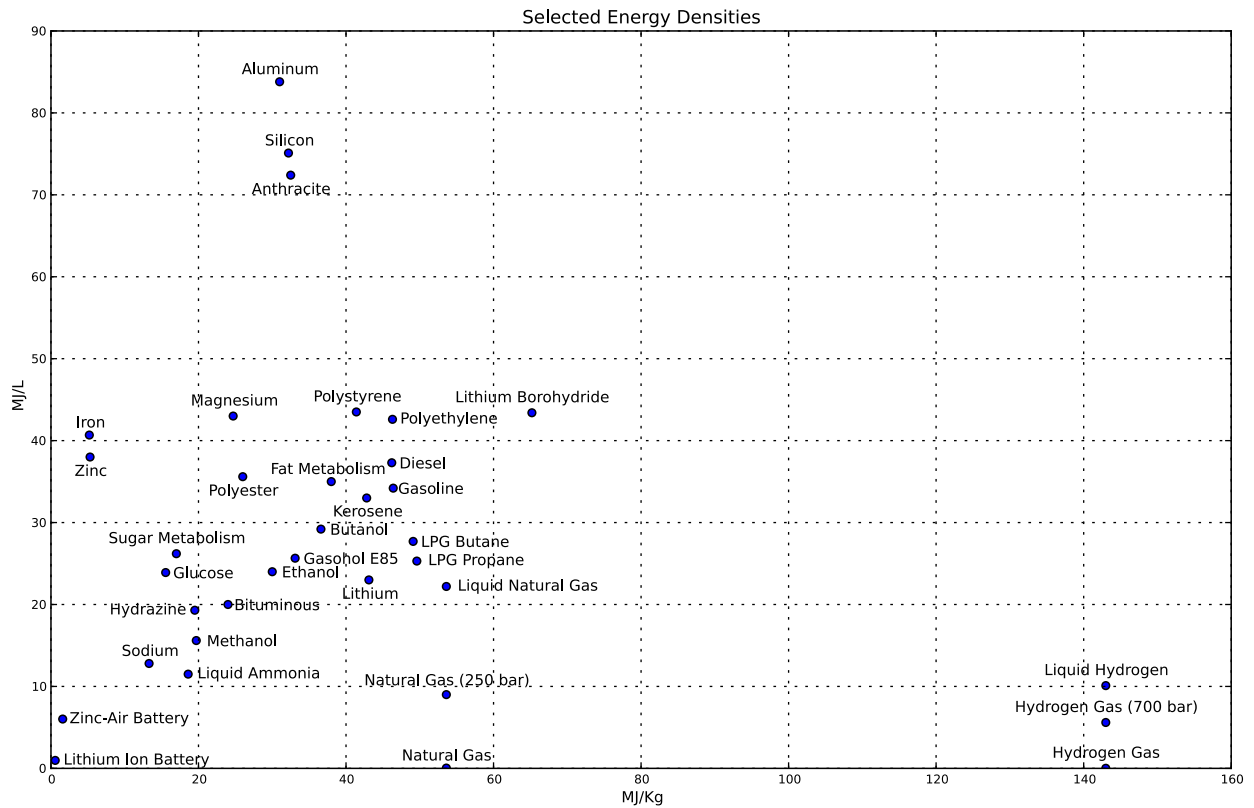
Figure 1: Plot of energy density vs specific energy for various compounds [30].

The most common methods for creating water-reactive aluminum include alloying the aluminum with large fractions of gallium (Ga), indium (In), or tin (Sn) [3], ball milling aluminum into fine powder [2], reacting the aluminum in the presence of strong acids [10], and surface treating the aluminum with Ga and In [4]. The use of strong acids, as well as the creation of aluminum powder, have largely been avoided in industry due to serious safety and logistical concerns regarding their inherently corrosive and combustible natures, respectively. Gallium and Indium are rare metals, and as such any alloys that incorporate large mass fractions of them into a fuel become very expensive and are largely cost prohibitive. The surface treatment method however, developed by Slocum in recent years, allows for the development of effective fuel while using only minimal concentrations of Ga and In, and requiring no use of acids or powders. This method is therefore considered to be significantly safer, cheaper, and simpler than other forms of aluminum activation currently being explored. For these reasons, the surface treatment activation method is used for all

17

tests and experimentation done in this thesis. A full procedure for the production of fuel using this method can be found in Appendix 8.1.

This surface treatment method requires that aluminum be treated with a eutectic mix that is 80% Gallium and 20% indium by mass. This eutectic is only absorbed into the aluminum in mass fractions ranging from 2-6%, meaning that the fuel retains a relatively low cost and minimal change in density. Additionally, this method of fuel production requires a simple surface treatment, meaning that it can be made readily from scrap aluminum. This is of great importance for applications such as military use, or use in the wake of a natural disaster, where fuel may need to be made on demand. Other processes require either melting the fuel or grinding it into fine powders which would be extremely difficult to do on demand without the proper equipment or without an outside power source. This ease of production from scrap is also advantageous because as much as 50% of end-of-life aluminum goes unrecycled in the U.S. [11]. While the production of aluminum does inherently produce carbon emissions, fuel can be made from otherwise unused, discarded, aluminum, and turned into recyclable AlOOH along with useful energy upon reacting. The surface treatment of scrap aluminum for fuel production could therefore allow this technology to have a positive environmental impact as well. Furthermore, aluminum pellets surface treated with Ga and In have been seen to maintain a stable shelf life of years, compared to gasoline or other carbon based fuels which generally maintain a shelf life of 3-12 months.

Due to these many advantages, reactive aluminum has incredible potential as a high energy density fuel source. Even looking at aluminum exclusively as a means of hydrogen storage, a single liter of aluminum would produce the equivalent amount of hydrogen gas as a 1 liter hydrogen tank pressurized to 50,000 psi. This is almost an order of magnitude higher pressure than any current hydrogen tanks are capable of achieving [12], demonstrating that aluminum is an incredibly effective means of hydrogen storage. Beyond its high energy density, the fuel is noncombustible, completely safe to transport, and produces no toxic emissions when reacted. This fuel has the potential to produce technologies such as emergency generators that run twice as long, use fuel with an indefinite shelf life, and that pose absolutely no risk of carbon monoxide poisoning.

2. THERMODYNAMICS OF ALUMINUM-WATER REACTIONS

Aluminum has an incredibly high chemical energy density however it quickly becomes inert in air and water due to an oxide layer that forms almost immediately on its surface and keeps any further reaction from occurring [8]. Various methods, such as those performed by Woodall and Slocum have found that this surface barrier can be bypassed in the presence of Gallium and Indium. This allows the aluminum to react in the presence of water, releasing large amounts of thermal and chemical energy in the process. This chemical oxidation could, in theory, take one of three naturally occurring forms, Aluminum Hydroxide (Al(OH)$_3$), Aluminum Oxyhydroxide (AlOOH), or Aluminum Oxide (Al$_2$O$_3$) as shown in Equations 2, 3, and 4.

$$2Al(s) + 6H_2O(l) \rightarrow 3H_2(g) + 2Al(OH)_3(aq) + Q_1 \qquad (2)$$

$$2Al(s) + 4H_2O(l) \rightarrow 3H_2(g) + 2AlOOH(aq) + Q_2 \qquad (3)$$

$$2Al(s) + 3H_2O(l) \rightarrow 3H_2(g) + 2Al_2O_3(aq) + Q_3 \qquad (4)$$
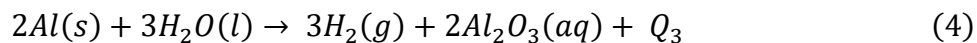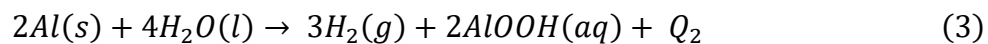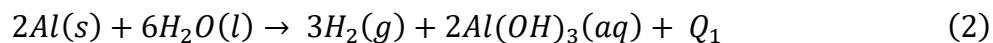
Where Q_n indicates the heat released, which varies across the three possible reactions. While experiments by Vedder et al. have shown the aluminum-water reaction to react via Equation 3 at atmospheric pressure and temperatures of 70 C [13], wider ranges of

ambient conditions have not been sufficiently explored. It was therefore unknown under which temperature and pressure conditions other reaction byproducts may become favorable.

While each of these reactions produces 3/2 moles of hydrogen per mole of aluminum reacted, the reactions vary in the amount of water stoichiometrically required, and the heat that each will produce as a byproduct. Understanding which of these reactions is occurring at a given operating temperature and pressure will allow the user to design the system for maximum efficiency and proper water consumption. In particular, the formation of aluminum oxide would be desirable in order to consume as little water as possible, thereby allowing for a higher system energy density.

Determining the most favorable reaction under a given set of pressure and temperature conditions was done using the thermodynamic quantity of Gibbs free energy. Reactions will always proceed to minimize the Gibbs free energy of the compounds. Therefore, any reaction in which the products have a lower Gibbs free energy than the reactants is said to have a negative change in Gibbs free energy across the reaction and will occur spontaneously. A reaction with a positive change in Gibbs free energy will not occur without outside stimulation. Furthermore, when multiple reactions are possible, the reaction that produces the most negative change in Gibbs free energy will be the most favorable to occur.

The Gibbs free energy was determined for each compound in reactions 2, 3, and 4 by looking at published data and applying temperature and pressure corrections to correspond to a wide range of working conditions. This was then used to find the total change in Gibbs free energy (ΔG) that occurs across each reaction, with lower values indicating a more favorable reaction. By performing this analysis across a wide range of temperatures and pressures, the most favorable reaction can be predicted across different operating regimes.

2.1   Analysis

The Gibbs free energy was analyzed to determine the favorability of each of the three possible reactions within a temperature range of 300-600 K, and a pressure range of 101-10,000 kPa. For any given reaction, the Gibbs free energy for each compound was calculated, and then the difference in Gibbs free energy between the reactants and products was determined. The reaction with the most negative change in Gibbs free energy is the most favorable to occur.

The first step in this analysis is to calculate the Gibbs free energy of formation for each individual compound in the reaction. While the Gibbs free energy of formation for many compounds are published and available online, these values must be corrected for variations due to changes temperature and pressure. Fortunately, the NASA ThermoBuild platform, which operates off of the NASA Glenn thermodynamic database, allows users to view the Gibbs free energy of a wide range of compounds at elevated temperatures. Using the data taken form this website, the only further correction that was needed was one for pressure. This can be done using Equation 5 for solids and liquids, and Equation 6 for gases.

$$\Delta_f g_i(T, P) = \Delta_f g_i^0(T) + v_i(p - p_0) \tag{5}$$

$$\Delta_f g_i(T, P) = \Delta_f g_i^0(T) + R * T * \ln\left(\frac{p}{p_0}\right) \tag{6}$$

Where v_i is the specific volume of compound i, R is the ideal gas constant, and P is the partial pressure of the gas in Equation 6, or simply the ambient pressure if using Equation 5. $\Delta_f g_i^0(T)$ is the Gibbs free energy of formation of compound i at temperature T and 1 bar, which provided by the NASA database.

Once these equations are used to determine the molar Gibbs free energy for each compound at the desired temperature and pressure, these values can then be summed to determine the net change in Gibbs free energy across a complete reaction. To do this, the

stoichiometric ratios in Equations 2, 3, and 4 are applied to the appropriate values for molar change in Gibbs free energy, and the difference between the reactants and products is found, as shown in Equation 7.

$$\Delta_f G(t,p)_{(2)} = \left(2 * g_{Al(OH)_3}(t,p) + 3 * g_{H_2}(t,p)\right) - \left(2 * g_{Al}(t,p) + 6 * g_{H_2O}(t,p)\right) \quad (7)$$

This gives the final change in Gibbs free energy, $\Delta_f G(t,p)_{(2)}$, for reaction 2, at a given temperature and pressure. This model makes several assumptions, the first of which is that no steam or other gasses are present during the reaction. This may not always be the case, particularly due to the exothermic nature of the reaction, but was assumed for the simplicity and generality of the model. If such gases were present, then the partial pressure of hydrogen used in Equation 6 would vary, causing a change in the final Gibbs free energy values. This variation would likely be minor however, because the Gibbs free energy varies only logarithmically with the partial pressure term. Additionally, this model assumes that the method by which the aluminum is activated does not impact the chemistry of the reaction. For experiments done here, this activation was achieved through the introduction of gallium and indium to the aluminum. It is believed that these compounds act only as a catalyst and have no true effect on the chemistry of the reaction, particularly because they are only present in concentrations of 1% by molar quantity.

This process was used to determine the change in Gibbs free energy for each of the three reactions discussed here. For each reaction, these values were evaluated in MATLAB over grid of 3100 points in a range of 300-600K and 101-10,000 kPa, and the results are shown in Figure 2. At any given temperature and pressure, the chemical reaction with the lowest change in Gibbs free energy is the most favorable, and the one that will be produced via the

aluminum-water reaction. This data can then be used to produce Figure 3, which shows the pressure and temperature regimes within which each reaction becomes most favorable.
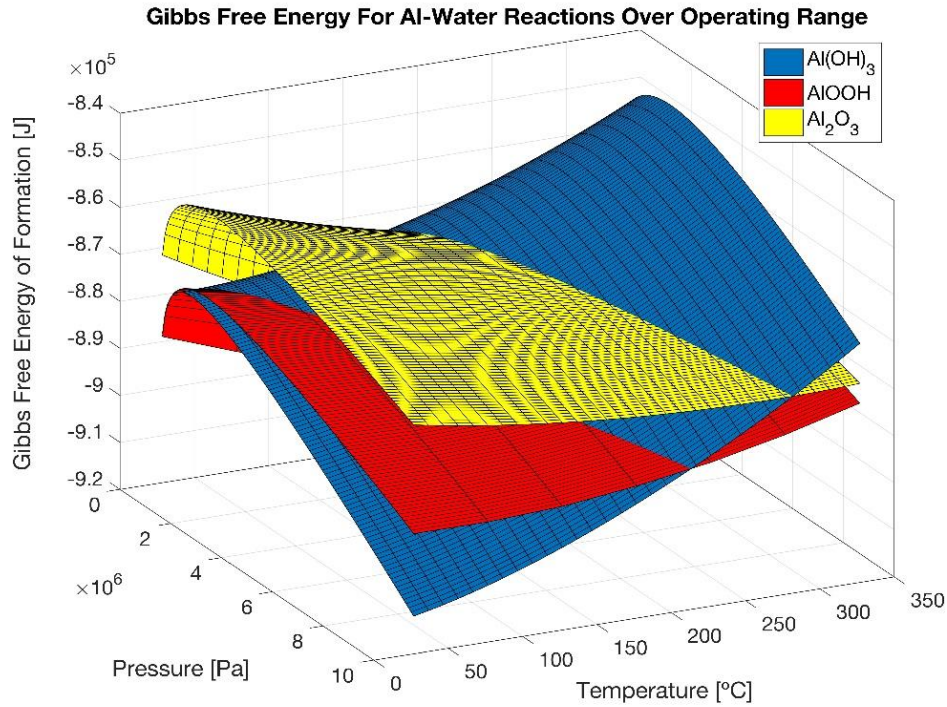
Figure 2: Calculated Gibbs free energy of formation at varied temperatures and pressures for each of the three candidate reaction byproducts.

This model predicts that at low temperatures, aluminum hydroxide is most favorable, while at slightly elevated temperatures, aluminum oxyhydroxide is the most favorable reaction product. Unfortunately, the region in which aluminum oxide would be produced requires temperatures above the boiling point of water and, therefore, could not be achieved by a liquid water-aluminum reaction.
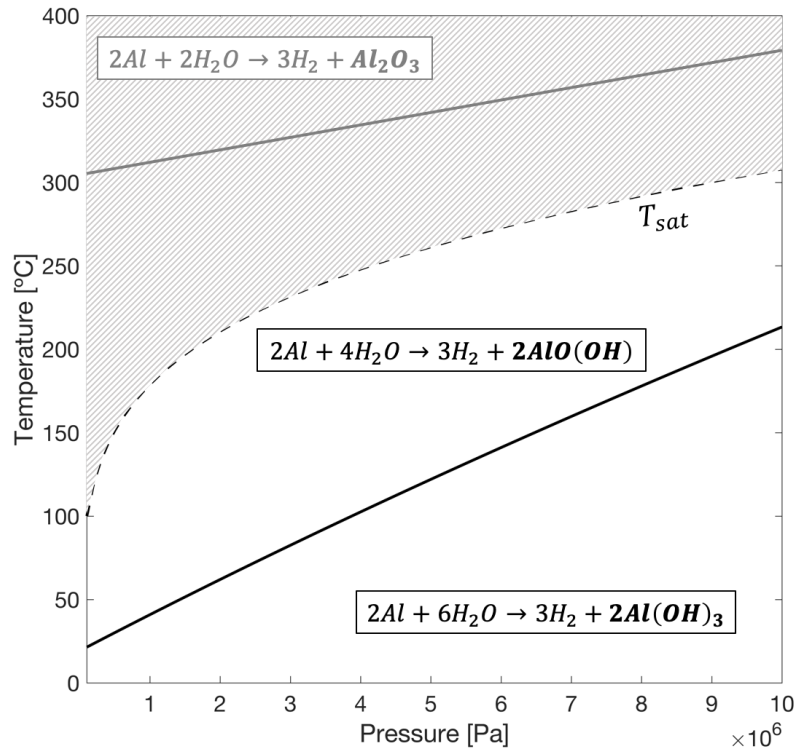
Figure 3: Transition diagram showing which reactions are most favorable under different reaction conditions. Conditions above the boiling point of water are greyed out, as aluminum-steam reactions have been unachievable using this form of aluminum fuel.

2.2 Experimental Validation

A series of four tests, at high and low temperatures as well as high and low pressure, were designed in order to validate the predictions made by this model. The values chosen, indicated in Section 2.2.1, allowed for two tests that were well within the expected aluminum oxyhydroxide regime, as well as two tests that were well within the expected aluminum hydroxide regime. Aluminum that had been activated using gallium and indium was reacted with water under each of these temperature and pressure conditions, and the reaction byproduct was recovered. The byproduct was then analyzed using x-ray

diffraction (XRD), as well as Fourier-transform infrared spectroscopy (FTIR), to determine its precise chemical makeup.

2.2.1 Experimental Setup

High Pressure Testing

Both high pressure reaction tests were done at 6.9 MPa, in the reaction chamber shown in Figure 4. This reaction chamber was made out of stainless steel tubing to avoid gallium or hydrogen embrittlement, and used Swagelok fittings in order to reduce leaking. The reaction chamber was pre-pressurized with compressed nitrogen and had a digital
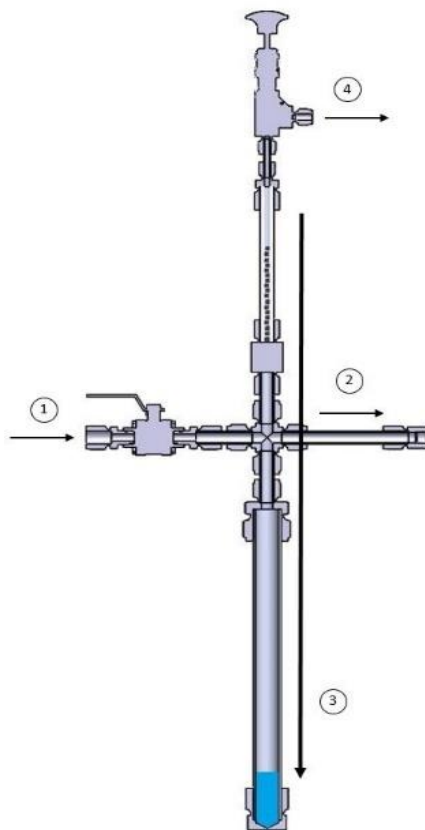
Figure 4: Cross section of the reaction chamber used for tests conducted at 6.9 MPa. 1) Inlet port for a tank of nitrogen gas that was connected to the chamber for system pressurization. 2) A mounted pressure transducer used to track the systems internal pressure. 3) A remote-controlled valve allowed the aluminum to drop into water below to begin the reaction. 4) Pressure relief valve used to prevent over pressurization.

pressure transducer to record the pressure, as well as an emergency relief valve in the case of accidental over-pressurization. Each reaction began with water already resting in the base of the reaction chamber, and aluminum placed in the topmost tube. This aluminum could then be dropped into the water using a remote-controlled ball valve.

High Pressure High Temperature Test:

During the high pressure, high temperature, test a resistive heater and a thermocouple were placed around the base of the reaction chamber. Both were then wrapped in insulation and the pressurized reaction chamber was allowed to heat up. Only once the reaction chamber had reached a steady state temperature of 230 C while still maintaining a pressure of 6.9 MPa, were the aluminum spheres released into the water. The reaction was then allowed to proceed for 30 minutes before the system was depressurized and the reaction chamber was slowly cooled. The contents of the reaction chamber were then recovered and allowed to dry in a fume hood at room temperature for 1 week.

High Pressure Low Temperature Test:

The high pressure, low temperature test was done by placing the pressurized reaction chamber within an ice bath and placing both the ice-bath as well as the reaction chamber within a 4 C refrigerator. The reaction chamber, water, and aluminum were all allowed to sit within the refrigerator for 30 minutes in order to pre-cool before the aluminum was released into the water. After being released, the aluminum was allowed to react in the high pressure, low temperature, environment for 72 hours. This long reaction time was chosen because it had been observed that the low temperature reaction tests proceeded at a much slower rate than those at an elevated temperature. After the reaction was complete, the system was depressurized, and the reaction products were recovered and allowed to dry in the fume hood at room temperature for 1 week.

Low Pressure, High Temperature Test:

The low pressure, high temperature, test was performed at 1 bar and 100 C. This was done by simply placing a preheated aluminum sphere into a beaker of boiling water. The aluminum was then allowed to react for 30 minutes after which the water eventually boiled off.

Low Pressure, Low Temperature Test:

The Low pressure, low temperature, test was performed at 1 bar and 4 C. This reaction was done by taking small fragments of aluminum and scattering them into an ice bath that was mixed to maintain a temperature of below 4 C at all times. Small fragments were used in order to reduce the magnitude of local heat generation, so that no pockets of water could be heated above 4 C. This reaction was allowed to proceed with a constant temperature below 4 C for 3 hours. The contents of the ice bath were then strained using a 200 μm sieve to remove any large remaining aluminum particles. The water and particles that passed through the sieve were then allowed to dry in the fume hood at room temperature for 1 week.

2.2.2 Experimental Results

Initial samples were tested using XRD with the assistance of the MIT Materials Science department. These results however, were largely inconclusive, and so samples were sent to Lehigh Testing Laboratories for XRD analysis. The results revealed that both high temperature tests produced aluminum oxyhydroxide, and that the high pressure, low temperature, test produced aluminum hydroxide, all as expected. Interestingly, the low temperature, low pressure, XRD results indicated that the sample analyzed was primarily elemental aluminum. This likely indicates that the reaction was not allowed to proceed for long enough and that not enough byproduct had been produced to be recognized by the XRD testing. These results can be seen in Figure 5 below.
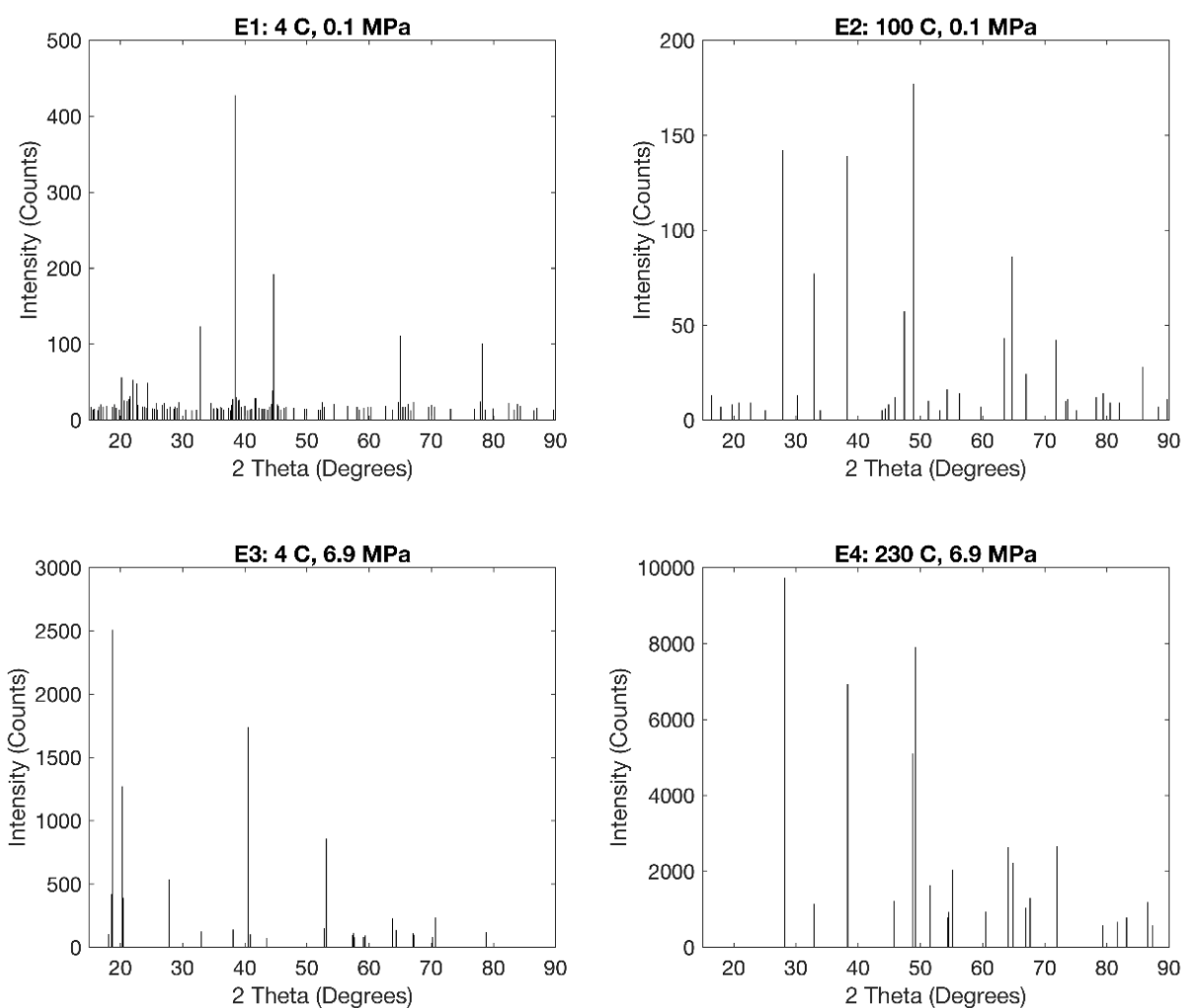
Figure 5: XRD peak results for reaction tests done at varying temperatures and pressures.

FTIR was also done with the help of the MIT Material Science department, and the results can be seen in Figure 6. Both high temperature results match the formation of aluminum oxyhydroxide, and both low temperatures results match aluminum hydroxide. The peaks on the lower pressure results however, are less distinct. This lack of clarity on lower pressure results is likely due to the fact that any residual water in the samples can obscure the results of an FTIR. While attempts were made to dry the sample, it has been shown that when reacting aluminum with water under atmospheric pressure, water can get trapped within the resulting oxyhydroxide crystalline lattice [13]. This water can be difficult to remove, and our attempts at drying the samples were therefore unable to increase FTIR

28

clarity. Notably however, when looking closely at samples E1 and E2, they can be seen to match their high-pressure counterparts. In E1, shoulders visible at 3656, 3548, 3465, 3435, and 3423 cm match well defined peaks in E3, and are indicative of aluminum hydroxide. In E2, peaks seen at 3307, 3095, 1074, 742, 613, and 493 cm are similarly seen to match those found in E4, and are indicative of aluminum oxyhydroxide. It is therefore believed that the 4 C, 1 bar, test also produced aluminum hydroxide, but simply not in a large enough quantity to be detected by XRD.
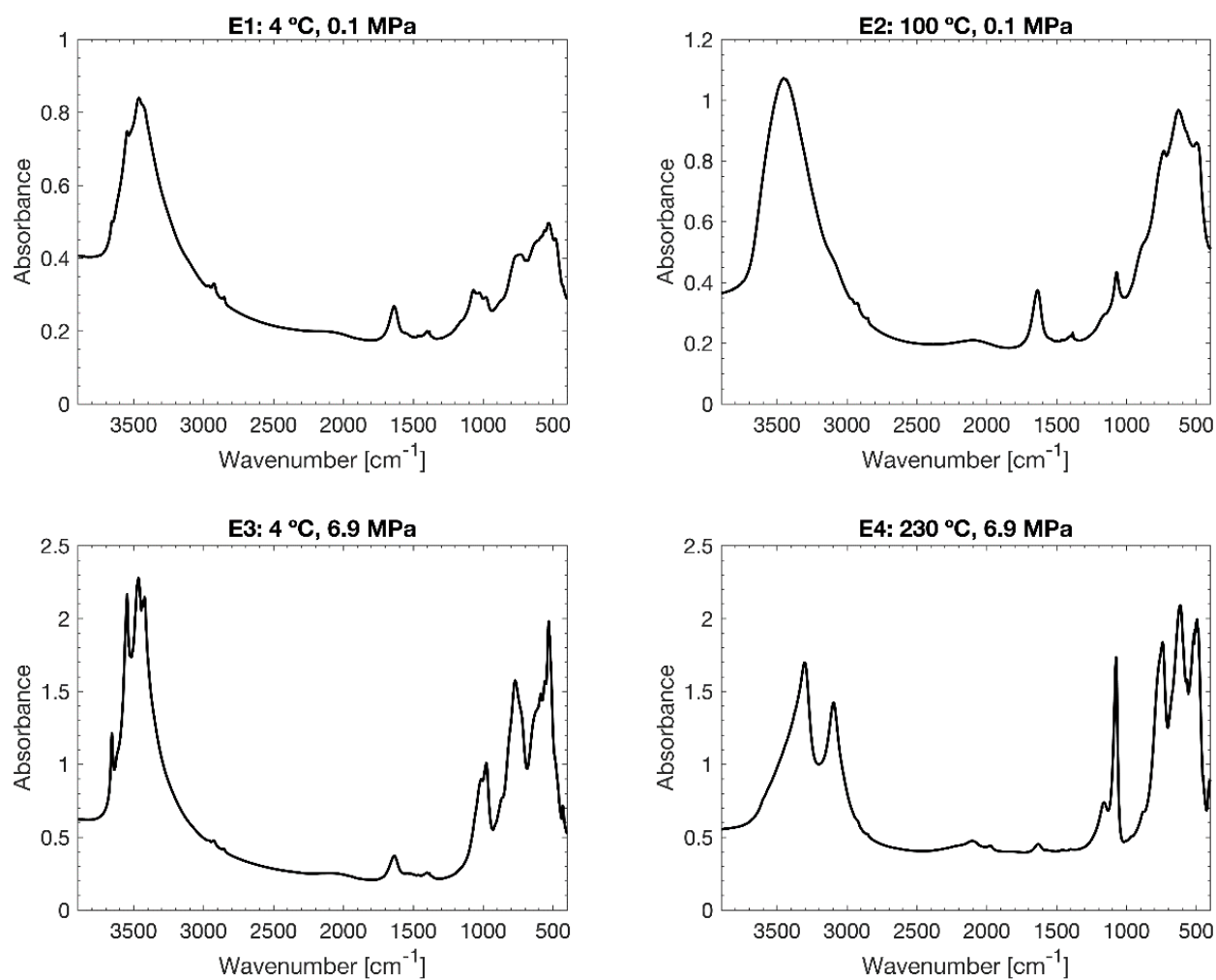
Figure 6: FTIR results for reaction tests done at varying temperatures and pressures.

Water Vapor Tests:

A series of tests were conducted to determine whether this reaction can be performed with steam, or whether it requires the presence of liquid water. These tests indicate whether the aluminum oxide region of Figure 3 could ever be reached. An additional motivation for this testing was that fuel was seen to slowly react and turn dark grey after exposure to air for several minutes. This was theorized to be due to a surface reaction, however it was unknown whether this reaction was an oxidation due to the oxygen in the air, or a reaction with water vapor.

An initial test was done in which two identically treated hemispheres of aluminum were placed into two separate jars. The first jar was filled with argon, but also contained a small bowl full of water. This water was never put in contact with the aluminum but was allowed to evaporate over time, thereby creating a gaseous atmosphere of argon at 100% relative humidity. The second jar was left open to atmosphere but filled with silica desiccant beads, thereby creating an oxygen rich environment with close to 0% relative humidity. The results can be seen in Figure 7 below, and after 4 hours only the aluminum that had been exposed to humid air showed any measure of surface reaction. This indicates that the observed surface reaction was occurring due to a reaction with water vapor in the air, rather than an oxidation due to oxygen in the air.
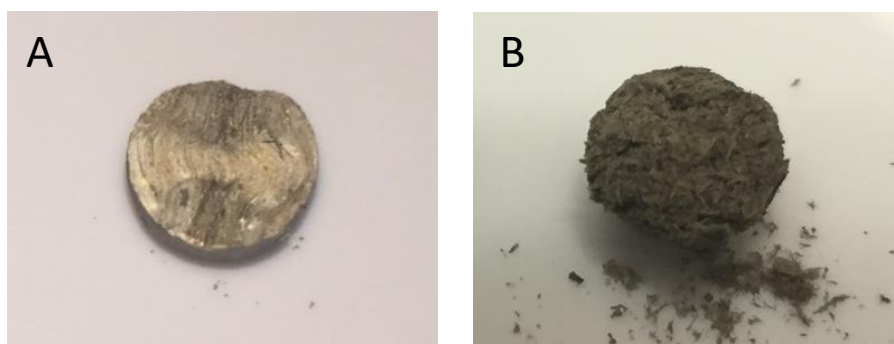
Figure 7: Image A is of an aluminum hemisphere that has been left in desiccated air for 4 hour, and B is of a hemisphere left in humid argon for 4 hours.

Once it was known that a reaction was possible using water vapor, an additional test was done to see if this reaction could be done with high temperature steam. A setup was used as shown in Figure 8, where boiling water was passed over an aluminum hemisphere. This aluminum sphere was heated to approximately 130 C, in order to ensure that no condensation was occurring on the surface of the aluminum.
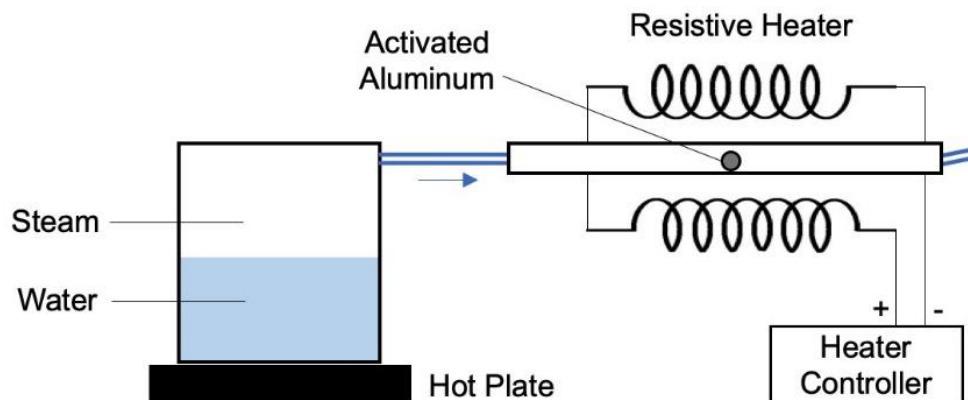
Figure 8: Diagram of experimental setup to test steam reactivity.

As a control, when this steam test was started, an identical hemisphere of aluminum was placed into a jar of humid argon, using the same method as described above. The hemispheres were observed at the start of the test as well as 35 minutes later, and the results are shown in Figure 9. While the aluminum subject to room temperature humidity was clearly seen to react within the 35 minute time period, no such reaction was observed for the aluminum that had been exposed to superheated steam.
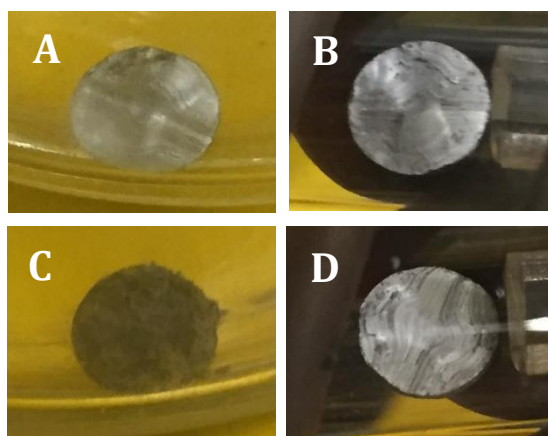
Figure 9: Aluminum hemispheres exposed to different gas. A) Before being placed in 100% humidity argon gas for 35 minutes. B) Before being exposed to steam for 35 minutes. C) After being exposed to humid argon, this hemisphere shows a visibly discolored surface. D) After being exposed to steam, this hemisphere shows no discoloration on surface.

This indicates that the treated aluminum used here is capable of reacting quickly with gaseous water vapor at room temperature but not at elevated temperatures. This is likely due to the adsorption of water onto the surface of aluminum at room temperature but not at elevated temperatures. Similar to condensation, the adsorption effect allows liquid water to form on the surface of the aluminum as a minimization of the metal's surface energy [14]. This effect would therefore cause the presence of liquid water on the surface of the aluminum, allowing a reaction to occur. At elevated temperatures, the adsorption effect decreases significantly, and would therefore not be observed. This lack of adsorbed liquid water would, in turn, prohibit any reaction from taking place, explaining why a surface reaction was seen only at room temperature but not at 130 C.

2.3   Discussion and Conclusion

An analysis has been done to determine the most favorable aluminum-water reaction to occur under a wide range of temperatures and pressures. This analysis indicates that aluminum oxyhydroxide is favorable under most practical conditions, however the production of aluminum hydroxide can be achieved if the reaction is done under

sufficiently low temperature or high pressure. Additionally, it is unlikely that aluminum oxide can be produced through this method, as the temperatures needed for its production are above that which can be reached by liquid water, and evidence suggests that the reaction of aluminum treated in this manner cannot occur with steam.

This analysis was then supported experimentally by tests at high and low temperatures and pressures. Analysis using both XRD and FTIR confirmed that both high temperature tests results produced aluminum oxyhydroxide and low temperature tests produced aluminum hydroxide, as predicted. While the XRD results for the low temperature, low pressure result was inconclusive due to the lack of sufficient reaction byproducts, FTIR data indicates that the minimal reaction that did occur did, in fact, produce aluminum hydroxide.

This model allows for the more accurate development of future aluminum fueled systems. The production of aluminum oxyhydroxide as compared to aluminum hydroxide will change the expected heat released in the reaction and reduce the amount of water needed by as much as 33%. Additionally, both aluminum hydroxide and oxyhydroxide have many industrial uses, and have different market values across the globe. By using this model, systems can now be designed for the optimal operating conditions, and for the ideal operating byproduct.

3. REACTION CONDITIONS OF ALUMINUM FUEL

Aluminum has long been sought after as a fuel source, due to its high energy density. Until recently, the two most common methods for producing reactive aluminum fuel required either alloying aluminum with high percentages of Gallium or grinding the aluminum into a powder. Unfortunately, alloying with high concentrations of gallium made the aluminum cost prohibitive, as Gallium is a rare, and fairly expensive, metal. While aluminum powders have been shown to be reactive with only small percentages of gallium or similar additives, they pose serious risks for explosivity, as well as inhalation health hazards. These cost and safety concerns have been major factors in keeping aluminum fuel from coming to market. Recently, a new method for creating reactive aluminum fuel, developed by Slocum, proposes a fuel that requires only small concentrations (2-6%) of gallium and Indium additives, yet boasts high (>80%) reactivity [4]. This method offers an energy dense fuel while having low costs and virtually no safety risks.

The Slocum method of placing raw aluminum in a heated gallium and indium eutectic bath is novel in many ways. In addition to being low cost and having significantly fewer safety concerns than reactive powders, it also has the ability to turn large pieces of raw aluminum into a reactive fuel without having to significantly change its state by either melting or grinding it. Unfortunately, however, this method is still in its infancy and current research has left many questions unanswered. For instance, it is known that two stages are necessary for fuel production, an initial heated phase where the eutectic is absorbed into the aluminum's surface, and a later eutectic permeation phase where the eutectic

permeates through the bulk of the aluminum. Previous research had not explored the time necessary for each of these stages and their effect on the fuel's reaction yield. Additionally, no studies had been done on how the concentration of eutectic within the aluminum effects the overall reactivity. Answering these questions is critical to producing fuel as quickly as possible and for as low a cost as possible, while maintaining high reaction yields. Additionally, the answers to these questions will hopefully shed light on the underlying mechanism of action of the reaction, as it is currently unknown how the introduction of gallium and indium allows for an aluminum-water reaction to proceed unimpeded by the naturally occurring oxide layer.

A series of tests to measure the reaction yield of aluminum that had been produced under different conditions were done. These tests included the measurement of reaction yield for aluminum that had been allowed varying permeation times post treatment, aluminum that had been treated at different temperatures, and aluminum that had been treated with varying concentrations of eutectic. By measuring the effects of each of these parameters on the final reaction yield of the aluminum, the fuel production method can be optimized for speed and high reaction yield.

3.1 Sphere Treatment

3.1.1 Sphere Composition

The aluminum spheres used in the following experiments were produced in the same way as those used by Slocum for the initial experimentation and development of this treatment method. These spheres were 6 mm in diameter and 99.90% aluminum in composition. They were manufactured by being extruded, forged, and polished, leaving them with a fine internal grain structure as well as residual internal stresses. This grain structure was measured to be 1-10 μm, which is significantly smaller than those seen in aluminum

produced via pure casting or forging, which typically produce grain sizes on the order of 10 -100 μm [15].

3.1.2 Surface Coating Method

In order to further characterize this fuel, a slight variation on Slocum's process was developed, in order to make fuel in a more reliable and controlled manner. Rather than placing aluminum in a heated bath of eutectic as described in Appendix 8.3, the aluminum was surface coated with eutectic as described in Appendix 8.1. In this method, a container of aluminum spheres was placed on a hotplate and heated to 120 C. After reaching the desired temperature, a small amount of eutectic was added to the container and it was mixed thoroughly until the aluminum spheres were seen to have an even surface coating of eutectic. The aluminum spheres were then allowed to sit on the hot plate for an hour and a half while being remixed every 20 minutes in order to promote consistent surface coatings and heat distribution within the container. This method produced fuel that showed remarkable consistency and displayed no pitting in the surface due to degradation from gallium, as can be seen in Figure 10. Additionally, this treatment method is eutectic-limited, which allows for the controlled addition of exact mass fractions of eutectic into different batches of fuel. Finally, it is notable that this method ensures that fuel can be made with significantly less Gallium and Indium overhead than the bath method. When treating a kilogram of aluminum using the bath method, several kilograms of Gallium and indium will be needed in order to properly cover the aluminum, however using this surface treatment method only ~50 grams of eutectic would be needed. While the same amount of eutectic would be absorbed into the aluminum in either case, having a eutectic bath requires large overhead and may become cost prohibitive for large-scale bath fuel production.
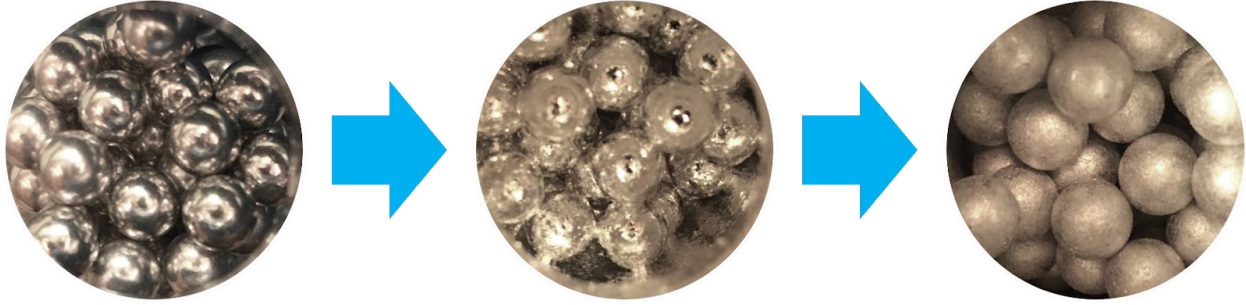
Figure 10: Progression of Aluminum surface treatment. Left image shows jar of untreated aluminum spheres. Middle image shows same aluminum spheres after being surface coated with eutectic. Right image shows these spheres after being heated and mixed for 1.5 hours, all liquid eutectic is gone and absorbed into the surface.

3.1.3 Batch Eutectic Consistency

A reference test was done in order to accurately measure the consistency of the new fuel surface treatment process described in Section 3.1.2. In this test, a batch of 24 spheres was treated with a single desired concentration of eutectic, and then the eutectic variation within each sphere from that batch was measured. This measured variation was then used as a standard reference variation, to be expected within each batch of fuel produced using this surface treatment method.

A microbalance with an accuracy of ±1 µg was used to select a set of 24 spheres that all weighed 0.301950 grams ±50 µg. These spheres were then surface treated with eutectic as a single batch. The final masses of each sphere were measured in order to determine the variation in final mass from sphere to sphere, and thus the total variation in mass fraction of eutectic present between spheres from a single batch.

One complication that arose during this test was that when a treated sphere was placed on the microbalance, the mass reading of the sphere would not stabilize, but rather, would steadily increase over time. As the sphere's mass increased over the course of several minutes, its color was also seen to darken. This increase in mass, and darkening of color, when exposed to air is a result of the reaction of the aluminum with water vapor in the air. This is believed to be due to adsorption effect, discussed previously in Section 2.2.2. As this

surface reaction occurs, some aluminum combines with water molecules in the air and is converted into aluminum oxyhydroxide which has a greater mass than the initial aluminum, causing the measured sphere mass to increase.

Looking closely, it was also seen that the rate of mass-increase for the aluminum sphere decreased over time. This is to be expected because as a surface reaction occurs, much of the surface becomes covered in the produced oxyhydroxide. This leaves less free surface area for continued reactions and therefore would cause the reaction rate to decrease over time. This decrease in reaction rate was measured on the microbalance and can be seen in Figure 11.
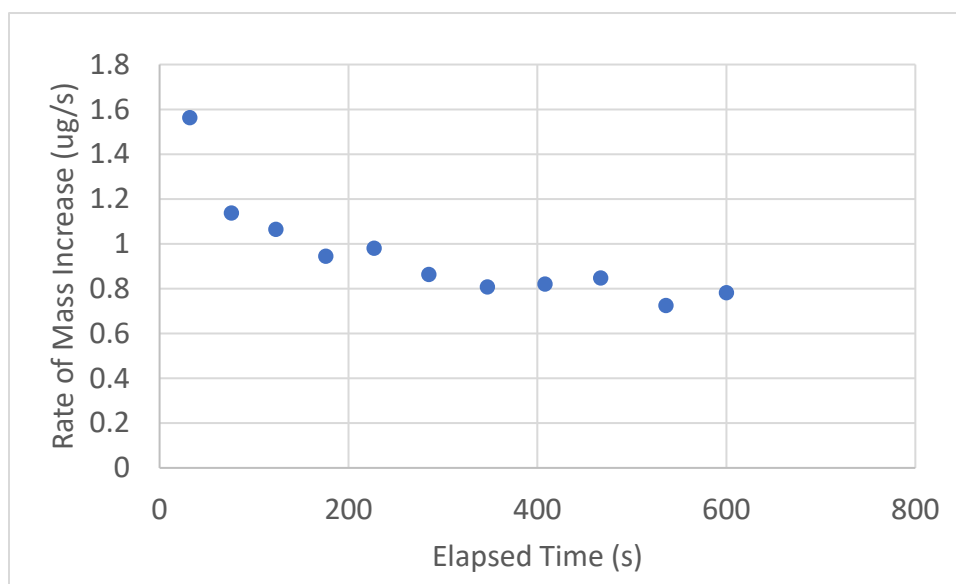
Figure 11: Plot showing mass increase over time for a treated aluminum sphere left out in air.

Due to this increase in mass over time, it was important to weigh each aluminum sphere as quickly as possible when determining the results of the consistency testing. Each sphere was removed from a jar and weighed after being exposed to open air for approximately 15 seconds, and any slight variation in this time was seen to be insignificant. The recorded increase in mass for each sphere can be seen in Figure 12.
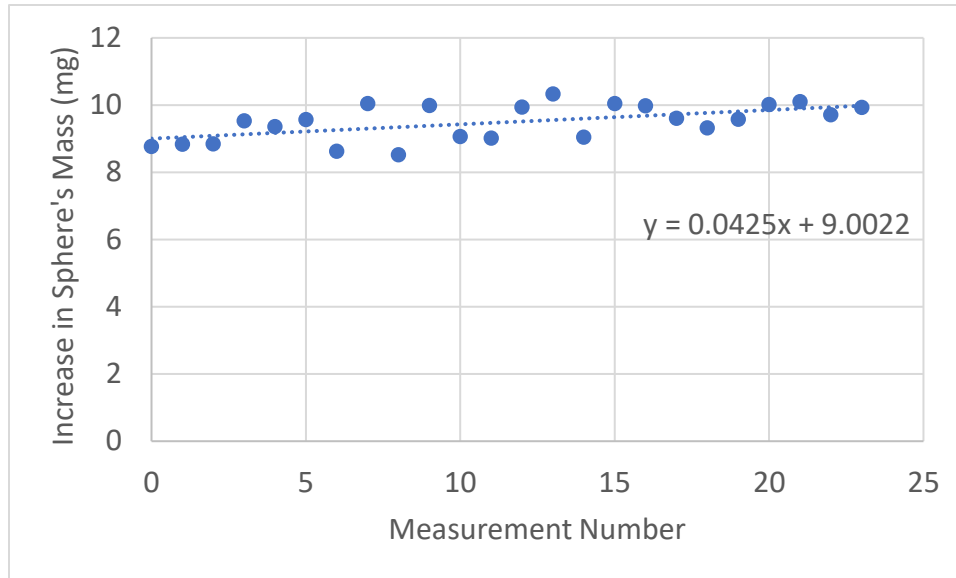
Figure 12: Plot showing the increase in mass measured for each treated sphere. The exact increase in mass corresponds to an exact concentration of eutectic added.

One error inherent within this experiment is that as the jar of aluminum spheres is opened and closed each time to remove a new sphere for measurement, the remaining spheres are being exposed to slight amounts of new, humid, air. This would result in later measurements being of samples that have been exposed to slightly more moisture and will therefore be slightly heavier, leading to a bias in the data. This trend can in fact be seen in the data recorded in Figure 12. In order to best account for this error, the line of best fit for the data was calculated, and the slope was subtracted away from each data point in order to produce a data set that shows no false positive trend. This slight data correction accounts for the sphere's increased moisture exposure over time.

The results of this consistency testing show that a batch treated with this new surface treatment method had a eutectic concentration of 2.90% with a standard deviation of only 0.14%.

3.2   Recoding Reaction Yield

In order to characterize the fuel, a method for measuring the reaction yield of a given piece of aluminum was needed. This was done by measuring the volume of gas produced when the aluminum was reacted with water. Given a known mass of reacted aluminum, and the fact that the aluminum-water reaction always produces 3 moles of H_2 gas for every 2 moles of reacted aluminum, the expected moles of hydrogen produced from a complete reaction can be calculated. This, in turn, can be mapped to an expected volume of hydrogen using the ideal gas law. Once this is done, this ideal volume of hydrogen can be compared to the actual recorded volume of hydrogen in order to determine a final percentage of reaction completion.

The experimental setup for measuring the volume of hydrogen produced in a given reaction can be seen in Figure 13.
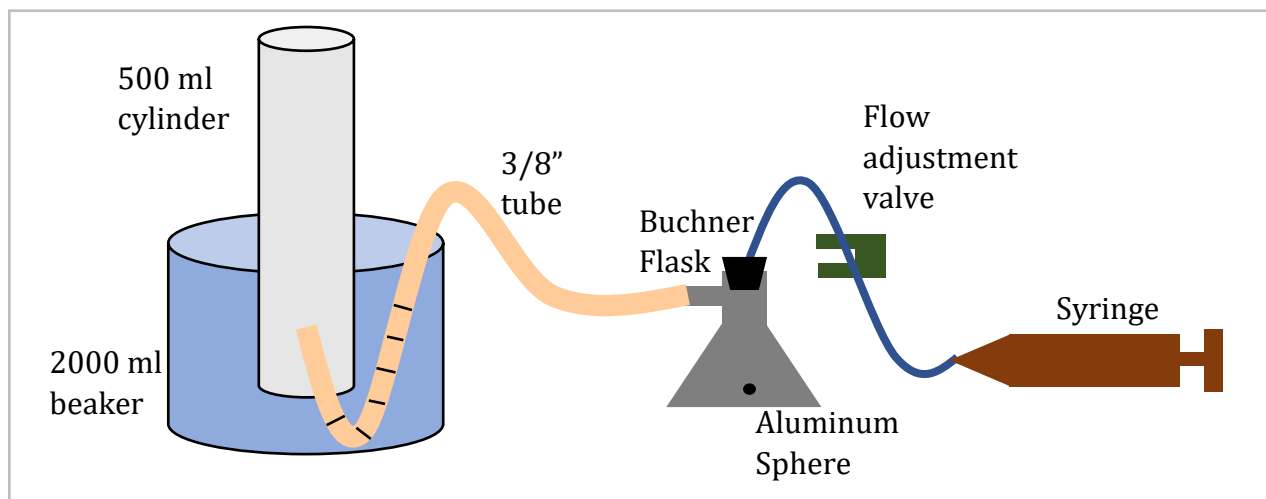
Figure 13: Diagram of reaction testing setup

An aluminum sphere was placed in a small 50ml Büchner flask, which was then corked, with its outlet leading into an inverted cylinder. This inverted cylinder was filled with water and placed in a large beaker. Through a hole in the cork in the Büchner flask, 5ml of purified water was inserted, commencing the aluminum-water reaction. The gas produced from the reaction was then allowed to bubble up into the overturned cylinder and displace

the water inside. The total volume of water displaced in the cylinder was then recorded as it represents the volume of gas produced in the reaction. Measurements of the volume of gas produced were taken every 15 seconds until the reaction rate dropped below ~0.5 ml/min at which point the reaction was considered to have run to completion. Following this, additional 5ml of water was inserted into the beaker and was allowed to sit for several minutes in order to ensure that the reaction was not water limited and that any aluminum that had become scattered throughout the flask had come into contact with water[1]. In most tests, no significant hydrogen generation was seen after 15-20 minutes. For further details of the measurement method, see Appendix 8.2.

3.2.1 Errors in Experimental Setup

Due to the complexity of the experimental setup, and the challenges of working with hydrogen, several errors were considered. These experimental errors include the effects of pressure and temperature changing the observed gas volume, any other gases that may contaminate the gas, and any hydrogen leaking that may have occurred. Each of these errors were analyzed and accounted for when determining the gas produced in the reaction.

Presence of Water Vapor:

Because the reaction occurs in the presence of water, and often forms steam in the process, it can be assumed that the hydrogen produced will be mixed with water vapor and will be at 100% relative humidity. Additionally, the hydrogen gas then bubbles through a water column and comes to rest next to exposed water, further ensuring that the gas will exist at 100% relative humidity. At 20 C, this means that water vapor will account for a full 2.3% of

---

[1] Temperature has been shown to impact the reaction rate and possibly even reaction completion, therefore the full 10 ml was not inserted at the beginning, so that reaction could more easily heat up to boiling with only 5ml of water, before it was flooded with additional water

the gas by volume. This water vapor volume is accounted for and subtracted away from any measured results when determining the actual volumes of hydrogen produced[1].

Increased Temperature Causing Gas Expansion:

The aluminum-water reaction is highly exothermic and the Büchner flask quickly becomes heated when the reaction begins. This leads to an expansion of the gas inside of the flask as per the ideal gas law. It is important that this expansion not bias the final volume measurements recorded, leading to a perceived increase in quantity of gas. Due to the low specific heat capacity of hydrogen, the gas cools very quickly once it leaves the flask, but the flask itself retains heat for several minutes after the reaction ends and will maintain its internal gas at an elevated temperature. For this reason, in all experiments done, once the reaction was considered to have gone to completion the flask was placed in a bath of cool water and allowed to cool to room temperature. The final volumes of hydrogen were only measured once this cooling stage was completed and any observed volume reduction was accounted for.

Pressure Compressing or Expanding Gas:

The pressure of the gas in the 500 ml cylinder will vary based on the water level in the cylinder, as per Bernoulli's equation. This change in pressure will then affect the recorded volume of the gas, as per the ideal gas law. This means that when the water level in the 500 ml cylinder is very high in the cylinder, the gas will be under a slight negative pressure, and will be seen to occupy a larger volume than that gas would normally occupy at 1 standard atmosphere of pressure. The opposite is true if the water level of the 500 ml cylinder was far below the water level of the 2000 ml beaker. All tests were therefore setup such that when an aluminum sphere had approximately 80% reaction yield, the resulting water level in the 500 ml cylinder would exactly match with the water level in the 2000 ml beaker,

---

[1] The dissolution of hydrogen into water was also measured but was found to be insignificant, especially compared to the error due to dissolution of water into hydrogen.

resulting in a gas pressure of 1 atm. This allows the volumetric measurements to assume a pressure of 1atm for most calculations and reduces any volume error due to change in pressure. Additionally, calculations show that the pressure differences created by variations in the water level that correspond to ±15% reaction yield[1], would add insignificant error to the system.

Hydrogen Leaking:

Due to H_2's incredibly small molecule size, it is known to leak very easily, and be permeable through most surfaces given sufficient time. Any hydrogen that were to leak out of the system would unaccounted for in the measurement, causing errors in the observed reaction yield. This was mitigated by using 1/8" thick flexible PVC tubing which has a very low hydrogen permeability, particularly in the case where there is no pressure differential across the tube. Additionally, all barbed seals and corks were wet before being sealed to allow for the water to act as a barrier to leaking. Using these methods, the setup was observed to have no detectable hydrogen losses even when left full of hydrogen for 24 hours.

3.3   Reaction Yield Results

3.3.1 Eutectic Permeation Time

A series of tests were done to determine the effect of permeation time on coated aluminum fuel. Four different batches of 60 aluminum spheres were surface treated as per Appendix 8.1, each with a different mass fraction of eutectic added. After the surface treatment, ten spheres were reacted immediately, followed by an additional 10 spheres 1, 2, 3, and 7 days

---

[1] This variation in reaction yield would lead to water level variations of approximately 2". This change in water level would only create a pressure differential of ±0.005 atm.

later. This set of experiments was done using batches that had been treated with 1.0%, 1.9%, 2.4%, and 4.3% eutectic by mass. The reaction yield was recorded, and the results can be seen in Figure 14.
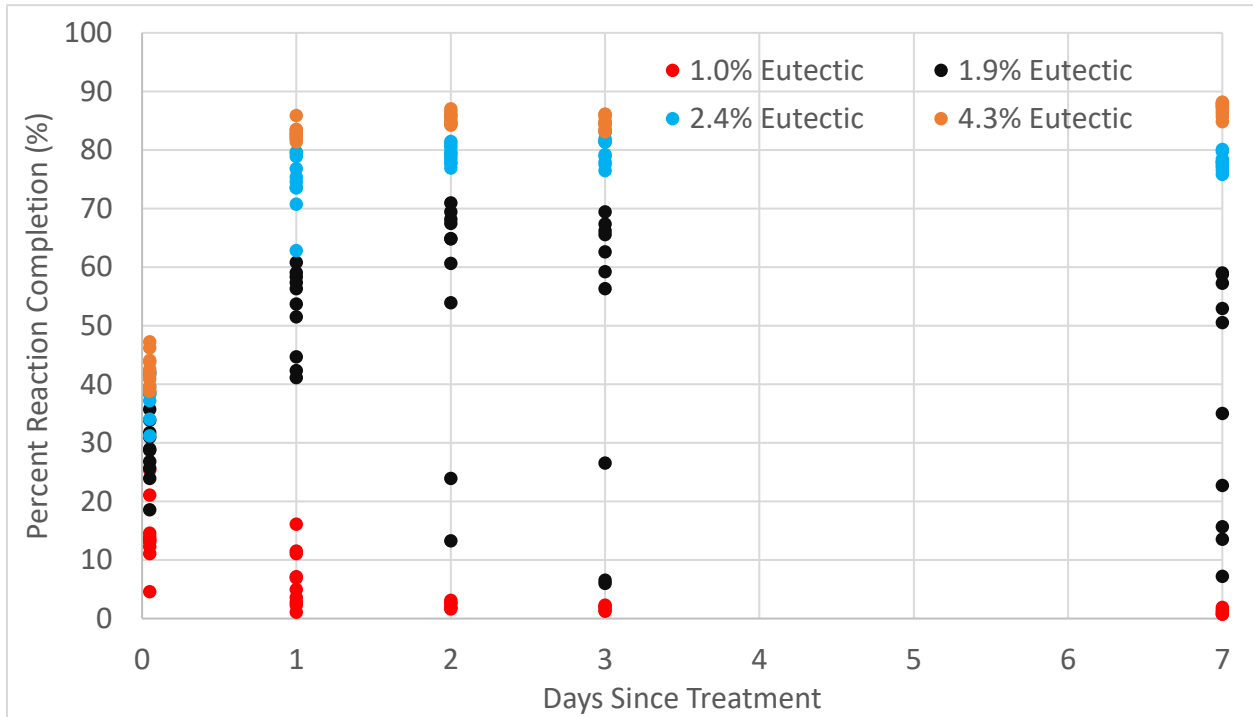
Figure 14: Plot of measured reaction completion of aluminum samples after increasing time since treatment. Aluminum samples were tested that were 1.0%, 1.9%, 2.4%, and 4.3% eutectic by mass.

It can be seen that for the 2.4% and 4.3% samples, the reaction yield climbs within the first 48 hours and the variation within the sample decreases significantly. After 48 hours, the reaction yields of these samples remain constant and do not vary. Additionally, the reaction yields of all samples remain distinctly different even after sufficient time for complete eutectic permeation. This demonstrates an inherent connection between the concentration of eutectic and the reaction yield of the aluminum which had not previously been studied.

When looking at the 1.0% sample it can be seen that initially there is a slight reaction, however as time commences and the eutectic permeates more completely into the sphere, the reaction yield declines to nearly zero. This indicates the existence of some threshold eutectic concentration that is necessary in order to commence a reaction. Immediately after the initial surface treatment, the entire 1.0% by mass of eutectic was concentrated on

the surface of the sphere and this was sufficient to allow for an aluminum-water reaction. As time went on however, and the eutectic is absorbed evenly throughout the sphere through a mixture of diffusion and wicking [16], the concentration at the surface drops. This decrease in concentration of eutectic at the surface means that there is no longer sufficient eutectic present pass the threshold necessary to initiate a reaction, and thus the reaction yield decreases to nearly zero.

Interestingly, the 1.9% eutectic sample seems to exhibit behavior from both regimes, with some of the samples having an increased reaction yield over time, and others having a decrease. This is likely due to the 1.9% samples being very close to this threshold concentration, such that with slight variation in eutectic concentration from sphere to sphere, some spheres had sufficient eutectic to react even after permeation away from the surface, and some did not.

The increase in reaction yield seen within the first 48 hours can also be used to give an approximation for the rate of eutectic permeation. By assuming that the increase in reaction yield is caused by the eutectic permeating deeper into the sphere, an approximate radius of permeation can be computed for the initial test at time zero, and for the 24 hour test. This, in turn, gives an approximate rate of permeation along the radius of the sphere. Permeation rates determined in this manner were 0.014 µm/s, which is on the low end of gallium permeation rates through aluminum studied by Hugo et al. [16]. This low permeation rate may be due to the particularly small grain structure found in these spheres or may be due to the presence of indium slowing the gallium penetration.

3.3.2 Treatment at Elevated Temperatures

Attempts were made to vary the surface treatment process in order to expedite the fuel development. The first attempt was to increase the temperature of the heated surface treatment stage. A series of test were done using the same procedure for as described in

section 3.3.1, however instead of heating the aluminum and eutectic to 120 C, they were heated to 180 C. The results for this experiment are shown below in Figure 15.
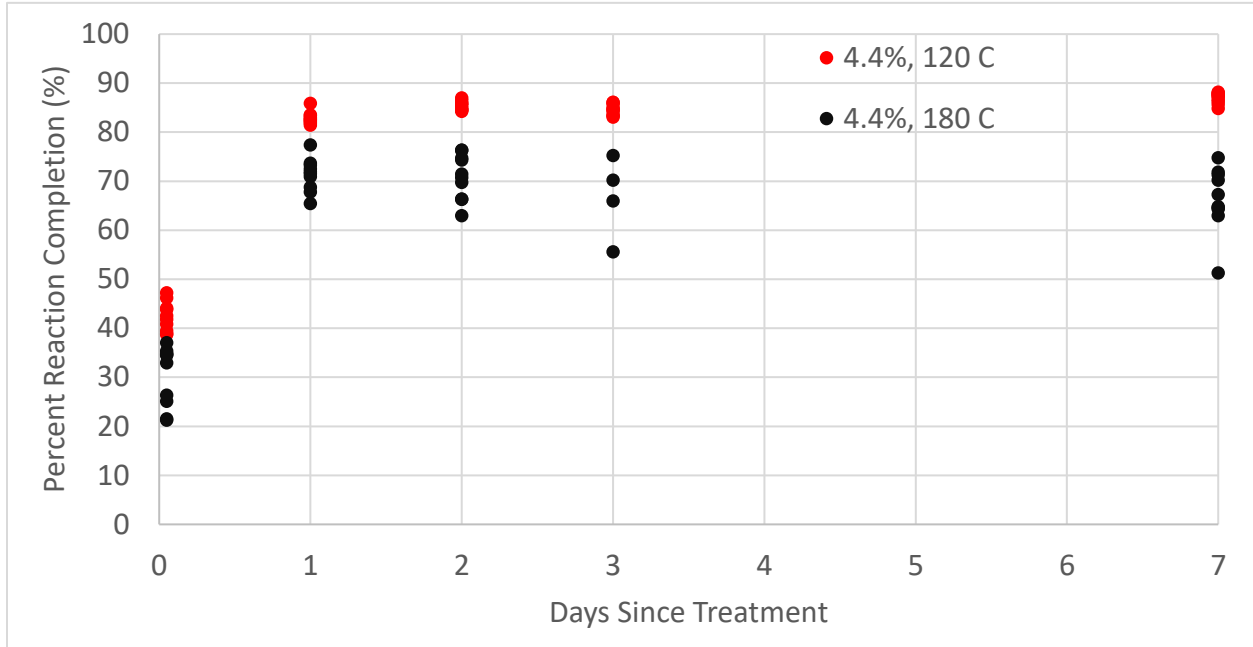
Figure 15: Plot of measured reaction completion for samples that were prepared with the same concentration of eutectic but at different temperatures.

While it is possible that this increased temperature did in fact decrease the total amount of time needed for the fuel to reach its final levels of reaction yield, it can be seen that this total yield is significantly decreased as compared to fuel heated to the standard 120 C. This is likely due to the fact that by heating the fuel in this test to 180 C, the fuel is being brought to a high enough temperature for it to begin to anneal. High temperature heating and annealing has previously been seen to cause decreases in reaction yield by Slocum [4], who reported similar 20% decreases in reaction yield for aluminum heated to 200 C prior to treatment.

3.3.3 Treatment for Extended Time

As a second attempt to decrease the time necessary for the fuel production process, fuel was surface treated while heated for 3 hours rather than 1.5. This was done with the hypothesis that heating expedites the eutectic permeation, and therefore a longer heat treatment time will necessitate less absorption time afterwards. The results of this test are shown in Figure 16 below.
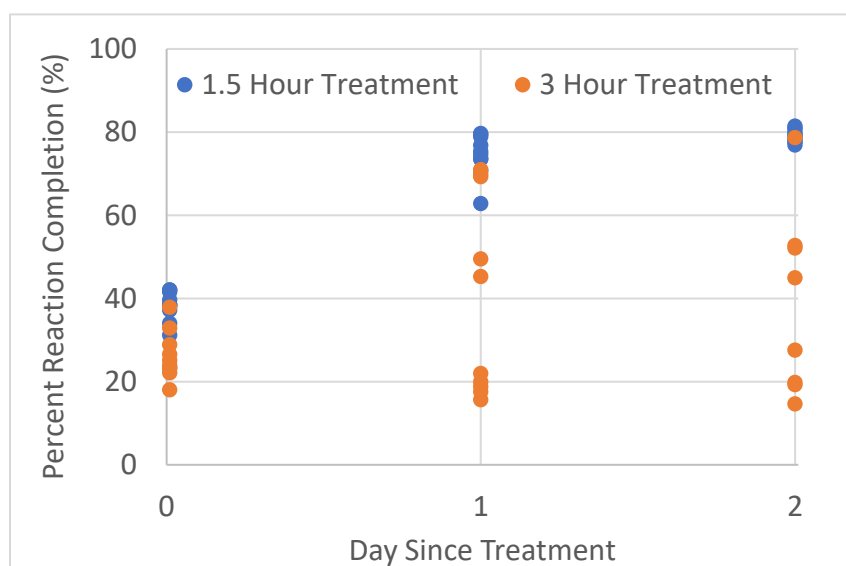
Figure 16: Plot of measured reaction completion for samples treated for 1.5 hours, and samples treated for 3 hours.

Interestingly, the longer heat treatment time does not seem to expedite the fuel production process and instead introduces significant variation into the final fuel reaction yield. While the aluminum spheres were mixed every 20 minutes during the heat treatment process, perhaps the inherent uneven heating that occurs across the spheres became exaggerated when heating over longer periods of time. This variation in heating from sphere to sphere would then result in a variation in reaction yield. Further tests should be done while heating the spheres using a more even heat source such as an oven, rather than a hotplate. Additionally, the general decrease in reaction yield observed for samples heated for 3

hours may be due to annealing of the aluminum. Future tests may also attempt to heat the aluminum at 120 C for the standard 1.5 hours and then at a lower temperature of 60 C for extended time so that permeation can be increased without running the risk of being so hot as to anneal the aluminum.

3.3.4 Varying Eutectic Concentrations

Considering both the high cost of gallium and indium eutectic, as well as the desire for high reaction yields in order to increase net energy density, it was necessary to further characterize the dependence of eutectic concentration on net aluminum reaction yield. One of the many advantages of the surface coating method is that it allows for batches of fuel to be made with precisely controlled mass fractions of eutectic. This allows the study of the correlation between eutectic concentration and reaction yield. A series of 7 tests were done where aluminum spheres were heated to 120 C for 1.5 hours and surface treated with varying mass fractions of eutectic. After waiting 72 hours, ten spheres from each of these batches was reacted in water and their reaction yields were measured as per Appendix 8.2. The results of these tests are shown in Figure 17.

These results show a clear increase in reaction yield as the mass fraction of eutectic is increased. A minimum threshold concentration for a reaction is observed as discussed in Section 3.3.1 at approximately 1.9%, below which there will be virtually no reaction and above which the reaction yield is >70%. Beyond this threshold, the increase in reaction yield can be seen to increases asymptotically as it approaches the low 90th percentile with as high as 6% eutectic. No further tests could be performed beyond 6%, because it was found that when higher concentrations of eutectic were added, the increased eutectic would not absorb past the surface of the aluminum within the 1.5 hour heated treatment period and could be easily centrifuged off. Because the eutectic is being absorbed into the grain boundaries of the aluminum, this limit may be due to a saturation of the free space within the grain boundaries of the aluminum, such that they cannot absorb more eutectic into the aluminum within the 1.5hr of the heated surface treatment. It is possible that if

aluminum were to be used that had a different internal grain structure or higher surface to volume ratios, then higher concentrations of eutectic could be absorbed into the surface, and higher reaction yields could be achieved.
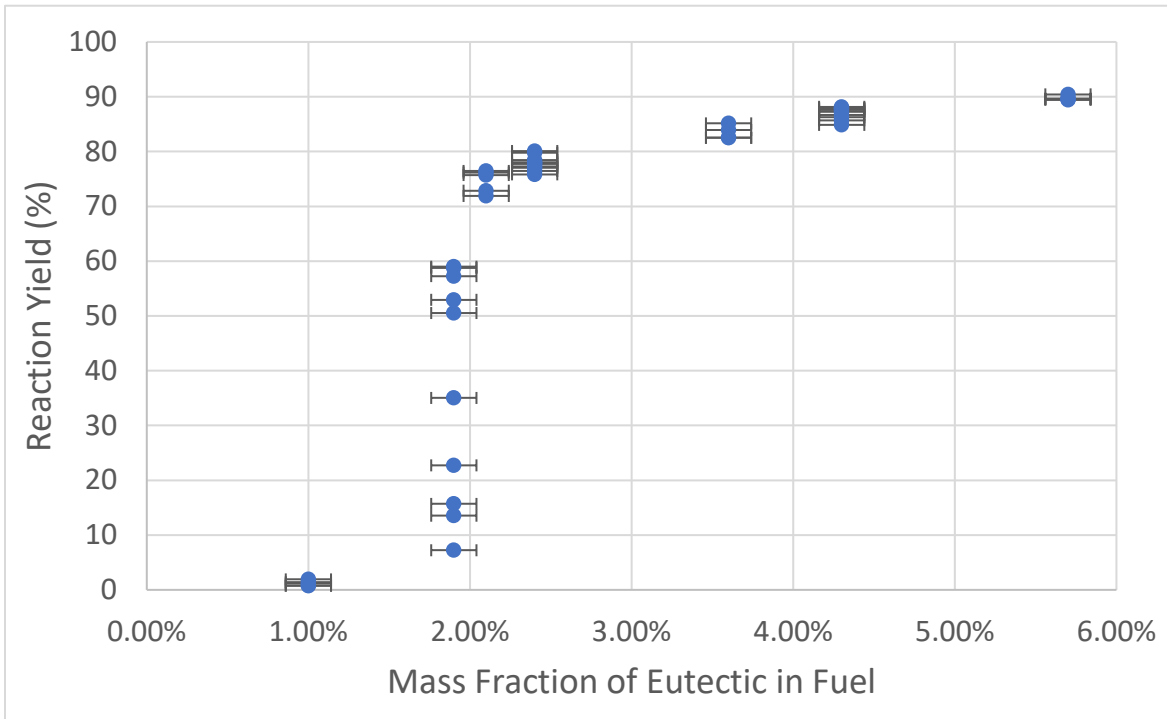
Figure 17: Plot of measured reaction completion for aluminum treated with different concentrations of eutectic. Error bars here represent 1 standard deviation.

3.4 Discussion and Conclusion

3.4.1 Surface Treatment Method

The new surface coating method proposed in this thesis was found to be an effective method for making large batches of consistent aluminum fuel using only small amounts of gallium and indium. The consistency of the fuel was measured and found to have a standard deviation of only 0.14% for spheres within a single batch, which is significantly

higher than what had been observed using the bath method [4]. No pitting was seen on the surface of the spheres, and the reaction yields within a single batch were highly consistent. Additionally, this surface treatment method gives the user the ability to finely select the desired concentration of eutectic used in each batch of fuel.

3.4.2 Eutectic Permeation Time

The eutectic permeation time for treatment of aluminum spheres was more finely characterized, at a necessary 48 hours for full permeation. While current attempts to decrease this time have failed, there has only been a slight exploration into possible options for minimizing the time needed to develop this fuel. Higher temperature surface treatment as well as longer heated surface treatment both proved ineffective in producing viable fuel in a shorter time, however, variations in several other properties have been shown to significantly impact aluminum reactivity and may allow for decreased permeation time. Foremost of these properties is the internal grain structure of the aluminum, which has been seen to significantly impact fuel viability [4]. Additionally, it is expected that variations in surface area to volume ratios for the aluminum may affect permeation rates of eutectic, as well as the presence of alloying elements which may impeded eutectic permeation through grain boundaries. A full investigation into the permeation rate of the gallium and indium eutectic would likely need to incorporate all of these properties and could have the potential to drastically decrease the time necessary to create an effective aluminum fuel using a surface treatment method.

3.4.3 Variation of Reaction Yield with Eutectic Concentration

The surface coating method for producing fuel batches with specific levels of eutectic absorption has allowed further characterization of the eutectic concentration requirements for this aluminum fuel. It was observed that a threshold concentration of eutectic exists,

below which the reaction yield of the aluminum will be negligible, but above which the reaction yield will be greater than 70%. The reaction yield was also seen to steadily increase from approximately 70%-95% as the eutectic concentration increased past the threshold.

It is likely that the exact values of this threshold concentration and reaction yields would vary when treating aluminum having different internal grain structures or containing varying alloying elements. However, it is expected that the trends observed, of a threshold concentration and of a positive yield correlation above said threshold, would still hold under most conditions. Regardless of whether the mechanism of action for the reaction is a dissolution of aluminum into liquid gallium, or an electrolytic reaction using indium as an anode [4], the observed trends are likely rooted in the mechanism of action, and therefore would hold true even with different forms of aluminum.

With the effects of eutectic concentration on net reaction yield more clearly understood, it is possible to use these results to optimize fuel production for various use cases. The net energy density and specific energy can be calculated for each variation of fuel discussed in this chapter, with the understanding that as the eutectic concentrations change from fuel to fuel, so will the fuel's net density, as well as its net reaction yield. Rather than using the standard energy density value of 83.8 MJ/l and specific energy value of 31 MJ/kg for aluminum, a more accurate effective energy density and effective specific energy can be determined. These are determined using Equations 8 and 9 , where the final mass fraction of aluminum is accounted for, as well as the predicted average reaction yield.

$$\frac{kg\ Aluminum}{1\ kg\ net\ fuel} \times \frac{31\ MJ}{1\ kg\ Aluminum} \times \%\ Reaction\ Yield = Effective\ Specific\ Energy \quad (8)$$

$$\frac{Liters\ Aluminum}{1\ Liter\ net\ fuel} \times \frac{83.8\ MJ}{1\ Liter\ Aluminum} \times \%\ Reaction\ Yield = Effective\ Energy\ Density \quad (9)$$
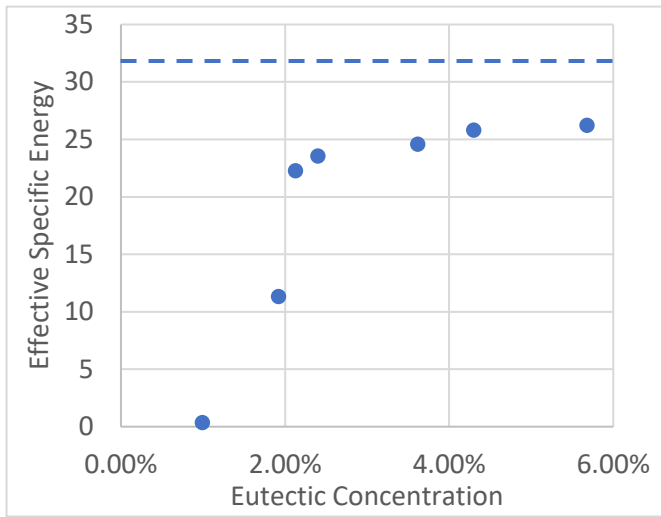
Figure 19: Plot of average effective specific energies for aluminum treated with different concentrations of eutectic. Dotted line indicates the specific energy of pure aluminum.
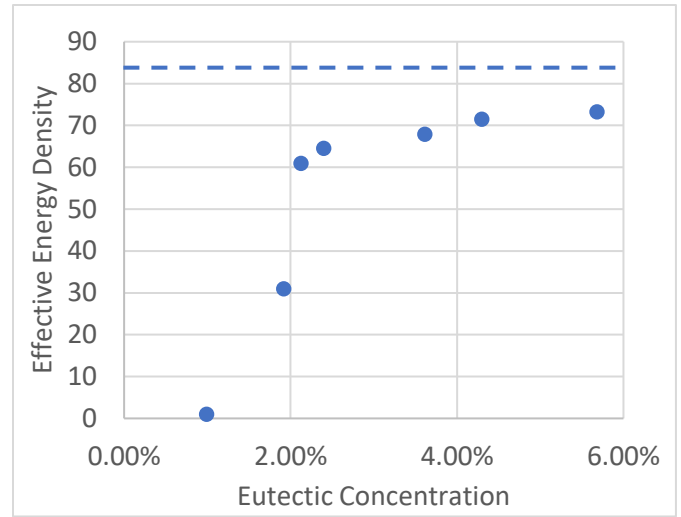
Figure 18: Plot of average effective energy densities for aluminum treated with different concentrations of eutectic. Dotted line indicates the energy density of pure aluminum.

As can be seen in Figure 19, the specific energy of the aluminum fuel increases as the mass fraction of eutectic increases. This increase has diminishing returns at higher values of eutectic for two reasons. The first is that the reaction yield does not increase greatly with increased eutectic beyond approximately 2% mass fractions, as has be shown in Figure 17. The second is that as the concentration of eutectic increases, the density of the net fuel increases, which lowers the effective specific energy. A similar trend can be seen when looking at the energy density of the fuel in Figure 18. This correlation shows slightly more increase in energy density at higher concentrations however, as compared to specific energy. This is because increasing the concentration of eutectic has very little effect on the net volume of the fuel[1] and therefore the only real correlation observed here is that of reaction yield versus eutectic concentration seen in Figure 17.

---

[1] The actual volume of the gallium and indium were used in these calculations. In actuality, for large blocks of fuel, the eutectic is believed to either dissolve the aluminum or occupy the otherwise vacant grain boundaries within the aluminum, and therefore may not take up additional volume beyond what would normally be taken up by the aluminum. This was not assumed however, because it is unknown if this is the case for fuels when ground up into powders or when suspended in liquid.

Additionally, the cost per kilogram and cost per liter of each fuel mixture can also be determined to allow for further use-case optimization. For these calculations, costs of $300/kg gallium [17], $500/kg indium [18], and $0.88/kg aluminum [19] were used.
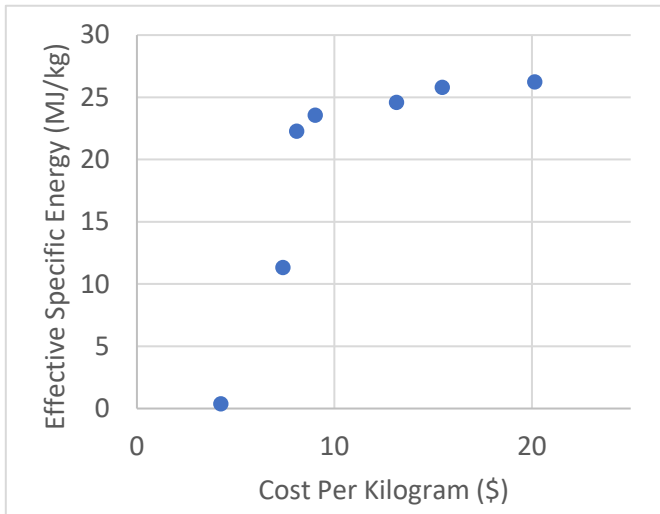
Figure 21: Plot of the effective specific energy of aluminum prepared for different costs. These costs each correlate to a different concentration of eutectic.
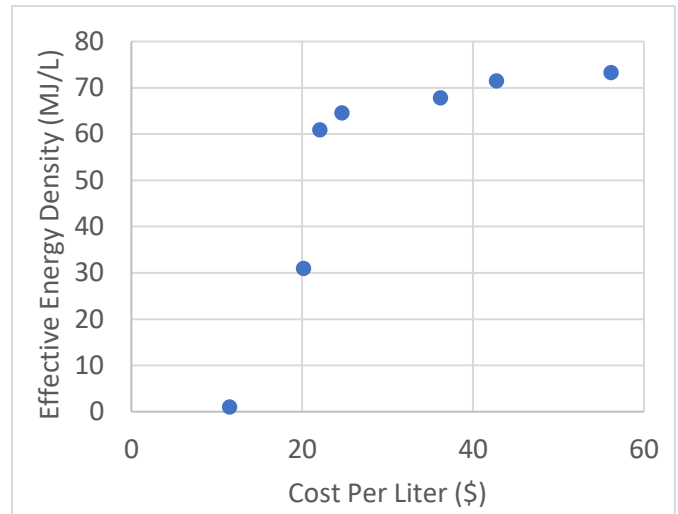
Figure 20: Plot of the effective energy density of aluminum prepared for different costs. These costs each correlate to a different concentration of eutectic.

Looking at both Figure 20 and Figure 21, a significant increase in cost is seen when attempting to increase the effective specific energy or effective energy density. This is because increasing either value necessitates the use of higher concentrations of eutectic. It is possible, however, that different forms of aluminum, perhaps with different internal grain structures, would be capable of achieving higher reaction yields and energy densities even with lower concentrations of eutectic. This could allow for cheaper and simpler fuel production while still retaining high levels of reactivity.

After determining the predicted cost for fuel made with varying concentrations of eutectic, the cost per kWh of energy can be determined as seen in Figure 22. As expected, fuel made with concentrations below the 1.9% concentration threshold needed for significant reaction would have an incredibly high cost per kWh. Above this threshold, the fuel reaches a minimum cost per kWh, because this is the regime where even a small increase in

eutectic concentration can significantly impact reaction yield. Beyond this point, the cost per kWh begins to increase, as the increased eutectic and increased cost has diminishing returns on the reaction completion.
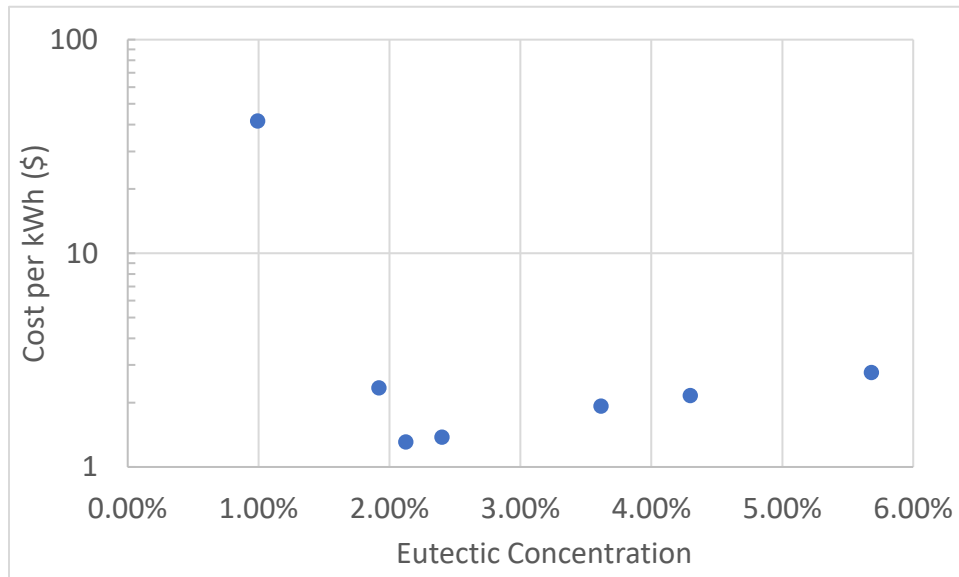
Figure 22: Plot of the expected cost per kWh of energy released for fuel made with varying concentrations of eutectic.

Notably, the eutectic is not actually consumed in the aluminum-water reaction and can be recovered and reused to treat new fuel. If such a recycling process were used, then the cost of the fuel would no longer scale with the cost of eutectic and the correlations shown in Figure 20, Figure 21, and Figure 22 would no longer exist. Instead, a fuel cost of simply $0.88/kg for aluminum, plus the cost of the recycling process, could be assumed.

4. DESIGN AND DEVELOPMENT OF AN ALUMINUM FUELED VEHICLE

With the aluminum-water reaction studied on a thermodynamic level, and the fuel production method further characterized, the next stage of development for this fuel was to prove its ability to generate electrical power. With that in mind, over the past year, the author, along with the help of several other students, designed and built an aluminum fueled vehicle. This vehicle was a BMW i3, that was successfully integrated with a 10 kW aluminum fueled power system, in order to charge the vehicle while driving. This was the first vehicle ever built of its kind, and the first demonstration of this aluminum fuel at power generation on this scale. While several generator systems had been built in the past using this aluminum fuel, they were limited in range from 50 W to 3 kW. The primary goal of this system was to demonstrate that not only could such a high-power system be made, but that the system could be fully contained and operated within the confines of a small vehicle.

This power system, referred to as the Sindri system, was designed to take the place of the BMW i3 range extender, which burns gasoline in a generator in order to recharge the battery of the car. Instead, the Sindri system uses an aluminum-water reaction to produce similar power levels and to extend the range of the vehicle by 50 miles. This was done by taking the hydrogen produced from an aluminum-water reaction and running it into two 5 kW PEM fuel cells. These fuel cells, in turn, generated electricity that could charge the battery of the car.

The Sindri system demonstrates that aluminum fuel is a viable power source for large scale, high power systems. These designs are not limited to a BMW i3 fitted with a fuel cell, but could be extended to a variety of high-power systems, such as underwater vehicles or emergency generators [20].

4.1   System Overview

The strategy of the Sindri charging system is to use an aluminum-water reaction in order to produce hydrogen. This hydrogen then flows into two 5 kW fuel cells which generate electricity to charge the BMW's battery. In order to successfully achieve this, keeping in mind safety requirements, stability requirements, and general equipment operating conditions, the full Sindri system was designed and implemented as outlined in Figure 23.
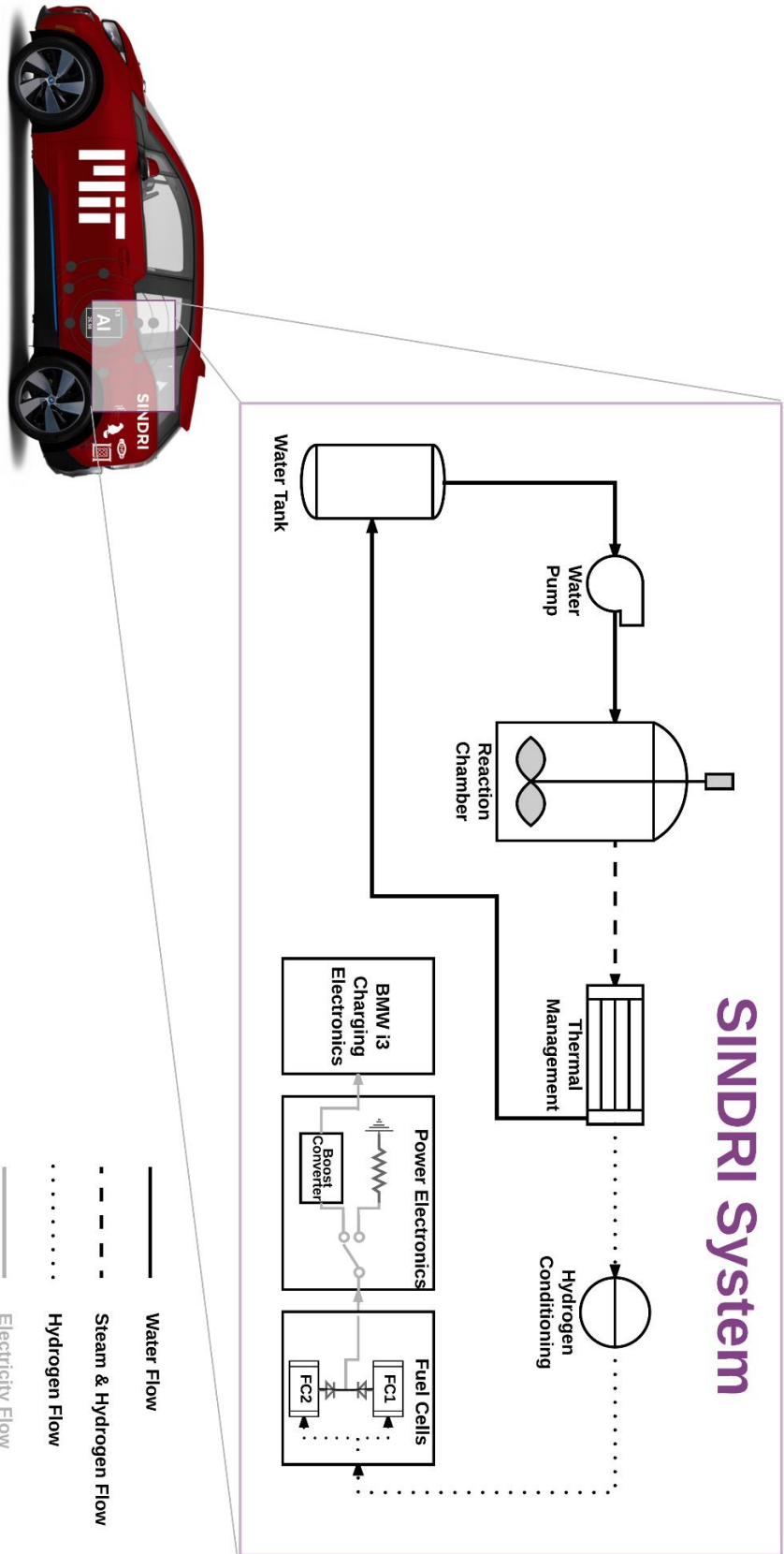
Figure 23: System diagram of the Sindri aluminum fueled BMW. [19]

The system begins by pumping water into a reaction chamber filled with aluminum fuel. When the water is added, a reaction begins, and hydrogen is produced. By controlling the rate of water addition, the reaction rate, and therefore the hydrogen production rate, can be controlled. In order to produce 10 kW of power from the fuel cells to power the BMW, the reaction chamber must produce a steady 120 slpm of hydrogen. This necessitates the reaction of 1.66 g/s of aluminum.

Due to the highly exothermic nature of the reaction, the gas exiting the reaction chamber is a mix of hydrogen and steam. This gas runs through two heat exchangers which condense the steam and drop the temperature of the remaining gas below a necessary 45 C. During this process, the thermal management subsystem dissipates 28 kW of heat and condenses 99.3% of the steam produced by the reaction and recycles it back into the system water tank. The remaining cooled hydrogen is then passed through an oxygen scrubber, desiccant, and pressure regulator. These ensure that the hydrogen is at the proper pressure level and 99.95% purity level required by the fuel cells.

At this point in the system the hydrogen is pure, cool, dry, and at the right pressure to be piped into the fuel cells to produce electricity. Within the fuel cells, the hydrogen delivered by the Sindri system is used in conjunction with oxygen from the outside air to produce electricity through an electrochemical reaction. Once this electricity is produced, the Power Electronics subsystem is then responsible for receiving electrical power at the voltage generated by the fuel cells and delivering it to the i3 battery at its proper charging voltage.

Throughout this process, a control subsystem is in place in order to monitor and control various elements of the Sindri system. This includes communicating with the relevant electronic components, reading from an array of sensors, and controlling various actuators. This control subsystem allows the system to maintain safe and efficient operating conditions at all times.

Finally, this entire system is integrated into the BMW. This system integration involves the installation and arrangement of all the various equipment within the i3 such that it is able to operate without compromising the safety of the car or driver, while still meeting the system's functional requirements.

4.2 Reactor Subsystem

The purpose of the reactor subsystem is to generate hydrogen by combining aluminum fuel and water. The reactor subsystem must be able to do this in a controlled manner, maintaining a relatively constant pressure and reaction rate of fuel and water. It must also incorporate safety features, as it contains a large pressure vessel filled with reactive material that can generating dangerous pressures if not properly controlled.

4.2.1 Fuel Generation

In an effort to lower the cost of aluminum used in this large-scale system, and to increase batch sizes, fuel production was attempted using cold rolled sheets of aluminum, as proposed by Slocum [4]. A 4'x2'x0.25" sheet of aluminum was cut into multiple strips which were each 4'x6"x0.25". These strips were then cold rolled in 0.015" increments until they reached a thickness of 0.18". After treating this aluminum in a bath of eutectic however, per the SOP found in Appendix 8.3, the aluminum had very poor levels of reaction completion. After consulting with Slocum, the following variations in testing were attempted:

-Making new eutectic with exactly 80% Gallium and 20% Indium.

-Cold rolling the aluminum in different thickness increments.

-Orienting the aluminum while it is being treated such that the surface of the eutectic bath was orthogonal to grains of the metal

-Letting all tests sit for a full week between being treated and being reacted.

While many of these tested versions of fuel were sufficiently embrittled to be hand-crushed using a pair of pliers, none showed high levels of reaction completion. Due to the time

constraints of this project, the exact reaction completion could not be measured as per Appendix 8.2, rather it was observed qualitatively. This reaction completion was observed by placing 0.3 grams of aluminum into 5 grams of distilled water and allowing the mixture to react to completion. For all testing variations described above, large chunks of aluminum were left over at the end of the reaction, which indicated very low levels of reaction completion. Eventually, it became necessary to abandon these attempts at creating fuel using cold rolled aluminum because the delays to fuel production were beginning to negatively impact the Sindri system timeline. The fuel production method then reverted to the original method of using aluminum spheres and surface treating them with eutectic as per Appendix 8.1. While it was not within the scope of this thesis, further research is needed on the use of cold rolled aluminum fuel and the limitations of using aluminum with varying internal grain structures to create effective aluminum fuel.

4.2.2 Subsystem Design

The reactor subsystem requirements are to provide the 120 slpm of hydrogen to the fuel cells that are necessary to generate the target 10 kW of power. The reactor subsystem also must maintain a local pressure of 15 to 20 psig in order to provide sufficient pressure to flow the hydrogen through the system and operate the fuel cells efficiently. Safety features include an automatic exhaust valve that opens at 30 psig and a passive relief valve that opens at 43 psig. The full design can be seen in Figure 24. Additionally, the reaction is run in a water limited fashion, where a water pump provides water to the reaction chamber as needed to produce the desired reaction rate. In the event of any failures or safety concerns water flow into the chamber is suspended, which will slow and eventually stop the reaction.
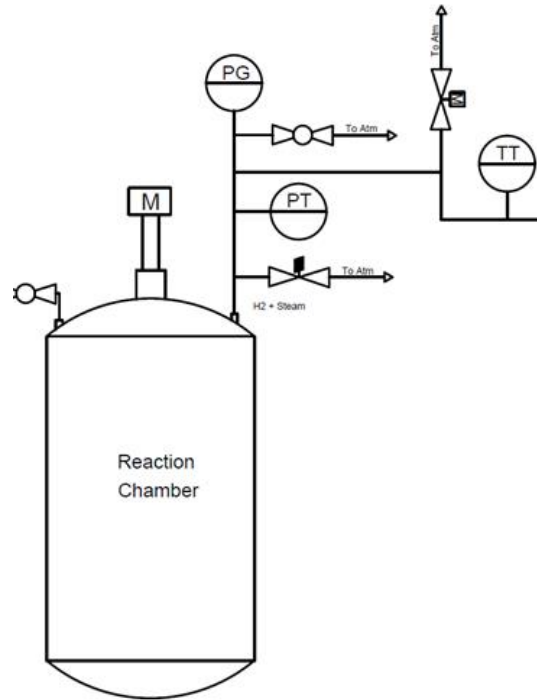
Figure 24: Diagram of the reaction chamber with mixer, digital pressure transducer, analogue pressure gauge, and multiple pressure relief valves.

Various control schemes were developed and tested to control the flow rate of water into the reaction chamber such that it maintains a constant pressure. Due to variability in system temperature, fuel reactivity, and oxyhydroxide buildup, the controls scheme needs to constantly monitor system pressure and adjust water flow rates during system operation. To ensure safety, testing was ramped up, starting with 50 g of fuel and stepping up incrementally to 500g in a smaller reaction chamber. Testing was then transitioned to the final system reaction chamber and ramped up further until the final testing size of 2 kg was reached. All testing was done with the approval of MIT EHS.

4.2.3 Subsystem Results

After significant time testing and adjusting gains, the final control scheme used was an integral derivative controller, seen in Equation 10.

$$FlowRate = 0.6 \frac{l}{min} + 300 * \frac{DeltaError}{second} + 8x10^{-6} * \sum TotalErrorsSinceStart \quad (10)$$

This set of variables and gains were found to produce a stable reaction rate that fell within the range needed for the Sindri system. During the final system test while operating at 120 slpm, the control scheme worked successfully to maintain a steady reaction as can be seen in Figure 25. Notably, this controller with these exact gains is limited to this system setup. If the reaction chamber geometry, mixer geometry, or fuel volatility were to change, the gains used here would be unlikely to stabilize the reaction.
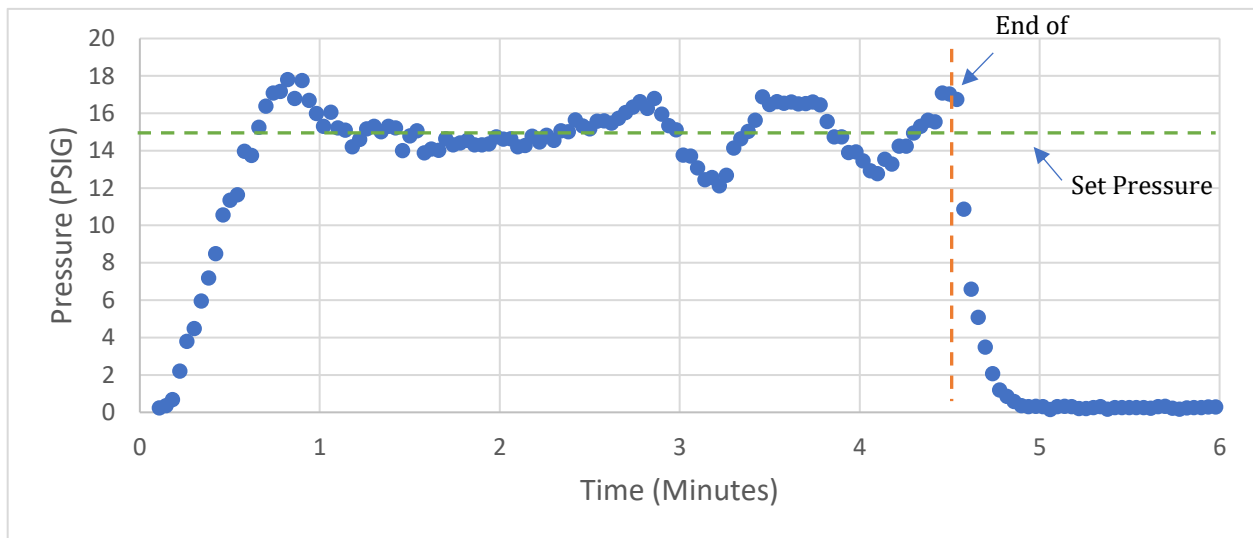
Figure 25: Pressure profile over time of final reaction test while system was operating and generating 7.5 kW of power. The controller maintains stable pressure control about the set operating pressure until end of test.

4.2.4 Subsystem Conclusions

The controlled, continuous reaction of solid aluminum with water is a difficult challenge for the future of this technology. This is primarily due to limitations inherent in using solid fuel, such as difficult metering properties and poor mixing capabilities as compared to liquids. Because the fuel is a solid and cannot be pumped, the reaction must utilize a batch reaction method which requires a single large reaction chamber that contains all of the

aluminum fuel and all of the eventual waste build up. This reaction chamber must therefore be rather large, heavy, and can become difficult to empty and refill between batches. Additionally, the fuel must be mixed thoroughly as the water is being added to the reaction chamber to ensure that the water can reach new fuel and does not get blocked by built up oxyhydroxide. Finally, a complex control scheme had to be developed in order to successfully control the solid fuel reaction and produce a continuous hydrogen output. While the control scheme developed in the Sindri system was, in fact, successful in controlling the hydrogen production rate and maintaining a stable pressure, this was only achieved after weeks of testing and would be difficult to adapt to other systems.

The use of a liquid aluminum fuel would solve many of these issues. A liquid fuel could easily be pumped into and out of the system and would therefore not require a reaction chamber large enough to fit all of the fuel being used. Additionally, the fuel could simply be pumped simultaneously with water into a single tube to allow for a mixed, steady, reaction to take place as it moves down the tube as described further in Section 5.7. In this scenario, the flow rate of both aluminum and water into the tube would both control the reaction, further ensuring a stable reaction rate. Finally, with the use of a continuous plug flow reactor, the reaction waste could be continuously pumped out of the reaction chamber and stored in an outside container to facilitate cleaning and refueling. The use of liquid fuel would therefore allow for smaller, lighter, reaction chambers, easier control of hydrogen output, and simpler system refueling.

4.3 Thermal Management and Hydrogen Conditioning Subsystems

Once the reactor subsystem produced the necessary 120 slpm of hydrogen, the gas must then be purified to 99.95% purity and cooled to below 45 C before entering into the fuel cells. To do this, a thermal management subsystem as well as a hydrogen conditioning subsystem were designed and implemented. The thermal management subsystem was responsible for cooling the hydrogen to below 45 C and thus condensing a large amount of the steam which is initially mixed with the hydrogen on the outlet of the reaction chamber.

The hydrogen conditioning subsystem was responsible for purifying the hydrogen and dropping its pressure to the required range of 0.45-0.55 barg.

4.3.1 Thermal Management

The aluminum-water reaction is highly exothermic, releasing 15 kJ of heat energy per gram of aluminum reacted. This means that during standard operation of the car, the reaction chamber will be not only generating hydrogen, but will also be generating approximately 28 kW of heat. This heat primarily goes into vaporizing water from the reaction into steam, causing the output gas from the reaction chamber to be a mix of both hydrogen and high temperature steam. The thermal management system must safely dissipate this heat outside of the vehicle without allowing the cabin temperature to exceed 35 C at which point it would be a safety hazard for the driver. Additionally, the steam produced must be condensed and recycled back into the system in order to reduce the necessary amount of water consumed by the system.

In order to dissipate such high levels of heat in the small enclosed space of the BMW i3, a two-stage cooling system was designed. This two-stage system consisted of two sets of heat exchangers and two sets of water traps for the condensed water. This layout, as shown in Figure 26, allowed for 94% of the steam to be condensed and separated out of the gas stream after the first high temperature radiator. This water represents the large majority of the thermal mass of the gas, and with it removed it ensures that the subsequent low-temperature heat exchanger is capable of lowering the temperature of the remaining hydrogen to below 45 C. An additional benefit of this two-stage configuration is that the radiator and heat exchangers are being used more efficiently. Assuming the radiator is being cooled by ambient air, the hotter that the fluid being cooled is, the higher the heat transfer rate that will be achieved across the radiator. If all of the steam and hydrogen were to be cooled to 45 C, then a large portion of the cooling would take place at lower temperatures and be highly inefficient. However, because the majority of the thermal mass

of the system is only being cooled to approximately 85 C in heat exchanger 1, then the majority of the system cooling is occurring in a more efficient regime.
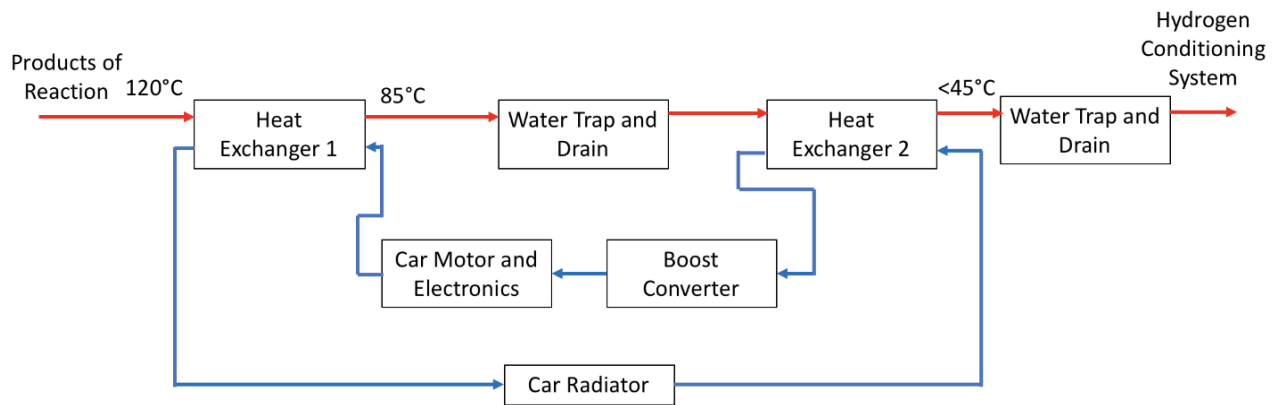
Figure 26: Diagram of the Sindri thermal management subsystem.

This thermal management system was successfully implemented and integrated into the BMW i3. The heat exchangers were connected to the internal coolant loop of the car, and the temperature of the coolant fluid was monitored during operation to ensure that no systems were overheating. Additionally, the output gas was, in fact, always kept below 45 C, and the water was successfully condensed and recycled back into the reactor subsystem.

4.3.2 Hydrogen Conditioning

Once successfully cooled by the thermal management subsystem, two primary contaminants must be removed from the gas before it is at the 99.95% purity needed by the PEM fuel cells. These contaminants are oxygen, and residual water vapor. The oxygen originates as a dissolved gas in the water used for the reaction that is released when boiled, totaling approximately 40 ppm. The water vapor is simply the residual water vapor present in air that has only been cooled to a dew point of 45 C.

Within the hydrogen conditioning subsystem, the gas flows into an oxygen scrubber to remove the expected 40 ppm oxygen from the hydrogen stream, a desiccant dryer to

reduce the water content to 128 ppm, and a pressure regulator to ensure that the output stream is between 0.45 and 0.55 bar. This pressure range is the acceptable range specified for the Horizon fuel cells used to ensure proper fuel cell operation. Upon exiting the hydrogen conditioning system, the hydrogen gas stream splits into two lines that go directly into the fuel cells. A diagram of the hydrogen conditioning system can be seen in Figure 27.
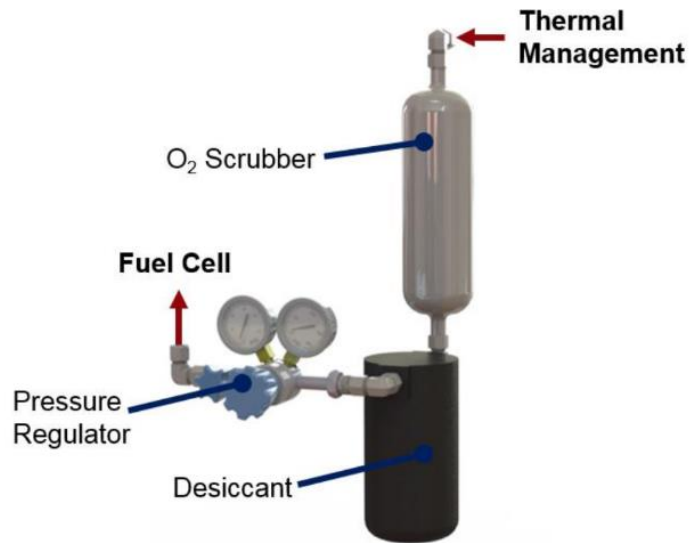
Figure 27: Layout of the Sindri hydrogen conditioning subsystem.

4.3.3 Subsystem Conclusions

By incorporating a two-stage cooling system, the car's coolant loop was sufficient to dissipate the 28 kW of heat given off by the aluminum-water reaction. Additionally, with careful analysis of contaminants and use of proper filters, the hydrogen was purified to the 99.95% purity level necessitated by the fuel cells.

This Sindri system was a proof of concept system that generated power exclusively through the use of PEM fuel cells. In future systems, however, much higher levels of efficiency can be achieved if the systems were to utilize the large fraction of waste heat that is produced

by the reaction. This subsystem alone dissipated 28 kW of heat, and the fuel cells, which work at 40% efficiency, dissipate an additional 15 kW of heat. This means that the entire Sindri system operates at only 20% efficiency. Additionally, while PEM fuel cells are relatively efficient, they are also expensive, fragile to mechanical shock, and must be run off of hydrogen at very high purity. This necessitated the use of additional ancillary equipment for hydrogen purification and shock absorption. In future work, the use of an engine in place of a fuel cell may solve many of these issues. The hydrogen and steam produced by this reaction can both be fed into a combustion engine directly, allowing for a simple, highly efficient system, as further outlined in Section 6.2.

4.4   Final System Performance

The Sindri system successfully operated at high power and in its initial phase of testing reached a power output as high as 7.5 kW. This power level was limited slightly below 10 kW in practice because the fuel cells had not been used in several months and require several hours of operation after such a break in order to resume operation at peak power. The fuel available during testing only allowed for the operation of the system for approximately an hour, during which time the output power steadily increased from 4kW to 7.5 kW. The limited fuel supply therefore necessitated the end of testing before the full 10 kW could be reached.

During system operation, the entire system was structurally mounted into hard points of the car designated as acceptable by BMW engineers, and laid out as shown in Figure 28. Additionally, the coolant system was completely integrated into the car's cooling loop and maintained the car cabin temperature below the designated 35 C during operation. Finally, the system was largely electrically integrated into the car with one exception due to a component failure. The low-power components in the Sindri system, such as pumps and sensors, all successfully drew power from the BMW's internal 12 V power line. The high-powered fuel cells, however, were unable to connect directly to the battery of the car because the boost converter, used to ensure compatible voltage between the fuel cells and

battery, malfunctioned. During testing, power was still generated within the BMW and was simply dissipated over large resistors rather than being used to recharge the vehicle. As of the date of this thesis submission, the vehicle is completed and on display at the Office of Naval Research in Maryland.
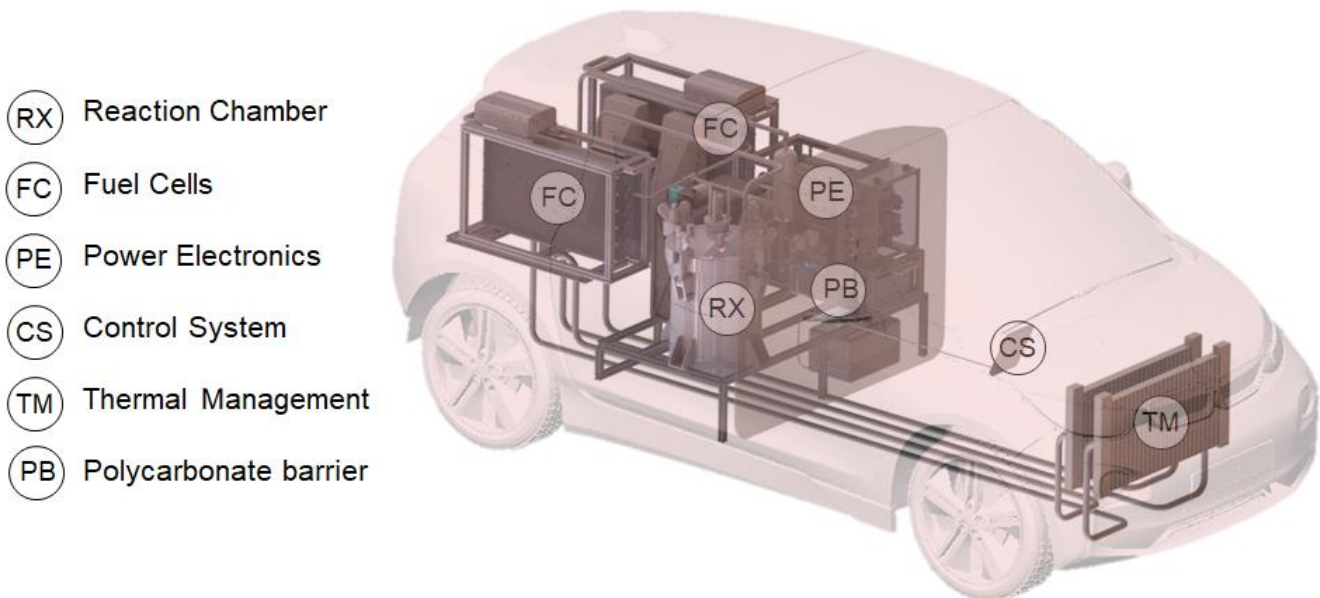
Figure 28: Labeled CAD showing the final layout of components within the BMW.

4.5 Future Work

The Sindri system was developed as a proof of concept to demonstrate the capability of this aluminum fuel to be used as a power source for large scale systems. The Sindri system was successful in doing so and demonstrated its capability to generate power on the scale of 10 kW and to operate self-contained within a small working environment. As this was the first system of its kind to be built, there were certainly challenges that arose and lessons learned along the way. Each of these challenges opens new doors to improvements and future work that can be done to make aluminum fueled systems more viable and more successful in years to come.

Fuel from stock aluminum:

As discussed in section 4.2.1, significant challenges were met when attempting to make effective fuel out of large aluminum plates, rather than the spheres that have been used for past testing. The development of such a capability is critical to the use of this fuel in industrial applications, because without the capability of making effective fuel out of low cost, bulk, aluminum, the use of this fuel would likely be cost prohibitive.

Liquid aluminum fuel

The use of solid fuels poses many practical challenges when designing large systems, foremost among which is the need for a large reaction chamber to perform batch reactions. With the use of a new liquid aluminum fuel as described in Section 5, this reaction chamber can be eliminated and replaced with much smaller storage tanks and a continuous tube reactor as shown in Figure 29. Additionally, liquid fuel is pumpable and would allow for simpler, safer, methods for controlling the reaction rate.

Steam-Hydrogen Internal Combustion Engine

PEM fuel cells are simple and high efficiency, making them ideal for use in the Sindri proof of concept system. For future systems however, the use of an internal combustion engine would be significantly smaller, cheaper, and would require no additional gas purification equipment, as can be seen in Figure 29. Additionally, using a theoretical steam-hydrogen engine cycle as proposed in Section 6, an engine could take advantage of the significant heat energy produced by this reaction and operate at total system efficiencies as high as 33%.
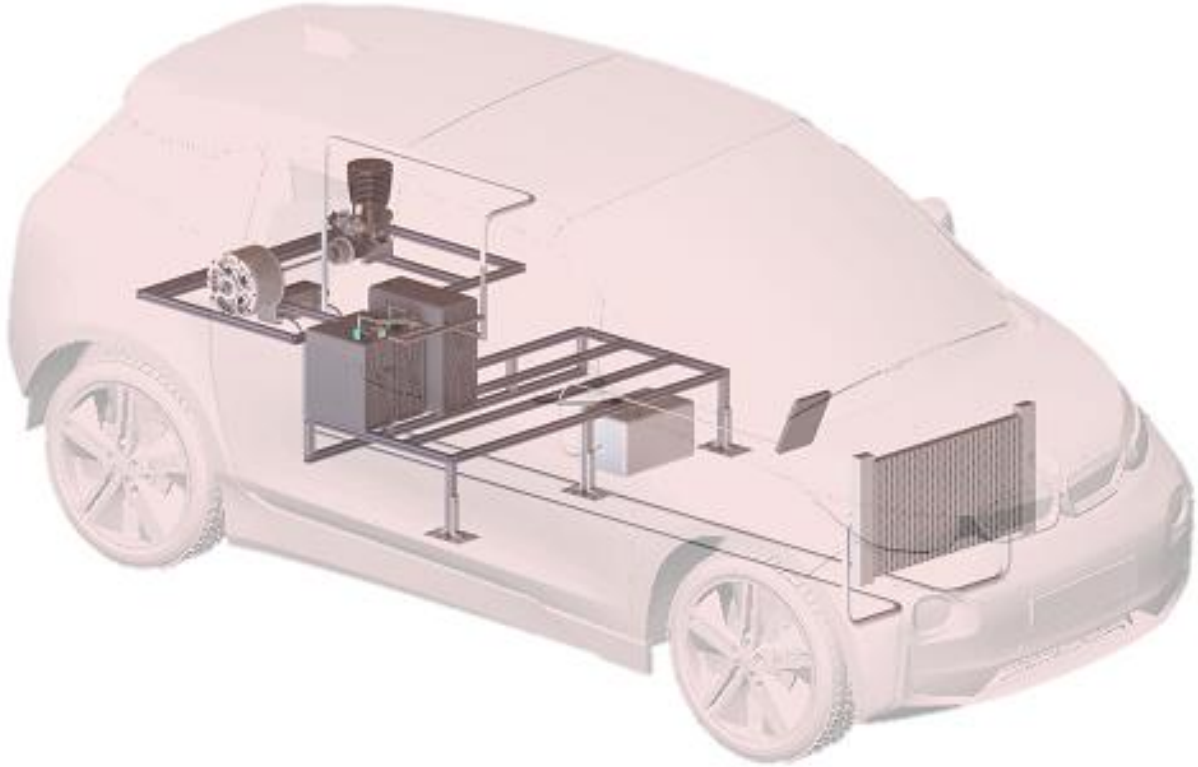
Figure 29: CAD model depicting the layout of a future aluminum fueled vehicle system. A liquid fuel reaction chamber is used to produce hydrogen, and an internal combustion engine is used to generate electricity, greatly simplifying the system.

5. DEVELOPMENT AND CHARACTERIZATION OF A LIQUID ALUMINUM FUEL

Working with solid aluminum fuel proved to be a significant challenge in the design and implementation of the Sindri system. Because solid fuels cannot easily be pumped through a system, the hydrogen generation systems that utilize this aluminum fuel have thus far been exclusively batch reactors. These systems require all of the fuel for the entire operation time to be held within a single, large, reaction chamber. This reaction chamber must also be large enough to fit all added water and waste buildup, greatly increasing its volume. If these systems are run at elevated temperatures and pressures, as is often the case, then the reaction chambers used also become quite heavy, because they need to be made from materials strong enough to maintain structural stability under these conditions. The reaction chamber employed in the Sindri system, for example, weighed as much as 65 kg when full, making it exceedingly difficult to unload, clean, and refill. Additionally, the use of batch reactors greatly increases the difficulty of the reaction control. This is because the large volumes of aluminum and oxyhydroxide buildup within a system make it difficult for the water to permeate evenly and for the reaction to occur at a uniform rate. Even with the incorporation of a large mixer into the system, it was clear that oxyhydroxide buildup within the system was slowing the reaction rate over time.

All of these challenges associated with solid fuel can be solved with the use of liquid fuel in a continuous plug flow reactor. This necessitated the development of a liquid aluminum

fuel that can be easily pumped and that maintains its high levels of reactivity with water. This was done by suspending high concentrations of small aluminum particles in viscous mineral oil. This oil-aluminum mix can be pumped easily through a system, and still reacts effectively with water.

5.1   Principles of Operation

As demonstrated by Hopkins [21], aluminum has natural oleophobic properties that allow it to preferentially wet to water rather than oil. This allows for the suspension of aluminum in oil without hindering its ability to react with water. When the aluminum-oil mix comes into contact with water, the oil that covers the aluminum particles will simply bead-up and separate off of the aluminum, making way for the water. This allows for a reaction to proceed, as demonstrated in Figure 30.
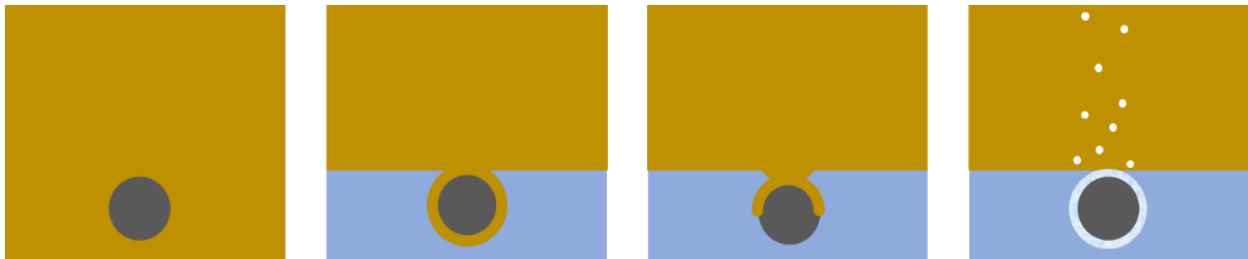
Figure 30: Graphic depicting the progression of oil separating off of aluminum in the presence of water. From left to right: aluminum sits in oil, water is added and oil remains on the surface of the aluminum, oil begins to bead up as water preferentially wets to the aluminum, water begins to react with the aluminum.

When attempting the suspension of dense particles, such as aluminum, in oil, there will be a natural tendency for these particles to fall out of suspension due to their density being greater than that of the carrier oil. The rate at which the particles will fall out of suspension can be generally calculated using Equation 11, which determines the terminal velocity of spheres through a fluid that is exhibiting creeping flow.

$$V_t = \frac{g * d^2}{18 * \mu} * (\rho_s - \rho)$$
(11)

Where V_t is the terminal velocity of the sphere, d is the diameter of the sphere, g is the acceleration due to gravity, μ is the viscosity of the liquid, and ρ and $ρ_s$ are the densities of the fluid and sphere respectively. Each of these variables can then be tuned with the objective of lowering a particle's terminal velocity, and thus increasing a particle's settling time. While g, ρ, and $ρ_s$ are relatively unchangeable, because aluminum has a set density and the density of commercial oils has only slight variability, both d and μ can be tailored to produce a slower terminal velocity.

Ideally, the diameter of the aluminum particles would be as small as possible in order to increase their settling time. In practice, however, the smaller that aluminum particles are ground, the more of a combustion hazard they become [8]. When making this liquid fuel, as described further in Section 5.2, the aluminum is ground into a powder, and then mixed into oil. Combustion is not a concern for the particles once they are suspended in oil, because they can no longer come into contact with oxygen. In the initial stages of being ground into powder however, there is still a serious combustion risk for small aluminum particles. This risk increases significantly as the particles become smaller than 100 μm in diameter, and thus, particles of this size were avoided [8]. For this reason, particles in this fuel were sieved to 200 μm, so that they can be as small as possible while still maintaining a low combustion risk during fuel production.

The viscosity of the oil can also be increased in order to decrease the terminal velocity of the particles. Increasing fluid viscosity, however, will also increase the pressure needed to pump the fluid through a tube. This trade-off is problematic, because low pumping losses, and long fuel shelf-life are both critical functional requirements for an effective liquid fuel. While several techniques were attempted to suspend the particles without increasing the fluid viscosity, such as using surfactants, the most successful was to make the oil shear-thinning. This meant that the oil would exhibit high viscosity under low shear rates, i.e. at rest, and would exhibit much lower viscosity under high shear rates, i.e. while being pumped. This allowed for a fuel that maintained a very long settling time, without necessitating large pumping losses.

5.2 Liquid Fuel Production Methods

The aluminum used for this fuel was activated using the surface treatment method described in Appendix 8.1. This fuel was then ground into powder using a grain mill, and the resulting powder was sieved, allowing only particles smaller than 200 μm to pass through and be used for the liquid fuel. This grinding was done in the presence of argon, and all work involving aluminum powder was done in a fume hood while wearing a face mask for safety. This 200 μm limit was chosen as it was the minimum size that was believed to be safe for grinding without risking combustion of the aluminum powder. The blades of the grain mill were also checked regularly to ensure that they exhibited no embrittlement or fracture. All powders ground for these tests were then stored in airtight containers that had been filled with argon gas.

Notably, the fuel was ground dry and then only later mixed with oil. This is because the grain mills used were unable to grind wet substances. If a different form of grinder could be utilized, such as a colloidal grinder, then it may be possible to grind the aluminum while it is already mixed with oil. This would mean that the aluminum powder was coated in oil at all times and would greatly reduce any inhalation hazards or risks of combustion that are associated with working with dry aluminum powders.

Initial observations of aluminum powder mixed into pure oil showed settling times of only a few minutes. This was seen for both silicone oil as well as mineral oil, even with viscosities as high as 1000 cst. Various methods were then attempted to increase this settling time. Surfactants and thickeners, such as xanthan gum, glycerol monostearate, and lecithin, were briefly explored, before settling on fumed silica, as it was seen to have the best results in initial tests. Fumed silica (FS) is a commercially available polymer that acts as a thickener and also creates shear thinning properties in a liquid when mixed into it. This occurs because the FS is a polymer chain that interlocks with other FS polymer chains when at rest creating a viscous fluid. When under shear, these chains straighten out and can easily slide past each other, allowing the liquid to flow more easily [22].

The fumed silica used in these tests was acquired from Aerosil and has several other advantageous properties as well. Aerosil fumed silica is advertised as an anti-settling agent, and as a free flow and anticaking agent. These properties are achieved by the distribution of FS particles around any suspended particles. The FS then forms a sort of shell around the particles, keeping them from clumping together as seen in Figure 31. The thickening properties, and anti-clumping properties of FS combine to make it the ideal additive for this application. FS can also be made in both hydrophobic and hydrophilic forms. Hydrophobic FS was used for these tests so that it would disperse well in the oil and so that it would separate easily from any water.
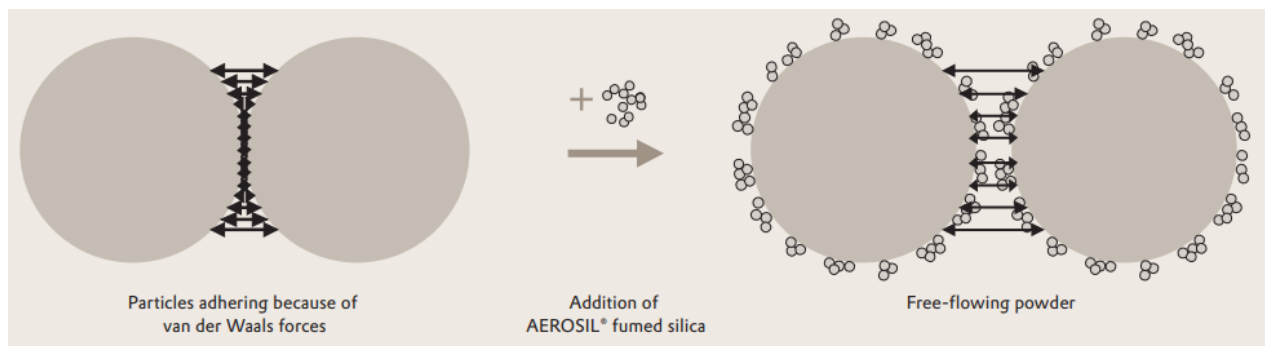
Figure 31: Visualization of fumed silica working to reduce particle clumping [7].

When preparing oil samples for testing, the proper masses of fumed silica and oil were carefully added to a jar and mixed lightly. This mixture was then brought to a high shear rate mixer where the liquid was mixed at 2000 rpm with a peripheral velocity of 4 m/s, for 3-5 minutes until the liquid was seen to become uniform. This mixing process was followed for all samples, as advised by the FS manufacturing corporation, Aerosil [23]. Once the oil-FS mixture was prepared, the desired mass of aluminum powder was then poured into the oil, and the two were mixed carefully until a homogenous suspension was observed.

Initial testing was done using silicone oil as the carrier fluid, however the viscosity of this oil was seen to degrade over time when mixed with FS. This effect has also been observed by Selimovic et al. [24]. For all later tests, and all data presented below, Light Mineral Oil supplied by W.S. Dodge Oil Co. Inc. was used as the carrier fluid. This mineral oil showed no

degradation to its viscosity over time and produced stable liquid aluminum fuel. The FS used in all tests was Aerosil R812 unless otherwise noted.

5.3   Rheology Testing

A rheometer was used to perform several sets of tests in order to characterize how different changes to the fuel's composition impacted its final viscosity. These changes include varied mass fractions of FS, varied mass fractions of aluminum, and changes in system temperature. For each of these tests, a rheometer was used to determine the viscosity of the liquid across a wide range of shear rates in order to understand how it would behave both at rest, and while being pumped. All tests were done on an AR G2 rheometer, and each test was done at least twice to ensure consistency and reduce sampling error.

5.3.1 Varied Mass Fractions of Fumed Silica

Four different mineral oil samples were prepared, each with different mass fractions of fumed silica added. These mass fractions were 0%, 4%, 6%, and 8%. The viscosities of these samples were then measured on a rheometer across a wide range of shear rates, and the results can be found in Figure 32. It is important to note that this set of testing was done before any aluminum had been added to the sample, in order to observe only the effects of the fumed silica on the oil.
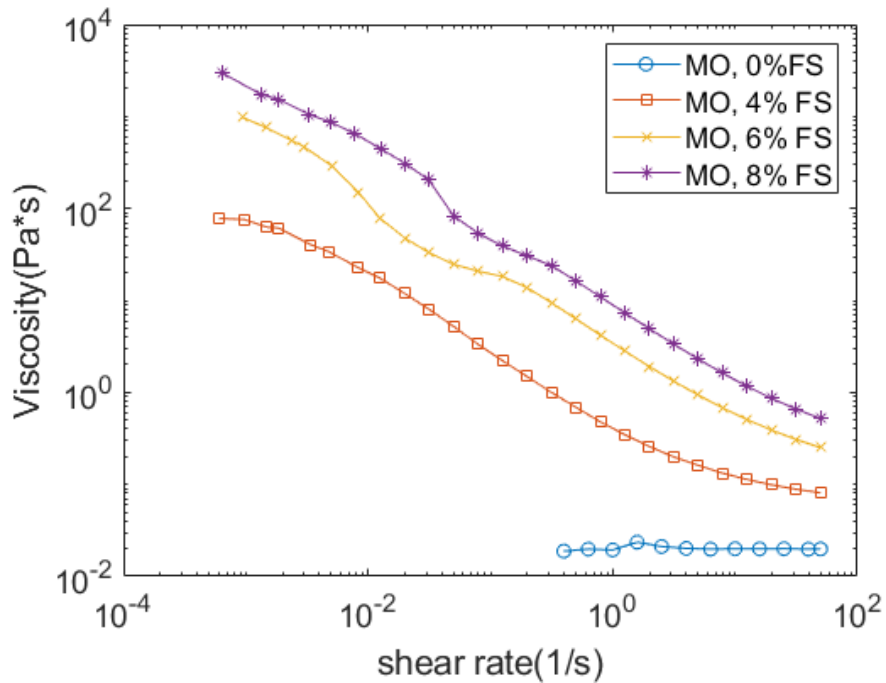
Figure 32: Plot of mineral oil viscosity as a function of shear rate. This was measured for mineral oil mixtures with 0%, 4%, 6%, and 8% mass fractions of fumed silica

As seen in Figure 32, the addition of fumed silica has a rather drastic effect on the viscosity of the oil. Additionally, the viscosity of the oil-FS mixture is linear when plotted against shear rate on a log-log curve. This means that the liquid fits a standard shear thinning profile that can be generalized by a power-law fluid as shown in Equation 12. In this equation, μ_{eff} is the liquids effective viscosity, γ is the applied shear rate, and K and n are empirically determined constants. Of course, this expression only represents an idealized fluid, as it would require an infinite viscosity as the shear rate decreased to zero, which is unachievable by of any fluid. This relationship, therefore, only holds true within a moderate range of shear rates and will taper off at particularly high or low shear rates as seen clearly in the 4% FS sample shown in Figure 32.

$$\mu_{ef} = K * (\gamma)^{n-1} \tag{12}$$

5.3.2 Varied Aluminum Concentration

As aluminum is added to the oil mixture, the final fluid viscosity will also increase. This is due to the fact that particles in suspension act as obstacles to one another during flow [25]. This effect was considered during the development of a liquid aluminum fuel because it meant that the final fuel mixture will be of significantly higher viscosity than the originally measured oil-FS mixture. This increase in viscosity was, in fact, seen when adding large mass fractions of aluminum particles to the carrier fluid, as shown in Figure 33.
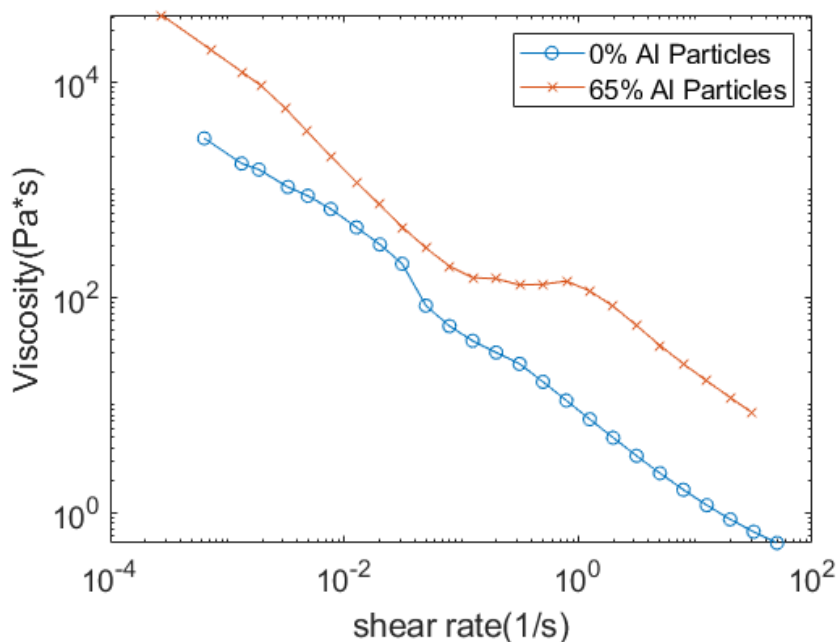
Figure 33: Plot of measure viscosity as a function of shear rate for two samples. The first is a mixture of mineral oil with 8% FS by mass, with no aluminum. The second is that same fluid mixture after adding sufficient aluminum particles such that the final mixture was 65% aluminum by mass.

5.3.3 Varied Temperature

It is common for liquids to become less viscous and to exhibit decreased surface tension when heated [26], therefore, testing was done to determine the effects of increased temperature on the viscosity of the liquid fuel. Use cases for this fuel can range across a

broad range of steady state environments, from deep ocean to deserts, and it is critical to ensure that the fuel would not degrade or have the aluminum fall out of suspension under any of these conditions. For this reason, viscosity tests were done at 7 C[1], 25 C, and 45 C, to observe the any changes that may occur. In each of these tests, the fuel mixture used was a mixture that was 32.2% Mineral oil, 2.8% FS[2], and 65% aluminum powder, by mass. The first, low temperature test was done where fuel was initially measured at a baseline of 25 C, then measured at 7 C, then brought back to 25 C and measured again. The elevated temperature test was similarly measured at a baseline of 25 C, then measured at 45 C, and again brought back to 25 C and measured. This measurement before and after the thermal change was done in order to ensure that no permanent degradation occurred during the change in temperature. The results of these tests can be seen in Figure 34 and Figure 35.
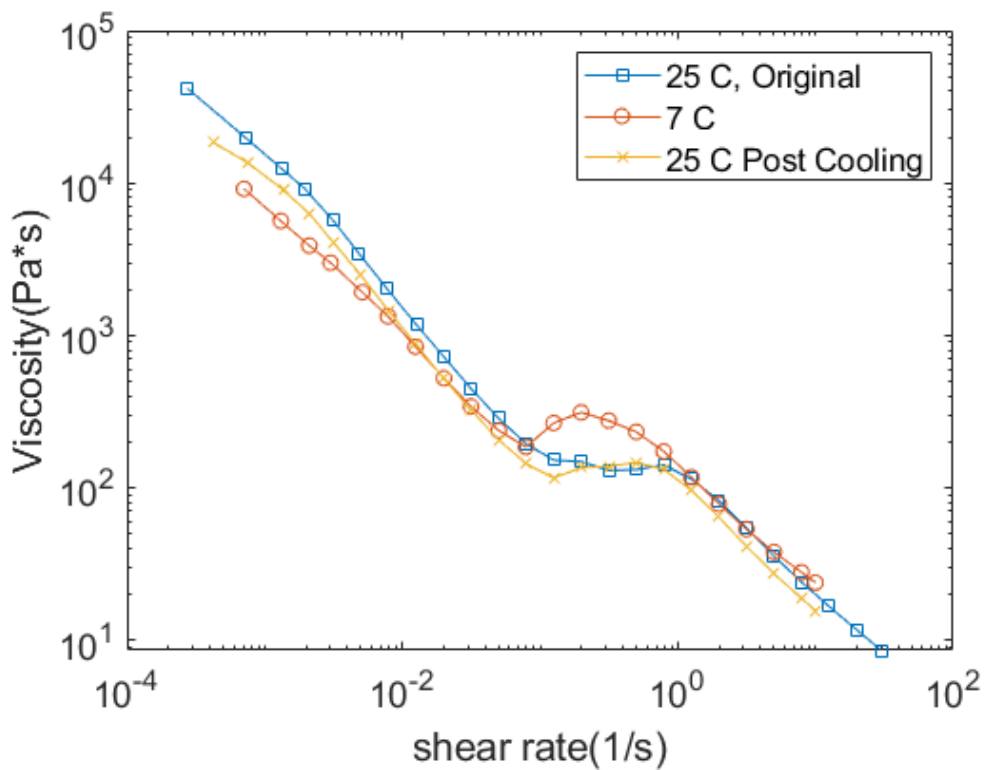
Figure 34: Plot of liquid fuel viscosity as a function of shear rate. This was measured for a suspension of aluminum powder in mineral oil and fumed silica at varying temperatures to determine the effect of low temperature on the liquid's viscosity

---

[1] Ideally test would be conducted at temperatures as low as 3 C, because that is average temperature of the deep ocean, however the cooling capabilities of the rheometer used only allowed for tests as low as 7 C.
[2] This corresponds to a carrier fluid mixture that was originally 92% Mineral Oil and 8% FS, as characterized in Figure 32
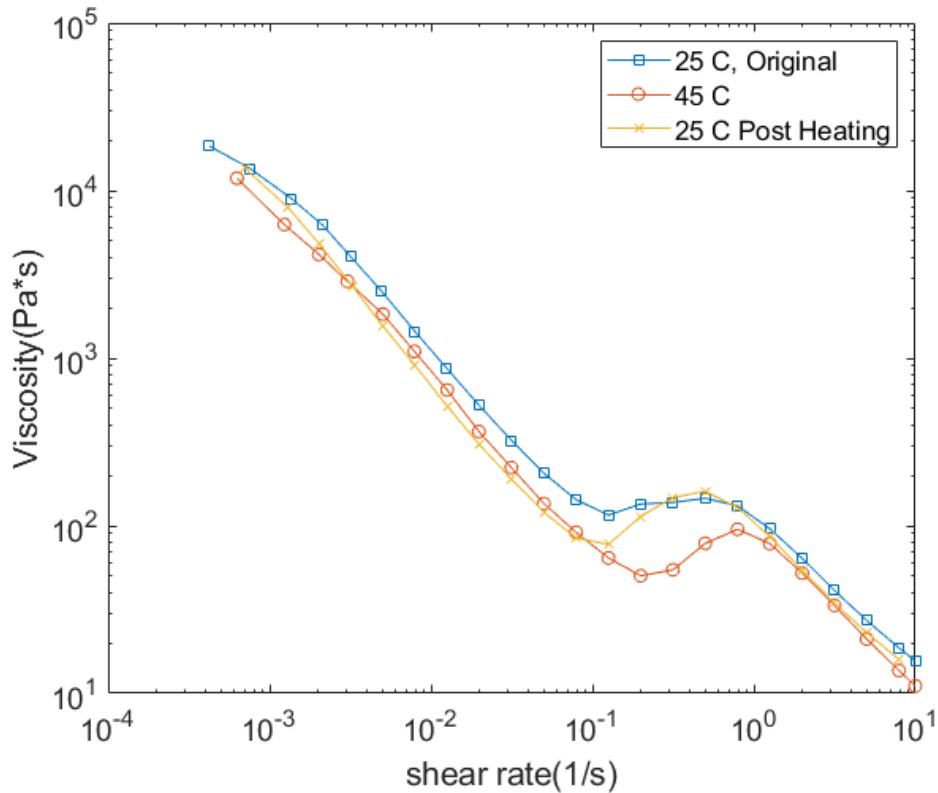
Figure 35: Plot of liquid fuel viscosity as a function of shear rate. This was measured for a suspension of aluminum powder in mineral oil and fumed silica at varying temperatures to determine the effect of high temperature on the liquid's viscosity

In both sets of temperature variation test, the observed changes in viscosity were incredibly low over the temperature ranges tested here. These variations were so low, in fact, that it is likely that any variation between the original and final 25 C tests observed here was due to the expected rheometer error. Additionally, several samples exhibited a viscosity peak at a shear rate of approximately 0.5. The cause for this is as of yet unknown, however, it may have been due to samples slipping slightly relative the rheometer as its rotational speed began to increase significantly and the fluid experienced a transition in flow regimes.

This lack of significant temperature dependence within a standard operating range is expected, as the mineral oil used is safe for long term storage in temperatures as high as 49 C [27], and the FS provided by Aerosil only begins to degrade at temperatures as high as 300 C [22].

5.3.4 Settling Time

It is critical that the liquid aluminum fuel have a long settling time so that the fuel can maintain a long shelf life and will not clog while flowing through a system. Initial attempts to calculate the settling time of the aluminum particles in thickened oil employed physics-based fluid models. These attempts were done using equations put forth by Chhabra et al. [28] [29] for the expected shear rate of a power-law fluid over a sphere. These equations however, assume that the fluid maintains ideal shear thinning properties even at incredibly low shear rates, which is not the case for the samples discussed here. This theoretical analysis therefore resulted in expected settling times much higher than what is actually observed. Additionally, the standard settling time analyses found in literature were not seen to address suspensions with such high-volume concentrations that particle to particle interactions become significant, nor were they found to address the significant particle spacing effect created by FS as shown in Figure 31.

For these reasons, an accurate predicted settling time could not be found and instead a simple experimental test was done. Three sets of samples were made, each prepared with 60% aluminum particles suspended in mineral oil and FS. The samples were 1.6%, 2.4%, and 3.2% FS, by mass[1] and therefore each had a significantly different viscosity. These samples were pipetted into a glass jar and allowed to sit undisturbed for 8 weeks. The results can be seen in Figure 36.

 As expected, the samples with higher mass fractions of FS showed less settling over the 8 week testing period. The 1.6% sample showed a significant oil layer buildup at the surface after 8 weeks indicating some settling of the aluminum particles out of the oil. The 2.4% samples also showed some slight oil layer buildup after 8 weeks as is indicated by the dark line forming at its surface. The 3.2% sample did not show significant oil buildup on its

---

[1] This corresponds to carrier fluid mixtures that were originally 4%, 6% and 8% FS by mass, as characterized in Figure 32

surface, indicating that 3.2% is a sufficient concentration of FS to prevent the settling of these aluminum particles on the time scale of months[1].
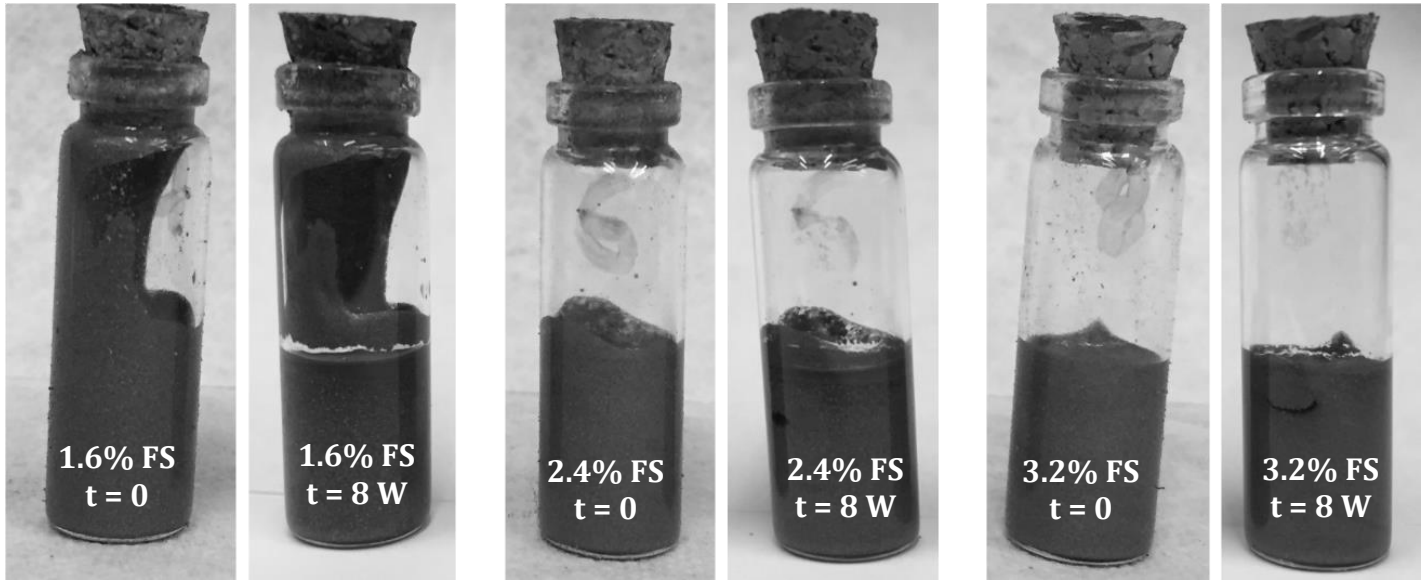
Figure 36: Liquid aluminum fuel settling time tests done with different mass fractions of FS. Leftmost set of images is of a sample with 1.6% FS after initial pipetting (left) and then 8 weeks later (right). Center set of images is a sample with 2.4% FS, and rightmost set of images is of a sample with 3.2% FS.

5.4 Pumping Tests

In a final system, it is crucial that a liquid fuel can be successfully pumped without clogging. Clogging could occur for two primary reasons within this mixture. The first of which is if the aluminum particles are not held in suspension long enough, and they settle so quickly that they settle, clump, and clog all while being pumped. The second, is if there is simply too much aluminum in the mixture relative to the oil. In this case the particles will cease to become suspended and behave as a fluid, instead behaving as moist granular flow which is

---

[1] A small bubble can be seen to have formed in the 3.2% sample, but that is simply due to initial pipetting error and not any settling within the liquid

subject to clogging. For these reasons, pumping tests were used to determine both the necessary viscosity of the fluid as well as the allowable aluminum concentration.

The pumping tests described in this section were done by using a syringe pump to dispense the fuel samples onto a mass balance in increments of 100 μl. The syringe used had a nozzle 2.5 mm in diameter, and the fluid was dispensed at a rate of 300 μl/min. Each sample was then weighed, and the density of the sample was determined. A successful pumping test is one in which the fuel can be pumped in a homogenous fashion, and the density from sample to sample has very little variation. In tests which exhibited clogging, large changes in density from sample to sample were observed and the syringe inevitably jammed.

5.4.1 Viscosity Selection

After observing that increasing the concentration of FS in the fuel can be used to increase the fuels viscosity, it became necessary to determine what concentration of FS would be sufficient to keep the aluminum particles in suspension. This was done by both settling time tests, as discussed in Section 5.3.4, as well as pumping tests. The pumping tests, shown in Figure 37, Figure 38, and Figure 39, were tests of three different liquid aluminum fuel samples. Each sample had the same concentration of aluminum particles but was made using different concentrations of FS and therefore had significantly different viscosities. The concentrations of FS used were 1.6%, 2.4%, and 3.2% by mass of the final fuel sample, which correspond to 4%, 6%, and 8% concentrations within the just the oil-FS mixture, respectively.

As seen in Figure 37, Figure 38, and Figure 39, the 3.2% sample was most stable, showing the least variation in mass flow between samples. The 2.4% sample similarly showed little variation between samples indicating a steady flow. The 1.6% sample, however, experienced significant variation in mass flow in later samples, due to the presence of a clog. This clogging indicates that the sample did not have sufficient viscosity to maintain a homogenous particle suspension throughout the flow test. Based on the stability seen for

the 3.2% sample here, as well as stability observations from the settling time tests discussed in Section 5.3.4, 3.2% FS was chosen as the minimum required FS concentration for all future samples. This corresponds to a carrier fluid mixture that is 92% mineral oil and 8% FS by mass.
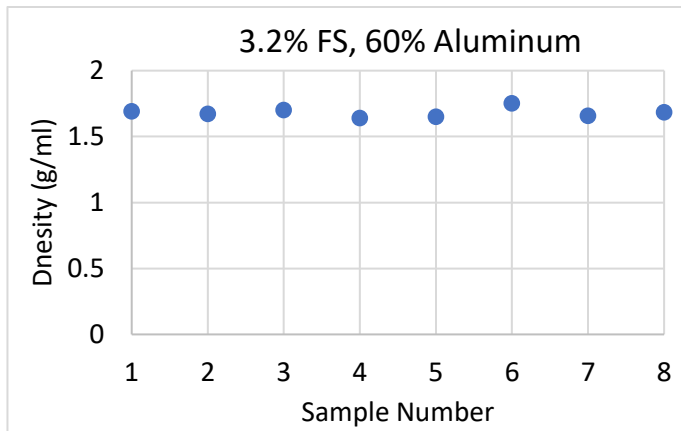
Figure 38: Plot showing the measured density of different 100 ul pumped samples of liquid aluminum fuel. The fuel mixture used for this test contained 3.2% fumed silica and 60% aluminum by mass. The fuel exhibited consistent density measurements, characteristic of a homogenous, freely flowing fluid.
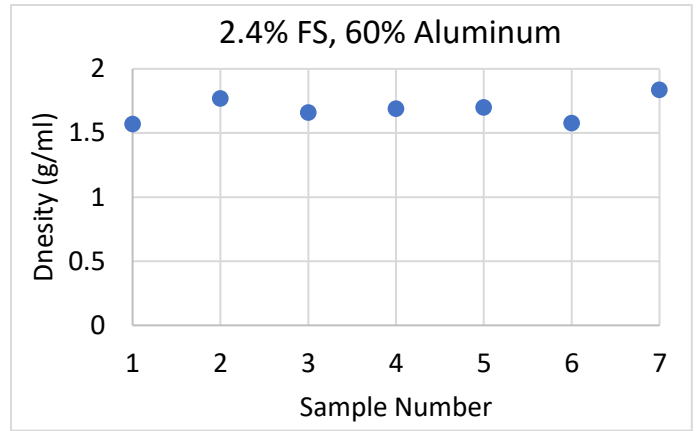
Figure 37: Plot showing the measured density of different 100 ul pumped samples of liquid aluminum fuel. The fuel mixture used for this test contained 2.4% fumed silica and 60% aluminum by mass. The fuel exhibited consistent density measurements, characteristic of a homogenous, freely flowing fluid.
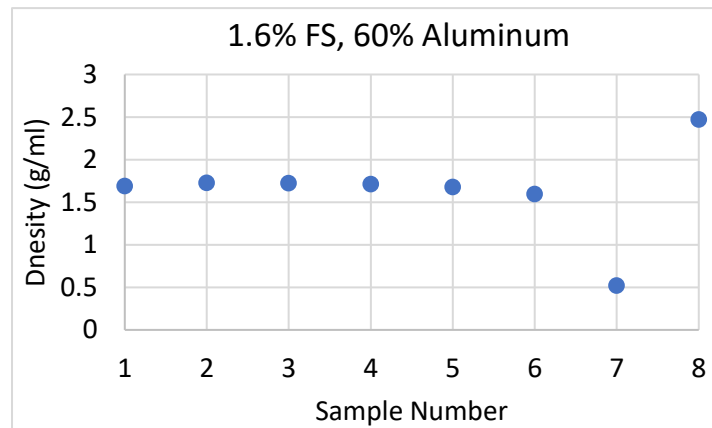
Figure 39: Plot showing the measured density of different 100 ul pumped samples of liquid aluminum fuel. The fuel mixture used for this test contained 3.2% fumed silica and 60% aluminum by mass. The fuel exhibited large variation in density as a result of clogging.

84

5.4.2 Aluminum Concentration Selection

One significant drawback to the use of a liquid aluminum fuel is that carrying around oil lowers the fuel's net energy density. For this reason, it is desirable that a liquid aluminum fuel have as high a concentration of aluminum in it as possible, thereby minimizing the presence of unnecessary oil and increasing the fuel's net energy density. These concentrations can only be taken so far, as a liquid suspension that contains too many particles and not enough carrier fluid will begin to behave more like a granular cluster of particles than a liquid.

A series of tests were done to determine the maximum amount of aluminum powder that can be added to the liquid fuel while still maintaining a pumpable liquid. Initial observations had shown that 60% aluminum was an acceptable concentration to add while still having fuel that behaved fully as a liquid. Therefore, for these tests, fuels with 60%, 65%, and 70% aluminum by mass were pumped, to determine at which point a sample would fail the pump test and show clogging.
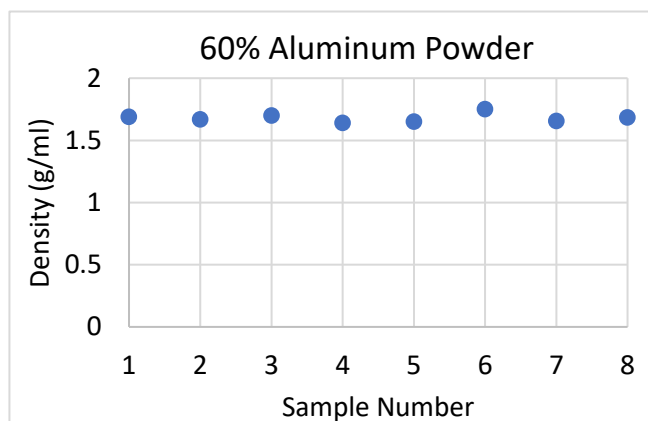
Figure 41:Plot showing the measured density of different 100 ul pumped samples of liquid aluminum fuel. The fuel mixture used for this test contained 60% aluminum powder by mass. The fuel exhibited consistent density measurements, characteristic of a homogenous, freely flowing fluid.
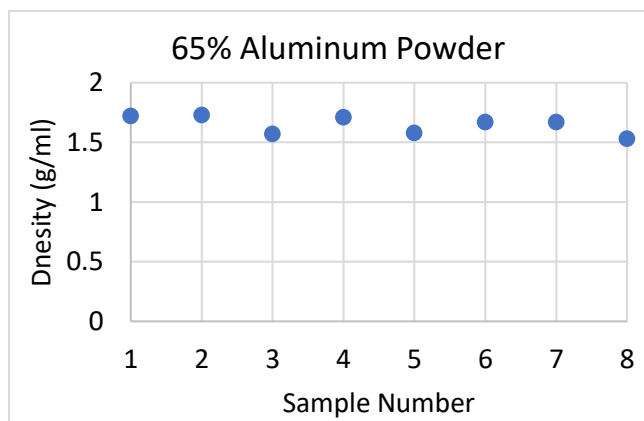
Figure 40:Plot showing the measured density of different 100 ul pumped samples of liquid aluminum fuel. The fuel mixture used for this test contained 65% aluminum powder by mass. The fuel exhibited consistent density measurements, characteristic of a homogenous, freely flowing fluid.
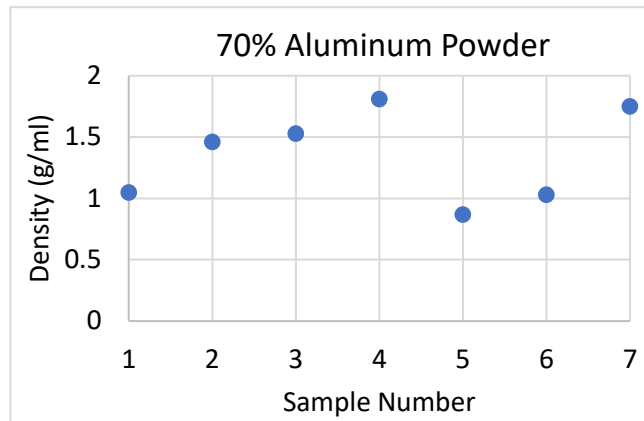
Figure 42: Plot showing the measured density of different 100 ul pumped samples of liquid aluminum fuel. The fuel mixture used for this test contained 70% aluminum powder by mass. The fuel exhibited large variation in density as a result of clogging.

As seen in Figure 41, Figure 40, and Figure 42 both the 60% and 65% aluminum samples showed stability and homogeneity between samples. Once the aluminum fuel concentration went as high as 70%, however, the mass flow began to vary significantly between samples, indicating significant clumping and clogging while being pumped.

For this reason, 65% aluminum concentrations were determined as a maximum allowable concentration of aluminum used in these liquid fuel samples. While these samples are 65% aluminum by mass, they are only 40% aluminum by volume due to the significant density discrepancy between aluminum and oil. Other industries, such as the ceramics industry, have shown the ability to maintain and flow particle suspensions with concentrations as high as 63% by volume [30]. It is therefore believed that in future work this 40% limit for current liquid aluminum fuels may be pushed further. Particularly with the use of smaller aluminum particles, it is believed that this concentration has the potential to be increased significantly while still maintaining smooth flow.

5.5   Reaction Tests

The final, and most critical, sets of testing that were done for the characterization of the liquid aluminum fuel were reaction completion tests. These were done to ensure that no aspects of producing the liquid aluminum fuel lowered the reaction yield in any way. These tests were done on 4 different types of fuel, solid aluminum spheres, aluminum powder, and two types of liquid aluminum fuel. Their reaction yields were then compared, to determine the relative performance of the liquid fuels.

5.5.1   Experimental Design

Baseline Aluminum Spheres:

Test 1 was of solid aluminum spheres and is the a baseline control. These spheres were the same 6mm spheres described in Section 3.1.1 and were surface treated as per the standard procedure in Appendix 8.1with 7% eutectic by mass. Their reaction completion tests were measured as per the procedure in Appendix 8.2.

Baseline Aluminum Powder:

Test 2 was of ground aluminum powder that was made out of pellets from the same batch used in test 1. Once ground into powder, and before being placed in oil, the aluminum becomes extremely volatile and may begin to react with oxygen or water vapor in the air. For this reason, the powder is ground and stored in argon, however it is still in contact with air at various transfer points in the grinding process. The difference between the reaction completions observed in test 1 and 2 may indicate the extent of this reaction with air.

The reaction tests for test 2 were done in much the same manner as test one, with only slight changes to account for the use of powder rather than solid pellets. At the start of each test, the jar of aluminum powder was thoroughly mixed, and a small bit of powder,

approximately 0.3g, was placed in the reaction flask. This flask was weighed before and after the placement of the fuel in order to determine the precise mass of powder added in each test. The water was then added, and the reaction yield measured as per Appendix 8.2. One notable occurrence is that the aluminum powder reaction was so violent that it often sent powder scattering across the flask walls when it began. When this was observed, the flask was shaken lightly to ensure that water could reach all of the powder scattered across the walls.

Liquid Aluminum Fuel, Hydrophobic FS:

Test 3 was of a liquid aluminum fuel mixture, comprised of 65% aluminum, 2.8% hydrophobic FS, and 31.8% mineral oil by mass. This hydrophobic FS was the same Aerosil R812 FS that had been used in all previous test. The aluminum powder used to make this liquid fuel was taken from the same mixed jar of powder as was used for test 2. Additionally, the powder was added to the oil sample immediately after all powder testing was complete. Therefore, any air exposure that was experienced by the aluminum particles in test 2 was also experienced by the aluminum particles in test 3. This was done to ensure that the differences in reaction yield observed between tests 2 and 3 were only differences due to the presence of the oil and FS.

The reaction testing for test 3 was done by using a 1 ml syringe to deposit a known volume of fuel into a flask. This flask was weighted before and after the deposition of the fuel in order to determine the mass of the fuel as well. Once the mass was determined, the flask was corked and connected to the reaction yield setup as described in Appendix 8.2. Notably, the reaction of liquid took significantly longer to occur as compared to solid aluminum fuel, and therefore all tests were allowed to proceed for at least a half an hour. The reaction rate was observed to be highly dependent on the manner in which the fuel was deposited into the jar, due to variations in the surface area of the deposited fuel from sample to sample. Additionally, the reaction rate was also seen to exhibit significant temperature dependence. This is to be expected, as not only is this aluminum fuel known to

react more quickly at elevated temperatures, but the oil's viscosity and surface tension will also decrease at elevated temperatures, expediting its separation from the aluminum.

Liquid Aluminum Fuel, Hydrophilic FS:

Test 4 was a liquid aluminum fuel mixture, comprised of 65% aluminum, 1.4% hydrophilic FS, and 33.4% mineral oil, by mass. While FS can be commercially purchased in both hydrophobic and hydrophilic variations, all tests described thus far have only used the hydrophobic FS. This is because it was theorized that the FS must be hydrophobic so that it will easily separate away from the aluminum when in contact with water. This hypothesis was tested here to determine if the use of hydrophilic FS would, in fact, obstruct the aluminum-water reaction.

A smaller concentration of FS was used for this test than what was used in test 3. This is because hydrophilic FS thickens oil more effectively that hydrophobic, and so 1.6% hydrophilic FS is sufficient to produce a fuel mixture at the same viscosity as 3.2% hydrophobic FS. It was desired that the fuel in test 3 and 4 have similar viscosities, so that any lack of separation between the aluminum and oil is not due to increased oil viscosity, but rather due to the hydrophilic nature of the FS. The FS used in this test was Aerosil 300, and the reaction completion tests were done in the same manner as was described for test 3.

5.5.2 Results

The results of the reaction tests can be seen in Figure 43. As expected, the fuel made using hydrophilic fumed silica, Aerosil 300, did not exhibit reaction completion at the levels of the hydrophobic fuel using Aerosil R812. Excitingly, the reaction completion levels for the hydrophobic liquid fuel were quite high. Notably, they were even higher than those observed for the aluminum powder and the aluminum spheres.
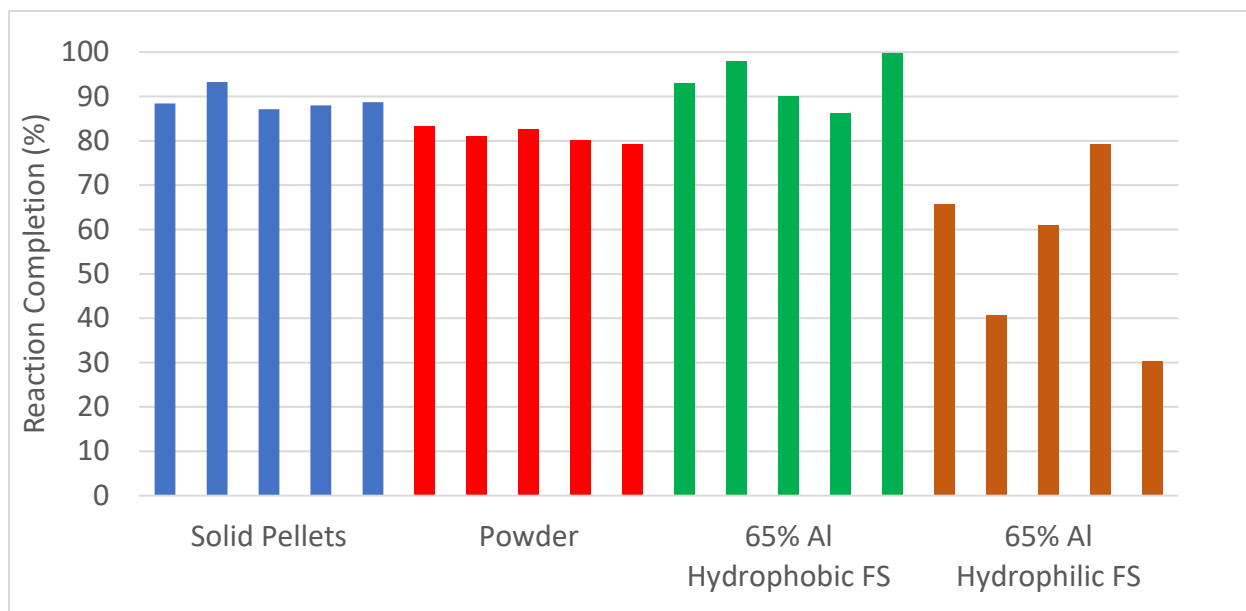
Figure 43: Plot of reaction completion for samples reacted as solid aluminum fuel, ground aluminum powder, and liquid aluminum suspensions that contained hydrophobic fumed silica and hydrophilic fumed silica.

This increase in observed reaction completion when using liquid aluminum fuel as compared to aluminum powder and spheres may be due to several possibilities. The first of which is the possibility that the mineral oil may be degrading and outgassing when elevated to the reaction temperatures of 100 C. Any gas produced by the mineral oil would be measured incorrectly as hydrogen and would therefore skew the results to indicate higher reaction yields than what actually existed. Upon further investigation however, a flask of mineral oil was heat to 100 C for 30 minutes and no outgassing was observed whatsoever, making this theory unlikely. Future work should still include gas chromatography of the output of a liquid fuel reaction, to ensure that no mineral oil breakdown is occurring.

The most likely possibility for this increase in observed reaction completion is that the liquid fuel mixture was not exactly 65% aluminum by mass. In order to determine reaction yield, the hydrogen produced in each reaction is compared against the ideal hydrogen output expected from that mass of fuel. If the fuel were to be a higher mass fraction of aluminum than expected, then the reaction would naturally produce more hydrogen than expected and the reaction yield data would be skewed. The mixture was made very

carefully to ensure accurate concentrations of each component, however, because these samples were being made at a scale of only 10 ml each, a slight error, or even the preferential wetting of oil versus aluminum to certain instruments, could easily throw off the mixture concentration by a few percent. In fact, when measuring the density of the fuel used for these tests, it matched more closely with the expected density for a 68% aluminum mixture. If the expected reaction yield is adjusted to account for a 68% mixture rather than a 65% mixture, then the average liquid fuel reaction yield drops to 89%, which is similar to the yield produced by the solid aluminum fuel. This also means that fuel can likely be produced in mass fractions as high as 68%, as no clogging was seen while pumping the fuel for the reaction testing.

An additional possibility for the reaction yield of the aluminum powder being measured as lower than the reaction yield of the liquid aluminum fuel is testing error. As mentioned earlier, the aluminum powder reaction is so volatile that the powder is often scattered across the reaction flask. This scattering can cause some powder to oxidize in the air within the flask or may keep some powder from coming into contact with water. This may explain the decreased reaction yield observed for the aluminum powder as compared to the aluminum spheres and the liquid aluminum fuel.

One final possibility is that the aluminum-water reaction simply occurs in a more optimal manner for high reaction completion when the aluminum is initially suspended in oil. This may be the case because the aluminum-water reaction is allowed to occur in a much more stable and controlled manner when reacting in liquid fuel. It has been theorized that breaking apart into small particles is a critical step for high reaction completions when using solid fuel. This stage is unnecessary when reacting aluminum powder, however the powder reaction is so volatile that particles may become scattered and oxidized. Reacting liquid aluminum fuel may pose an ideal combination of both forms, where the fuel is already ground into particles small enough to ensure high levels of reaction completion, but the reaction also occurs in a steady and controlled manner to allow for all particles to react completely.

5.6 Discussion and Conclusions

Aluminum fuel poses many advantages over other commonly used fuels such as gasoline or compressed hydrogen. It is significantly more energy dense, it is safer to store and transport, and it has a shelf life of years. In the past, the use of aluminum fuel has also come at the cost of having to use either unsafe powders, or solid fuels that add logistical challenges and require batch reaction systems. This section outlines the development of a liquid aluminum fuel that successfully reacts with water to high levels of completion. Liquid fuel has been made with mass fractions as high as 65% aluminum powder, while maintaining steady flow and showing no clogging even at low flow rates in tubes as narrow as 2.5 mm. This fuel also shows no significant settling over 2 months, and its viscosity shows very little temperature dependence within standard operating ranges of 7 C to 45 C. The liquid aluminum fuel has also been shown to react effectively with water to high levels of reaction completion, comparable to those of solid fuels discussed in Section 3.3.

Based on the final fuel mixture which consists of 65% solid aluminum fuel, 3.2% Aerosil R812 and 31.8% mineral oil, the final mass and volumes of the constituent components can be accounted for and a final fuel energy density can be determined. Additionally, the effective energy density and specific energy of the fuel, defined in Equations 8 and 9 which account for the reaction yield, can be determined. These final properties of the fuel can be found in Table 1.

Table 1: Properties of final liquid aluminum fuel configuration.

Measured Density of Liquid Fuel	1.64 g/ml
Measured H2 Production Per ml Liquid Fuel	1270 ml
Effective Energy Density	28.7 MJ/l
Effective Specific Energy	17.5 MJ/kg

Utilizing aluminum fuel in a liquid form allows the use of a high energy dense fuel, while eliminating all the challenges of pressurizing, pumping, refueling, and continuously reacting solid aluminum. Despite the large volume of this fuel that is occupied by oil, this

liquid fuel still has approximately 3x the energy density of liquid H2. Additionally, this liquid fuel maintains a comparable energy density to gasoline, while being safely non-combustible, and producing hydrogen which can be utilized more efficiently than gasoline to produce electricity.

Future work can be done to further optimize the energy density and specific energy of the liquid aluminum fuel. By grinding the aluminum into powder while it is already suspended in oil, smaller particle sizes can be achieved without risking powder combustion. The use of finer particles should allow for higher mass fractions of aluminum to be introduced into the oil while still maintaining fluidic properties and not clumping or clogging while being pumped. Higher mass fractions of aluminum will, in turn, increase the total fuel energy density and specific energy. Additionally, using smaller particles will allow for easier particle suspension in oil, which would and increase the overall homogeneity of the fluid and decrease the need for fumed silica.

5.7   Liquid Aluminum Fueled System Design

With the development of a working liquid aluminum fuel completed, a big step forward will be the design and implementation of a continuous flow reactor using this liquid fuel. As mentioned previously, continuous flow reactors have several significant advantages over batch reactors, such as smaller and more easily pressurized reaction chambers, ease of waste management and refueling, and ease of reaction control. Different concepts for this continuous flow reactor system are considered and analyzed in the following sections.

5.7.1   Continuous Flow Reactor

The two primary concepts considered for a liquid aluminum fuel continuous flow reactor are the water trap concept, and the permeable membrane concept. The water trap concept, shown roughly in Figure 44, is one in which both the liquid fuel and water are pumped into

a single solid tube reactor. At the end of the tube reactor, this concept incorporates the basic principles of a gravity driven water trap to allow the AlOOH and oil to drain into a waste container below while the hydrogen and steam continue upward through the rest of the system. This system concept is promising, and its principles are well understood, however it does rely on gravity, meaning that the system must always be operated in the correct orientation and flipping it over can cause internal flooding.
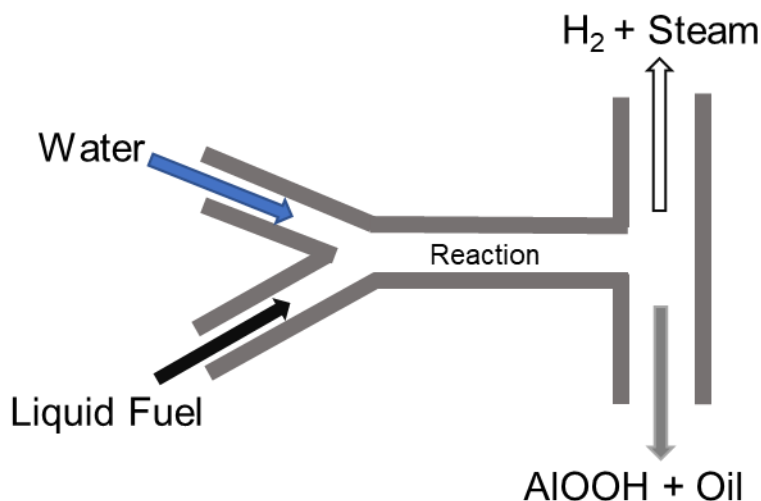
Figure 44: Diagram of continuous flow reactor concept, where waste drains downwards due to gravity while hydrogen and steam continue to travel through the system.

In the permeable membrane concept, shown in Figure 45, the water and liquid fuel are pumped into a single tube, but rather than the tube being solid, it is permeable to hydrogen. This allows the hydrogen to pass through the tube walls into the rest of the system while the other components continue on through the tube and are removed as waste. This concept is very promising, although the permeability rate of current marketed gas permeable membranes may limit the achievable hydrogen flow rates. The necessary permeability was calculated for an example system where a gas permeable tube 0.64 cm ID, 0.15 cm thick, and 50 cm long is used as a reaction chamber, with a pressure drop to the outside of the tube of 5 psi and a desired H_2 flow rate is 5 slpm. This was used to calculate a necessary hydrogen permeability for the tube material of 5×10^7 Barrer via Equation 13,

which is significantly higher than the rating for any materials currently found on the market. Perhaps with changes in system design and significantly greater reaction tube surface area, the necessary permeability can be decreased to a value achievable with future technology.

$$1 \; barrer = \; 10^{-10} * \frac{cm_{STP}^{3} * cm}{cm^{2} * s * cmHg} \tag{13}$$
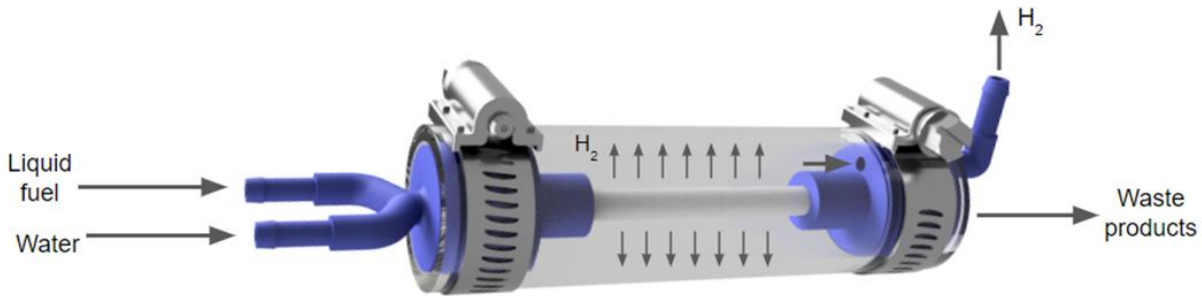
Figure 45: Design of a continuous flow reactor for liquid aluminum fuel, where a hydrogen permeable tube is used to separate the hydrogen from the waste products.

An alternative form of the gas permeable membrane concept is to use a porous tube as the reaction chamber. Tubes with pores in the range of 10-100 μm are easily manufactured and could be used to allow hydrogen to flow out of the reaction chamber while maintaining the liquid and solid waste inside. The pore sizes in this concept will not limit the achievable hydrogen flow, as first order calculations show that with 10 μm pores even small pressures should allow for large volumetric flows of hydrogen out the tube. One serious concern however, is the clogging of the pores with water, oil, or aluminum oxyhydroxide. As the hydrogen flows outward, there is little to keep the water and oil from flowing outward as well, obstructing the individual pores. This concept would therefore require significant experimentation to determine its feasibility, particularly with variations to pore size and the use of hydrophobic or hydrophilic coatings on the porous tube to minimize the extent of clogging.

5.7.2 Analysis of Pumping Losses

As mentioned previously, using a liquid fuel allows the fuel to be easily pumped throughout a system. While this is an advantage over solid fuel, it can easily become impractical if the fuel is too viscous and necessitates large pumping losses. For this reason, the fuel has been engineered to be shear thinning, so that its viscosity will decrease significantly when being pumped through a pipe. In order to determine expected pumping losses, a conservative example system can be analyzed with a pipe diameter of 0.32 cm, a length of 1.5m, and a desired flow rate of 0.13 ml/s, which is approximately the fuel flow rate needed to produce 10 slpm H_2. The shear rate experienced at the walls of this tube can be calculated via Equation 14 to be approximately 40 s^{-1}.

$$Shear\ Rate = \frac{4 * Q}{\pi * r^3} \tag{14}$$

Given this shear rate, a conservative estimate of 10 Pa*s can be made for the viscosity of the fuel using the data shown in Figure 34. Using the viscosity, pipe geometry and flow rate, the necessary pressure drop across such a system can estimated using Equation 15 to be 7.6 bar.

$$Pressure\ Drop\ Along\ a\ Pipe = \frac{8 * \mu * L * Q}{\pi * r^4} \tag{15}$$

Finally, the necessary power needed to pump this fluid can be determined through the simple relationship shown in Equation 16. This leads to a pumping pressure as low as 0.1 W. Even after accounting for inefficiencies, and assuming a necessary pumping power of 1 W, small electrical peristaltic pumps at this scale can be easily procured. These pumps can weigh as little as 100 grams and can be easily incorporated into a reactor system.

$$Power = (Change\ in\ Pressure) * (Volumetric\ Flow\ Rate) \tag{16}$$

5.7.3 Water Recovery

An additional system consideration is the amount of water that must be included within the system to effectively react the aluminum. Accounting for an expected 90% reaction yield, approximately 1.26 ml of water is necessary to react with every 1 ml of liquid fuel. While this can add up to an appreciable fraction of the system weight and volume, the amount of water needed can be decreased significantly if it recovered through the later stages of the system. In both fuel cells, as well as internal combustion engines, energy is extracted from hydrogen by combining it with oxygen to form water. Water is therefore produced as the byproduct of the electrical generation stage of most any hydrogen system. If this water is recycled back into the reaction, the volume of water that must be carried with the system can be reduced by as much as 75%. This greatly reduces the required volume and mass of water needed and increases the system energy density significantly.

Overall the development of a liquid aluminum fueled system appears to be not only feasible but has the potential to be much smaller and more manageable than its solid fuel counterpart systems. Such a system does not require a large, heavy, reaction chambers, and instead can store its fuel in lightweight bladders and react it in a single small pressurized tube. Looking beyond aluminum fuel, this liquid system can also be used to produce hydrogen on-demand without the need for heavy and dangerous pressurized hydrogen canisters. The development of a viable liquid aluminum fuel represents a significant step forward in the development and commercialization of aluminum fueled power systems.

6. DESIGN AND ANALYSIS OF A HYDROGEN-STEAM ENGINE

The Sindri system, as well as all smaller power systems built using this aluminum fuel thus far have used hydrogen fuel cells to generate electricity. These fuel cells work by a controlled reaction of hydrogen and oxygen, where the affinity of these molecules for each other is utilized to produce an electrical potential. Standard PEM fuel cells, such as the ones used in the Sindri system, have efficiencies in the range of 40-60%. This is significantly higher than standard gasoline engine efficiencies of approximately 20%, making fuel cells very desirable for high efficiency systems. While less efficient, current engine technology has several significant advantages over fuel cell systems. Engines have been designed to be incredibly cheap, capable of producing kilowatts of power for a few hundred dollars where fuel cell systems would easily be thousands at today's costs. Engines have also been designed to be incredibly robust to mechanical shock, or low-quality input gases. This is in contrast to PEM fuel cells which require special shock mounting to ensure that their internal membrane will not fracture, as well as hydrogen that is 99.95% pure, with small impurities of CO_2 or CO capable of causing serious long-term damage to their performance. Finally, engines are also significantly more power dense than fuel cells, meaning that generating a given amount of power can be done is a significantly smaller footprint using an engine as compared to a fuel cell, as indicated in Figure 29. Given these advantages of engines over fuel cells, there are many applications for which using an engine-based generator would be preferable.

An aluminum-water reaction releases approximately half its energy as hydrogen, and half as heat. Engines that run off of hydrogen have been found to be as high as 40% efficient, which is higher than standard gasoline engines primarily due to hydrogens higher compression ratio and faster flame speed [6]. This efficiency is already comparable to that of fuel cells, making hydrogen engines a very viable concept for future aluminum fueled generators. However, because both of these systems are only using the hydrogen released from the reaction, they are really are only utilizing half of the system's energy and therefore only have system-wide efficiencies of approximately 20%.

In an effort to significantly increase the system wide efficiency of aluminum fueled power systems, an engine concept has been designed that utilizes both the hydrogen energy, as well as the thermal energy released by the reaction. This system requires only a slight change to the standard Otto cycle engine used in most generators and can therefore be implemented easily in future systems. Initial analysis of this proposed engine cycle suggests ideal system wide efficiencies as high as 33%. This would allow for a power system with the low cost and robust nature of an engine, while still retaining the efficiencies achievable by fuel cells.

6.1   Engine Background

Engines have been used for centuries as a means to convert chemical and thermal energy into mechanical energy. The two primary forms are steam engines and combustion engines. A steam engine uses pressurized steam to push a piston, producing mechanical work. A combustion engine uses the pressure produced by fuel combustion to push a piston. Essentially, each of these engines utilizes high pressure gas to produce mechanical work.

6.1.1 Steam Engines

A basic steam engine works by pumping water into a boiler, where it is vaporized into steam. This steam is then piped into the compressed cylinder of a piston. The pressure of the steam then pushes the piston outward causing the gas to expand and producing mechanical work in the process. A slide valve then changes the passage of the steam so that it is directed to the opposite side of the piston. This allows the new incoming pressurized steam to now push the piston in the opposite direction while it expands. While this happens, the expanded air on the original side is pushed outwards through an exhaust valve. This process can be visualized in Figure 46. The efficiency of a steam engine varies with the temperatures and pressures used, with the highest recorded values primarily in the range of 10-20%.
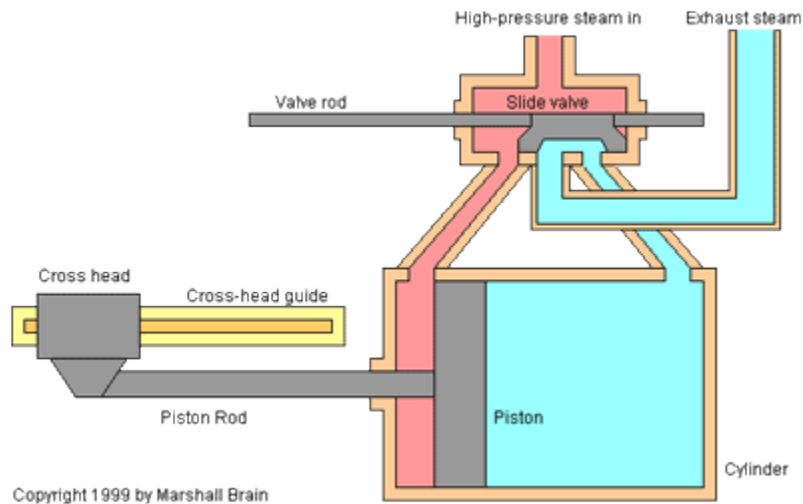
Figure 46: Diagram of a steam engine [32].

Modern steam generators primarily use turbines, in which high pressure steam moving past a turbine will cause the turbine to spin, generating electricity. This process is used in steam-electric power plants, which comprise the majority of electrically generating power plants in the world, including coal, nuclear, and geothermal. In all of these power plants, the

heat produced by the fuel is used to boil water into steam, and the steam is then run past a turbine. These high-power steam turbine plants can operate at as high as 80% efficiency [31].

6.1.2 Internal Combustion Engines

Internal combustion engines, which power most automobiles and home-generators, come in many variations. These variations primarily vary the type of fuel used, as well as the engine cycle that generates power from the fuel. Common fuels used in a combustion engine are gasoline, diesel, natural gas, or hydrogen, and the exact fuel used may change how the fuel is ignited, and what temperatures and pressures the engine can operate at. The engine cycle can be either a 2-stroke cycle, or a 4-stroke. A 4-stroke cycle pressurizes the fuel, ignites it, expels the exhaust, and then intakes new gas as outlined in Figure 47 [32] [33]. A 2-stroke engine is similar but doubles up steps by intaking new gas as it expels the exhaust, this shortens the cycle allowing it to produce more power than an equivalent 4-stroke engine. This higher power density comes at a loss of efficiency however because some new fuel can become lost with the exhaust in every step. Four stroke engines are the most commonly used small engines, and a modern, automobile, gasoline fueled 4-stroke will typically operate at up to 20% efficiency.

Direct injection has also been used to increase efficiency in modern engines. Direct injection is when fuel is not mixed with the initial intake gas but rather is injected into the engine at high pressure once the intake gas is already compressed and the piston is at top dead center (TDC). This fuel injection occurs immediately before the ignition stage and allows for the more accurate control of injected fuel fractions, which in turn allows for engines to operate more efficiently.
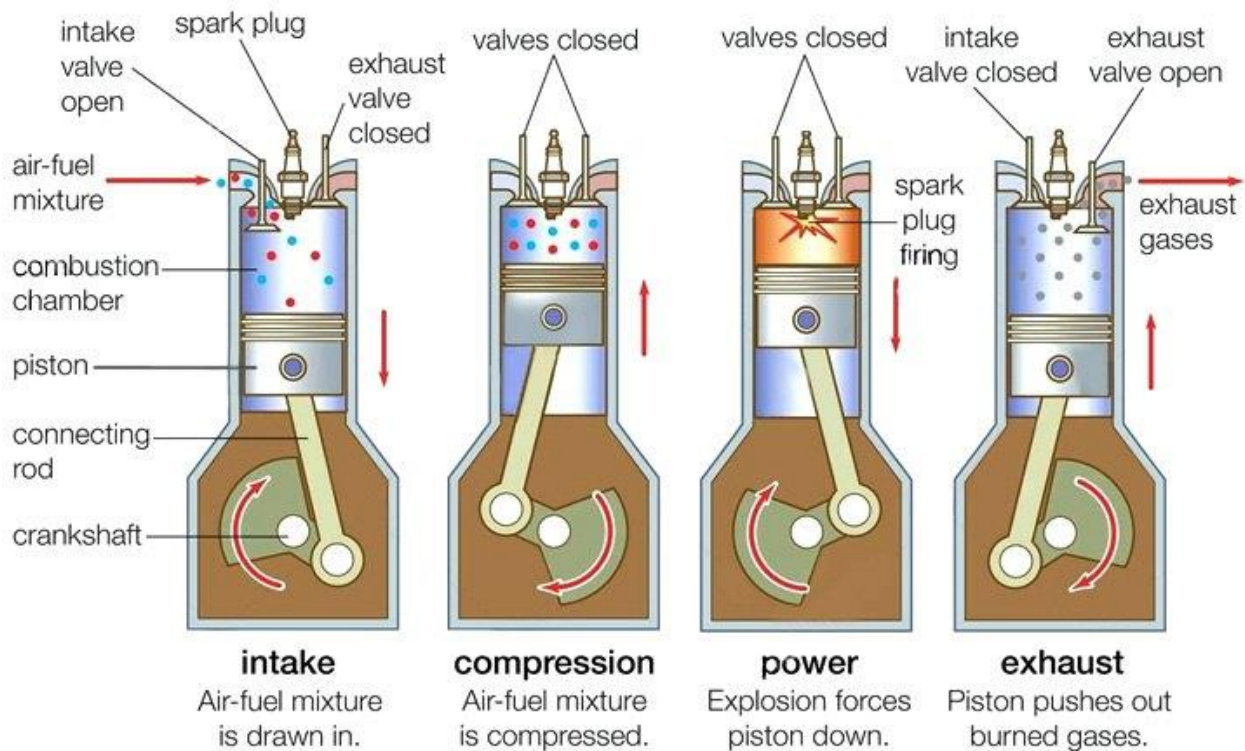
Figure 47: Diagram of a 4 stroke combustion engine following the Otto cycle. Each image presents a different stroke in the cycle, progressing from intake, to compression, to combustion on the power stroke, to exhaust. [39]

6.2   Combined Hydrogen-Steam Engine

The joint hydrogen-steam engine cycle proposed hear aims to take advantage of both the thermal energy as well as the hydrogen chemical energy that is released by an aluminum-water reaction. This is done by taking the mixed hydrogen and steam output gas from an aluminum-water reaction and injecting it directly into a combustion engine when it is at top dead center. The pressure from the steam will immediately begin to push the piston downward, followed by the combustion of the hydrogen which will increase the pressure and exert force on the piston as well. The steps of this cycle are detailed in Figure 48, and

can be thought of as a direct injection engine where the injected fuel is both steam and hydrogen.
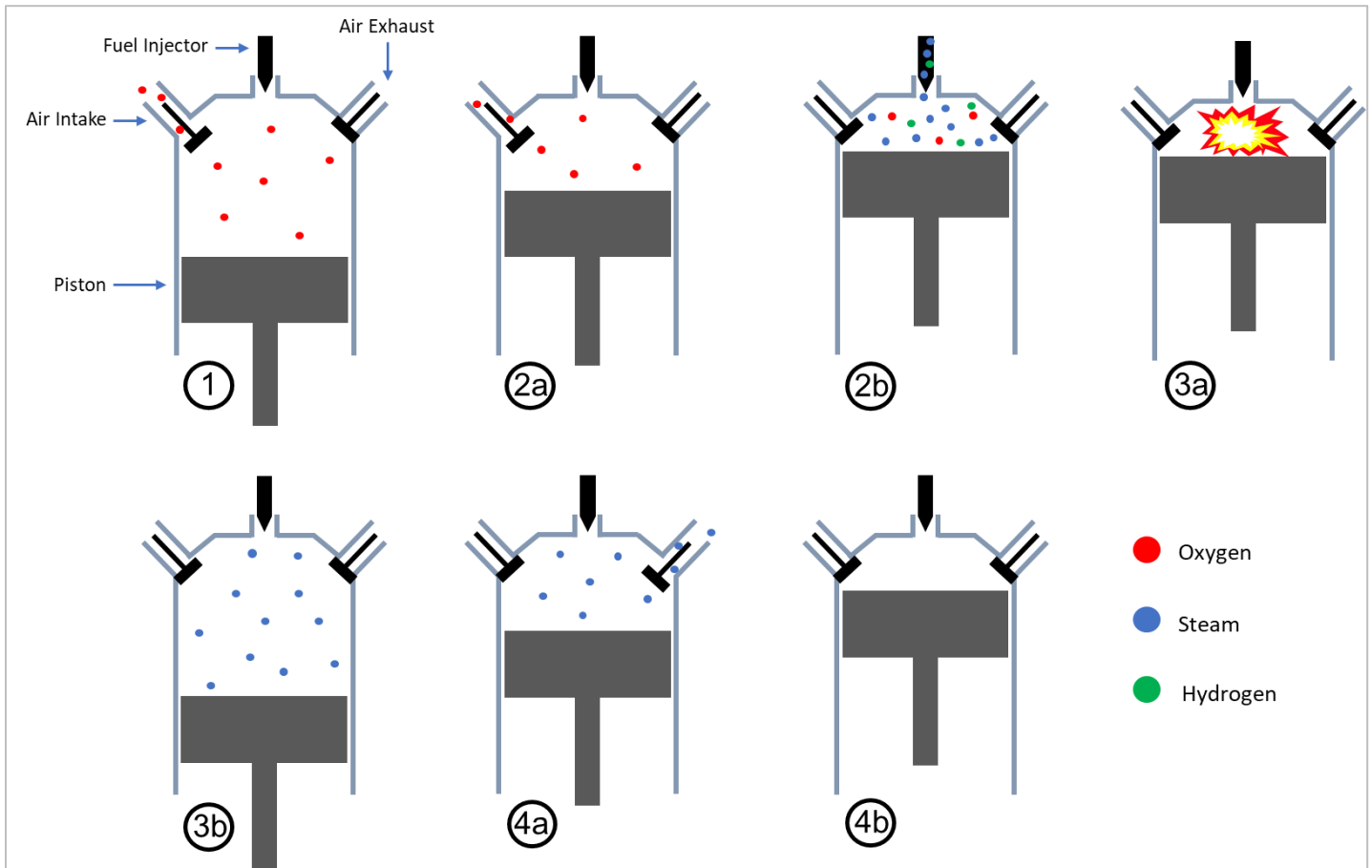
Figure 48: Diagram depicting the proposed hydrogen-steam engine cycle. In stage 1, oxygen is taken in to the cylinder. In stage 2a, the piston moves upwards, and the intake valve initially remains open until some middle point at which the intake valve closes, and the remainder of the air is compressed in the cylinder. In stage 2b, immediately following the slight oxygen compression, the steam and hydrogen are injected at high pressure into the cylinder. In stage 3a the hydrogen combusts with oxygen to produce steam, creating a high pressure that forces the piston down as shown in stage 3b. In stage 4a the exhaust valve opens allowing the gas to escape until the piston reaches TDC in stage 4b at which point the exhaust valve closes and the cycle starts anew.

This engine concept is a hybrid between a steam engine and an internal combustion engine. In this engine, the pressurized steam is injected when the piston is compressed and used to push the piston down, similar to a steam engine. Additionally, internal combustion is used to ignite the hydrogen, superheating the steam and increasing the cylinder pressure. This

103

engine also has the advantage of only using hydrogen as a fraction of the fuel, meaning that it requires less oxygen than most combustion engines. A standard gasoline engine requires large amounts of oxygen to burn all of the inputted gasoline fuel, meaning that a large amount of gas must be pressurized before the fuel is ignited. This pressurization stage requires a lot of energy and decreases the system efficiency. Hydrogen, however, requires significantly less oxygen to burn than gasoline does per mole, and because the hydrogen only comprises a fraction of the input gas, only a small volume of oxygen is needed to burn it completely. This means that less air needs to be compressed into the cylinder to effectively burn the hydrogen, leading to fewer energy losses in the system.

Notably, the water in this proposed engine system can be found to follow the T-S curve of a standard Rankine cycle with superheating as seen in Figure 49. In this comparison, the aluminum-water reaction acts as the boiler, moving the water form point **a** to **b** on the curve. The combustion of the hydrogen then acts to superheat the gas moving it from point **b** to **c**, and the expansion of the cylinder takes the place of standard steam turbine expansion, moving it from point **c** to **d**. The water vapor is then condensed and recycled back into the system bringing it from point **d** back to **a**. The proposed engine concept can therefore be thought of as operating similarly to both a direct injection Otto cycle, and a Rankine cycle with superheating.
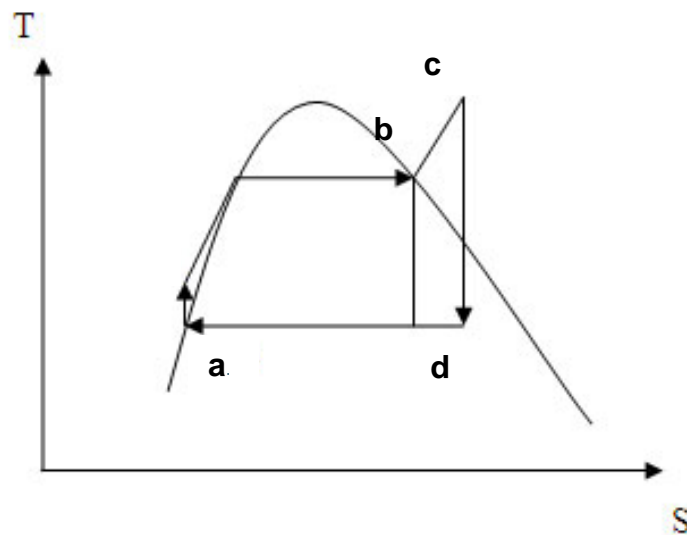
Figure 49: Temperature Entropy diagram of a standard Rankine cycle with superheating [34].

6.2.1 Cycle Analysis

Fuel Composition:

The first step in the analysis of this proposed system is determining the ratio of steam to hydrogen that will be produced by an aluminum-water reaction. This can be done by assuming that all of the thermal energy released by a reaction of 1 mole of aluminum will first go into heating up the reaction products until they reach the boiling point of water. At that point, any excess heat will go into vaporizing water into steam, which keeps the reaction from ever reaching a temperature above the boiling point of water. Determining the exact amount of steam produced per mole of reaction can be done by simply performing an energy balance as shown in Equation 17.

$$n_{Al} * E_{Al} = m_{AlOOH} * Cp_{AlOOH} * \Delta T + m_{H2} * Cp_{H2} * \Delta T$$
$$+ m_{H2O} * Cp_{H2O} * \Delta T + Hvap_{H2O} * m_{H2O} \tag{17}$$

Where n_{Al} represents the number of moles of aluminum reacted, E_{Al} represents the heat released per mole of aluminum reacted, m_i represents the mass of compound i that is heated by the reaction, Cp_j represents the specific heat capacity of compound j, $Hvap_{H2O}$ represents the heat of vaporization of water, and ΔT represents the change in temperature between the reaction inputs and the boiling point of water that they are heated to. Assuming a reaction of 1 mole of aluminum, n_{Al}, m_{AlOOH}, and m_{H2} can all be determined stoichiometrically. All specific heat capacities and the heat of vaporization of water as also known constants. This leaves the mass of excess water that is heated and vaporized as the only unknown in the equation. Solving for the mass of water then gives a mole ratio of water to hydrogen in the final gas of approximately 12% hydrogen and 88% steam by volume. This ratio assumes an initial reaction pressure of 14.7 bar[1] but will vary depending on the pressure that the reaction is operated at, as many of the constants used in Equation 17 vary with pressure. Additionally, the ΔT used here was only 10 C, as it was assumed that

---

[1] The pressure used as a baseline for this analysis as 14.7 as it is the compression ratio suggested in literature for the operation of hydrogen ICEs.

the reactants would be preheated before being reacted, possibly with the residual heat present in the system's exhaust gas. Varying this ΔT will affect the final gas mixture slightly, although the ratio is not very sensitive to ΔT as most of the energy is being used for the vaporization of water.

Necessary Oxygen Intake and Piston Volume at TDC:

Once the number of moles of hydrogen is known, the number of moles of oxygen needed to burn it is simply half of that, as hydrogen burns in oxygen as per Equation 18.

$$2H_2 + O_2 \rightarrow 2H_2O \tag{18}$$

The necessary volume of gas needed to intake this much oxygen can then be determined using the ideal gas law. Of course, this volume will also vary based on whether the input gas is pure oxygen or if it is air which is only 21% oxygen. Once the necessary intake volume is reached, the intake valve will close, and the gas will begin to be compressed until it reaches TDC. At TDC the oxygen will be slightly compressed, and the pressurized steam and hydrogen will then be injected. The necessary volume at TDC can be determined, as the reaction pressure of the steam and hydrogen must be sufficient to inject it into the remaining cylinder volume while still being able to mix with oxygen in the proper ratios. This volume at TDC can be determined using the ideal gas law as shown in Equation 19.

$$V_{TDC} = (n_{H2O} + n_{H2} + n_{O2}) * R * T * \frac{1}{P_{rxn}} \tag{19}$$

Where n_{H2O} and n_{H2} are the number of moles of steam and hydrogen produced by the reaction of 1 mole of aluminum respectively, n_{O2} is the number of moles of oxygen necessary to burn n_{H2}, R is the ideal gas constant, and T is the temperature of the gas. This gas temperature is equal to the boiling point of water at the reaction pressure, P_{rxn}. The reaction pressure is used as the final pressure at TDC because the injection of the

pressurized steam-hydrogen mix will naturally raise the cylinder pressure to this reaction pressure. Additionally, if air is used as the intake gas, then an n_{N2} term must be incorporated as well.

This analysis was done assuming that the exact moles of gas present result from the reaction of 1 mole of aluminum. This is an arbitrary fuel quantity for each engine cycle and therefore the exact volume of fuel is not important, but rather what is important is the volume ratio between the necessary intake gas volume and the TDC volume. This ratio of necessary intake gas volume to TDC volume is 0.479 for the intake of pure O_2 and 1.9 for the intake of air. This means that if pure O_2 is used as the engine intake, then the amount of oxygen needed to burn the hydrogen is actually so small that even the slight amount left in an uncompressed cylinder at TDC is more than enough to combust the hydrogen that will be input into the chamber. This is not the case when using air as an intake gas. If air is used, then some air must be compressed in the cylinder before TDC is reached in order to have enough oxygen to burn all of the hydrogen that will be injected into the engine.

Compressing gas requires work to be put into the system, which lowers overall system efficiency. This work energy can be calculated using Equation 20 [33].

$$W = \frac{P_i * V_i^\gamma * \left(V_f^{(1-\gamma)} - V_i^{(1-\gamma)}\right)}{1 - \gamma} \tag{20}$$

Where V_i is the initial volume of the intake air at an initial pressure of P_i which is assumed to be 1 bar. V_f is the final volume of the air after it is compressed by the piston, and γ is the ratio $\frac{Cp}{Cv}$ for air, which is 1.4 at STP and varies insignificantly within the temperature and pressure ranges considered. This final work used to compress the gas must then be considered as energy input into the system when calculating the final system efficiency.

Hydrogen Combustion:

With the steam, hydrogen, and oxygen in the cylinder, and the piston at TDC, a spark plug will then ignite the hydrogen gas, leading to a large release of chemical energy. Assuming complete, constant volume, combustion, this energy goes entirely into raising the temperature and pressure of the gas. This change in pressure and temperature can be determined using the first law of thermodynamics as shown in Equation 21.

$$J = \sum m_i * Cv_i * \Delta T + \Delta P * V_{TDC} \tag{21}$$

Where J is the energy released during combustion, m_i and Cv_i are the mass and specific heat of each gas present respectively, ΔT is the change in temperature caused by the combustion, ΔP is the change in pressure caused by combustion, and V_{TDC} is the volume of the cylinder when the piston is at top dead center. As it stands, Equation 21 has two unknowns, the change in temperature and the change in pressure. This can be solved by relating the change and temperature and change in pressure to one another by the ideal gas law, and rearranging Equation 21 to form Equation 22.

$$\Delta T = \frac{J}{\Sigma (m_i * Cv_i) + \Sigma (n_i) * R} \tag{22}$$

Where n_i is the number of moles for each gas present, and R is the ideal gas constant. This allows ΔT to be calculated, and ΔP can follow using the ideal gas law.

Unfortunately, calculating the change in temperature and pressure for the complete combustion of hydrogen all at once cannot be done, because too many of the constants necessary for these calculations vary over the course of the combustion process. Many of the specific heat capacities vary with such a significant increase in temperature and pressure, and even the masses and total volumes of gas change throughout combustion as the hydrogen and oxygen react to form water vapor. This combustion analysis must therefore be done iteratively, where the combustion of slightly more hydrogen is calculated

in each step, and the proper constants are used and updated for the current conditions with every step. Using this iterative process, the hydrogen combustion considered here would lead to a final gas temperature of 870 C and a pressure of 34 bar, assuming the initial reaction pressure of 14.7 bar used above. These temperatures and pressures are well within the range of standard engine operating conditions [34].

Gas Expansion:

After the hydrogen has combusted and raised the temperature and pressure of the resulting gas, the piston will begin to move downwards, expanding the cylinder volume and extracting energy from the gas. This process causes an adiabatic expansion of the gas, which cools it and reduces its pressure. The change in temperature caused by the adiabatic expansion of a gas can be expressed via Equation 23 [33].

$$T_f/T_i \ = \left(V_i/V_f\right)^{(\gamma-1)} \tag{23}$$

Where T_i and T_f are the initial and final gas temperatures, V_i and V_f are the initial and final gas volumes, and γ is the ratio of $\frac{Cp}{Cv}$ for the gas. Again, this calculation must be done iteratively because the specific heat values for each gas vary significantly across the temperature range analyzed. Additionally, each gas will have different specific heat capacities and must therefore be considered individually. To do this, a temperature change of -5 C was imposed on the system, and the resulting volume change for each gas was determined. Given the new gas volume and temperature, the partial pressure for the gas was also calculated via the ideal gas law. The partial pressures of all gasses were then summed to find the total system pressure after such an incremental change in temperature. This stepped analysis was done repeatedly, until the total system pressure reached 1 bar, at which point the cylinder pressure will no longer push down on the piston and no further work can be extracted from the gas. Assuming the same initial reaction pressure of 14.7 bar as described above, this final cylinder pressure of 1 bar was reached when the gas had expanded to 16 times the original TDC volume, and the final gas temperature was 415 C.

An additional concern during this expansion analysis is that the water vapor must never get within a temperature and pressure regime that will allow it to condense within the engine. This would cause logistical issues with internal engine lubrication and part wear, and should therefore be avoided. Fortunately, at all temperature and pressure ranges considered in this analysis the conditions for condensation were never reached.

Exhaust Gas and Engine Efficiency:

The final engine exhaust gas will be expelled at approximately 400 C and will be comprised primarily of water vapor, with nitrogen as well if air is used as the intake gas. This heated gas still retains a lot of thermal energy, and because it is expelled it represents energy that is completely lost from system. By determining the amount of energy that is held with this exhaust gas, and assuming that all other energy is successfully converted to mechanical work on the piston, the total ideal engine efficiency can be determined as per Equation 24.

$$Ideal\ Engine\ Efficiency = \frac{Energy\ Input\ to\ System - Energy\ Losses\ to\ Exhaust}{Energy\ Input\ to\ System} \quad (24)$$

Where the energy input into the system is the total chemical energy released by the reaction of aluminum with water, as well as the work energy input to compress the intake gas as mentioned previously.

The thermal energy contained within the output gas can be determined by looking at the energy that would need to be added to that gas at room temperature in order to heat it to its current temperature. This can be expressed as a sum of the specific heat and latent heat as described in Equation 25.

$$E_{Lost} = \Sigma\ m_i * Cp_i * \Delta T + Hvap_{H2O} * m_{H2O} \quad (25)$$

Where m_i and Cp_i are the masses and specific heat capacities of each gas present, and ΔT is the change in temperature from the system's starting temperature to the current exhaust

temperature. Again, this calculation must be done incrementally, because the specific heat constants of each gas change significantly over the temperature range considered.

6.2.2 Results

A MATLAB model was used to perform the complete engine analysis described in Section 6.2.1. Published data of the Cp and Cv of each compound were found at varying temperatures and pressures and were incorporated into the analysis to improve the overall accuracy. For any analysis temperatures and pressures that were in between the data points found, a simple linear interpolation was used. The boiling point, heat of vaporization, and heat of formation for water were also found at varying temperatures and pressured and were incorporated into the model as well. This model then analyzed the complete engine cycle assuming various initial aluminum-water reaction pressures.
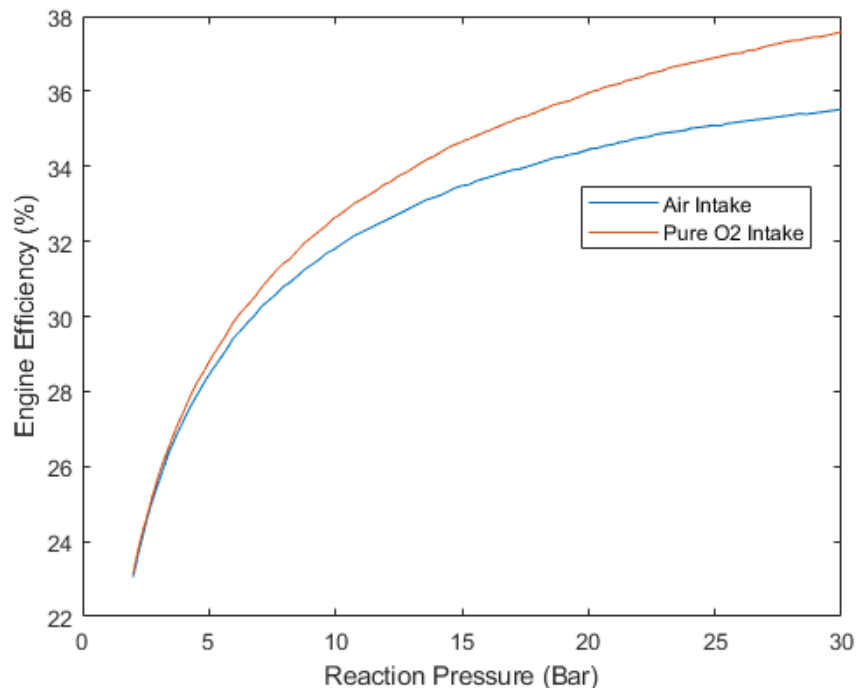
Figure 50: Plot of calculated ideal engine efficiency as a function of the aluminum-water reaction pressure. This plot shows results for a system analysis where air was assumed as the intake gas and an analysis where pure oxygen was assumed.

As seen in Figure 50, the engine efficiency increases with initial reaction pressure, with diminishing returns at higher pressures. Additionally, the engine is slightly more efficient when using pure O_2 as an input as compared to using air, and this difference becomes more exaggerated for higher reaction pressures. This increase in efficiency at higher reaction pressures is to be expected, as the higher the reaction pressure, the more pressure can be utilized from the initial steam generated by the reaction.

The temperature of the exhaust gas was also plotted for varying reaction pressures, and the results can be found in Figure 51. The temperature of the exhaust gas can be seen to decrease at higher reaction pressures, which in turn allows the system to reach higher efficiencies. When the system operates at a higher pressure, it can expand the gas to a greater extent before it reaches 1 bar, allowing for a more complete adiabatic expansion stage and less residual energy remaining in the exhaust gas.
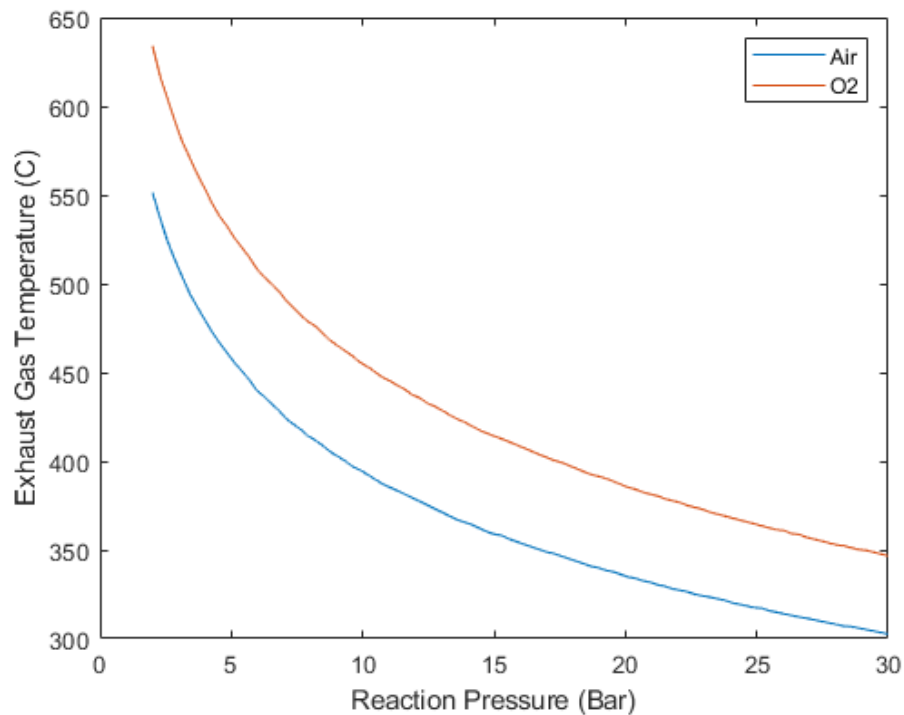
Figure 51: Plot of calculated engine exhaust gas temperature as a function of the aluminum-water reaction pressure. This plot shows results for a system analysis where air was assumed as the intake gas and an analysis where pure oxygen was assumed.

The maximum engine temperatures and pressures were also plotted for different reaction pressure configurations as can be seen in Figure 52 and Figure 53. These plots demonstrate the peak pressures and temperatures that are achieved within the cylinder immediately after the combustion of the hydrogen gas. It is important that these be considered when designing an engine, to ensure that the cylinder and housing can maintain complete structural integrity while operating under these conditions. Fortunately, the pressures and temperatures seen here are largely within the operating range of modern engines [34].
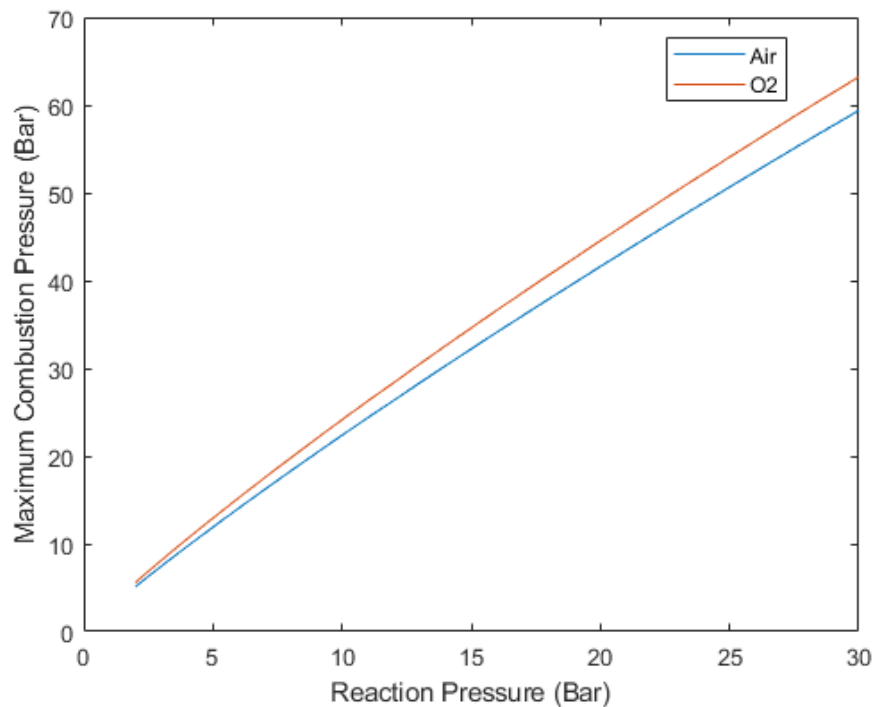
Figure 52: Plot of calculated maximum combustion pressure experienced in the engine cylinder as a function of the aluminum-water reaction pressure. This plot shows results for a system analysis where air was assumed as the intake gas and an analysis where pure oxygen was assumed.

While this analysis considers all of the major steps in the proposed engine cycle, it is still an analysis of an ideal engine. This analysis does not include many realistic system energy losses such as friction losses, wall heat losses, and the non-instantaneous timing of different stages. Future models should aim to incorporate these as best as possible, in order to more accurately predict the proposed engine's efficiency.

113
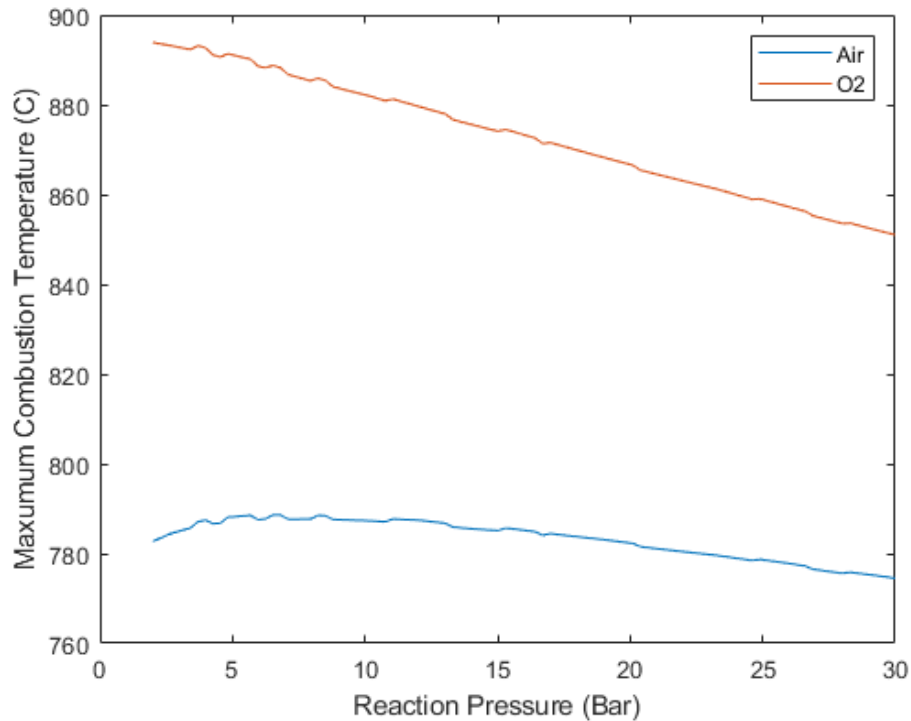
Figure 53: Plot of calculated maximum combustion temperature experienced in the engine cylinder as a function of the aluminum-water reaction pressure. This plot shows results for a system analysis where air was assumed as the intake gas and an analysis where pure oxygen was assumed. Slight tremors in the plot are insignificant and are simply a result of the stepped nature of the analysis done.

6.2.3 Conclusions

Combustion engines have many advantages over fuel cells for power generation. They are lower cost, more robust, and far smaller for a given power output. These advantages make engines a great candidate for generating electricity form an aluminum-water reaction. Until now, fuel cells had always had the advantage of having higher efficiencies than even the best combustion engines, but with the development of the joint hydrogen-steam engine proposed here, this may no longer be the case. Analysis of this engine cycle gives potential system wide efficiencies as high as 33% while still retaining realistic system pressures. This is in contrast to a fuel cell that may use hydrogen at 40-60% efficiency but would have

a system wide efficiency of only 20-30% when running off of aluminum fuel because it cannot utilize the reaction heat. Even with slight losses that will accompany unideal implementations of the engine, by utilizing both the steam energy as well as the hydrogen energy, this engine concept can achieve system level efficiencies on par with fuel cells. Creating this engine requires only the slight redesign of valving within a standard Otto cycle combustion engine, allowing for easy implementation. This engine concept has the potential to be a significant step forward in aluminum fueled technologies, allowing for cheap, robust, efficient, and highly power-dense generators.

Future work:

Further analysis should be done to incorporate realistic losses and timing errors into the system. Even the combustion of hydrogen in the presence of high concentrations of steam must be further considered as its flammability can decrease at such high concentrations of steam as those considered in this analysis [35]. This analysis may require the use of more advanced thermodynamic software, or the collaboration with groups that have performed similar engine analyses, such as the engine concept proposed by Haller et al. [6]. Performing a more detailed analysis will give further insight into the realistic operating conditions and efficiencies that such an engine could be operated at in practice.

Future work may also attempt to incorporate steam reforming into this proposed engine system. Steam reforming, the most widely used method for producing hydrogen gas, produces hydrogen by reacting hydrocarbons with high temperature steam. Current methods for steam reforming require steam in the range of 700 C [36], but research into lowering the necessary temperature is ongoing. As high temperature steam is the primary exhaust from this engine, it could potentially be utilized in a steam reforming process. While current analysis indicates that the exhaust gas will only be in the range of 400 C, incorporating the engine exhaust into a steam reforming process would produce more hydrogen that can be fed back into the engine. Simply completing this loop and creating a more hydrogen rich fuel mixture may be enough to heat the exhaust gas to the desired 700 C and allow the steam reforming process to continue. Steam reforming may also be

incorporated via the use of a liquid aluminum fuel. If the oil suspension holding aluminum particles in a liquid aluminum fuel were to be a hydrocarbon capable of producing hydrogen, then the high temperature exhaust steam need only be exposed to the reaction waste in order to produce more hydrogen for the reaction. Such a system which incorporates hydrocarbon-based liquid aluminum fuel to power an internal combustion engine and steam reforming process would have the potential for an incredibly high energy density.

7. CONCLUSION

With an energy density over double that of gasoline, aluminum has incredible potential as a fuel source. Additionally, reacting aluminum with water to produce hydrogen allows for the production of hydrogen on demand for low cost, using no pressurized gas, and with incredibly high storage densities. This makes aluminum fuel an ideal storage system for hydrogen, and a serious candidate technology for finally bringing about a hydrogen economy.

Aluminum-water reactions were analyzed under a wide range of temperatures and pressures to determine which reaction was most favorable under each operating condition. Results of this model showed a transition in favorability from aluminum hydroxide to aluminum oxyhydroxide at higher temperatures and lower pressures. This model matches results found in literature and was corroborated by a series of four experiments at high and low temperatures and pressure. These experiments used XRD as well as FTIR to confirm the production of both aluminum hydroxide and aluminum oxyhydroxide under the various conditions predicted, further verifying the model. Because each reaction requires different amounts of water and produces different amounts of heat, using this model to predict the expected reaction is critical for the more accurate design of aluminum-water reaction systems.

The aluminum fuel used here was made using the surface treatment recently developed by Slocum. This fuel can be made by simply placing aluminum in a heated bath of Gallium and Indium eutectic. Notably, this fuel does not require the grinding or alloying of the fuel, allowing it to be made from scrap aluminum without extensive processing. A new coating method was also developed to allow for more consistent fuel production and the controlled

addition of eutectic. Testing aluminum treated with different mass fractions of eutectic revealed a minimum threshold of 1.9% eutectic necessary to make the aluminum reactive with water, with demising returns for the addition of higher concentrations. While this exact concentration may vary in aluminum that contains different internal grain structures, these trends are believed to be inherent to the mechanism of action for the reaction. This knowledge of a minimum threshold concentration can therefore inform system design in the future development of aluminum fuel technologies. Understanding this relationship now allows users to optimize their fuel production for energy density, specific energy, or cost.

The world's first aluminum fueled car was developed to demonstrate the significant potential of this technology. The car used an aluminum-water reaction to produce hydrogen, and then used the hydrogen to generate electricity in a set of PEM fuel cells, which in turn charged the car. This was a 10 kW system capable of producing enough power to drive the car at 40 mph. This system incorporated a complex reaction control scheme because of the large batch reactor used. Additionally, the system used a multi-stage thermal management subsystem to safely dissipate the large amounts of waste heat generated. In the end, the system was successfully integrated into the car and generated 7.5 kW power, demonstrating that this fuel can be effectively used for high powered systems even within the space constraints of a small vehicle. This system was proof of concept however, and only operated at approximately 20% system efficiency and took up the entire rear cabin of the car. Future systems utilizing liquid aluminum fuel as well as a hydrogen-steam engine could take up a fraction of the volume while producing higher system level efficiencies.

A liquid aluminum fuel was developed to allow for simpler and more controllable system operation using plug flow reactors. This fuel contains 65% mass fractions of aluminum, is easily pumpable, shows no settling over months, and retains high levels of reaction completion. The use of this fuel can open many new doors for the design of aluminum fueled power systems. By being shear thinning and easily pumpable, this fuel can greatly simplify logistics of reacting as well as refueling aluminum fueled power systems. Future

118

work hopes to push these fuels to even higher mass fractions of aluminum and higher levels of homogeneity.

An engine concept was proposed to utilize both the thermal and chemical energy released in an aluminum-water reaction. Current models of this hydrogen-steam engine cycle show system level efficiencies in the mid 30% range, with variation depending on the intake gas, and the initial reaction pressures utilized. This is very promising, as fuel cell systems typically have hydrogen efficiencies of 40-60% but no means of generating energy from the reaction heat, leaving them with system level efficiencies of only 20-30%. Future work must be done to better understand the operating limitations of such an engine system, and to better characterize its losses due to friction, timing errors, and other such nonidealities. The development of such an engine can allow for a system with an efficiency on par with that of a fuel cell, while maintaining the low cost, small footprint, and robustness of an internal combustion engine.

This body of work aimed to further characterize aluminum fuel and to advance the research and development of aluminum fueled power systems. For this reason, this work is not only concerned with the production methods of aluminum fuel, but also with identifying and solving the key challenges that aluminum fueled systems currently face. This fuel has significant potential for use in emergency generators or other lifesaving technologies, and it is hope of the author that this work helps bring these technologies closer to becoming a reality.

8. APPENDICES

8.1 SOP for Fuel Production Using a Surface Coating Method

Procedure:

1. Weigh out the desired amount of aluminum to be treated
2. Put aluminum into lidded jar, close lid, and place on hot plate
3. Weight out Ga-In eutectic, equal to ~5% of the original aluminum mass from step 1
    a. Different mass fractions can be used for different desired eutectic concentrations.
4. Place eutectic on hot plate
5. Turn hot plate to ~200c, wait for 20min
    a. Entire jar of aluminum should be heated. Although there will be a temperature gradient over the height of the jar, the topmost aluminum should not be cooler than ~70c and the bottommost aluminum should be approximately 120c.
6. Once the desired temperature is achieved, pour the aluminum into the jar of eutectic, mix **thoroughly**
    a. Lidded jars are recommended so that the lid can be closed and the entire jar can be shaken.
    b. Aluminum should be mixed until the eutectic can be seen to coat all surfaces of all aluminum pieces
7. Leave aluminum and eutectic on hot plate for 1.5hr, mixing approximately every 20min
8. Remove aluminum jar from hot plate
9. If excess eutectic is observed on the surface of the aluminum, centrifuge aluminum pieces to remove excess eutectic from the surface
    a. Centrifuging is done at 4000 RPM for 1 minute
    b. Rocks should be placed at the bottom of the centrifuge in order to allow eutectic to pool there without still coating aluminum
    c. If there is sufficient treated aluminum that the centrifuge needs to be run several times, leave the jar of excess treated aluminum closed whenever not

being handled. This is done in order to decrease the surface oxidation of the treated aluminum

10. Put centrifuged aluminum pieces into airtight containers and fill with argon if possible
    a. Because some eutectic will inevitably stick to the walls of the treatment containers used, the aluminum should be weighed before and after treatment to determine the average eutectic concentration
11. Clean jars and beakers using a mix of muriatic acid and water

Notes on eutectic:

The eutectic is a mixture that is 20% Indium by mass and 80% Gallium by mass. The eutectic can be made by taking a block of indium and cutting off ~1 gram chunks into a beaker until the desired mass is achieved. Then put a bottle of gallium in a pool of water and heat it until it is completely melted. Once the gallium is melted, pipette 4x the mass of the indium it into the beaker that contains the chunks of indium. This mixture should then be left on a hot plate at 100 C for ~20 minutes without mixing.

The eutectic is mixed in a percentage such that at room temperature it can only remain liquid in the 80/20 ratio used. This means that if there is too much of either metal the excess will precipitate out and leave a liquid that is properly 80/20.

Notes on cleaning eutectic:

Pouring small amounts of muriatic acid into beakers or pipettes covered in eutectic will cause the eutectic to ball up and precipitate. This muriatic acid can then be heavily diluted and disposed of. The balled-up eutectic at the bottom of the beaker can then be pipetted or poured into a desired storage container. Before using the eutectic for fuel treatment, it is advised that the eutectic be rinsed with water to remove any muriatic acid on its surface.

Notes on safety:

It is advised to assume everything in the lab and on the lab bench is covered in Gallium. Do not bring lab notebook into space, but rather take notes on paper and copy over data later. Wear gloves when touching anything and wash hands often.

All exposure of muriatic acid to aluminum or to eutectic that likely has aluminum dissolved within it should be done within the fume hood. If beakers or jars that contained a mix of muriatic acid and aluminum or muriatic acid with recently used eutectic must be taken out of the fume hood, wait until they have finished reacting entirely, and dilute heavily with water before removing from hood.

8.2   SOP for Measuring Reaction Yield Based on H$_2$ Production

Equipment:

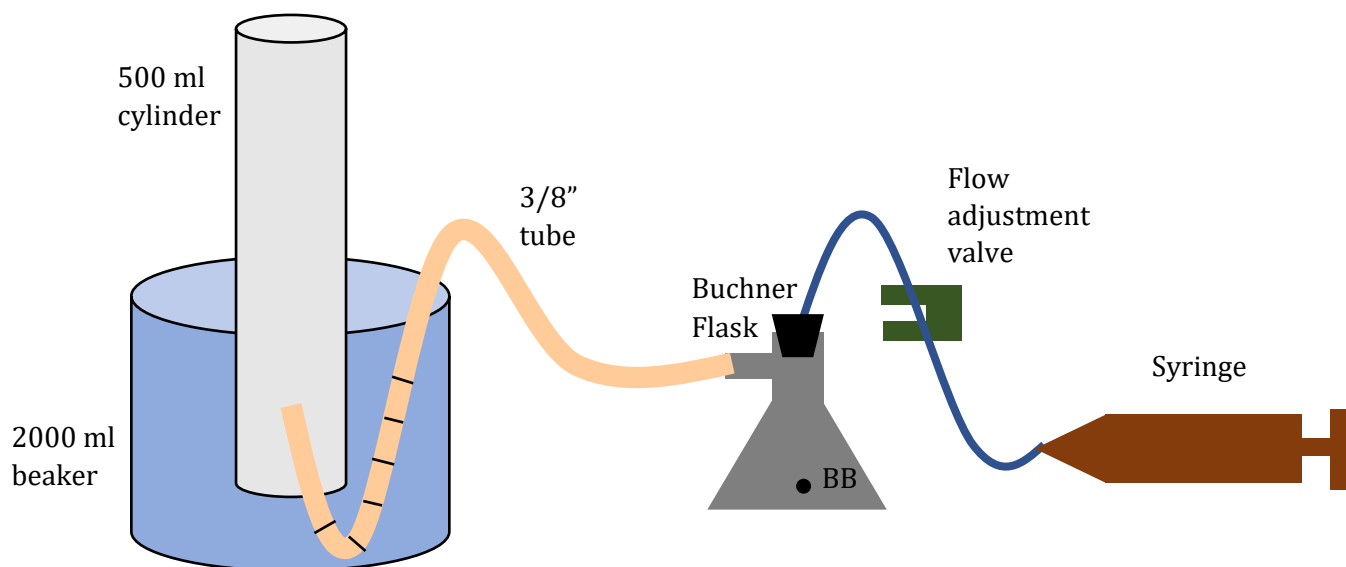500 ml narrow cylinder

2000 ml, 5" diameter beaker

3/8" ID flexible tube with tick marks every inch

50 ml Buchner flask with 3/8" barbed connection

Cork for flask that has hole in it, in this hole is placed a tube connected to syringe

Flow adjustment valve

Diagram of Setup:

Procedure:

1. Fill both the 2000 ml beaker and 500 ml cylinder with water, quickly overturn 500 ml cylinder into 2000 ml beaker.

2. Feed 3/8" ID tubing into 500 ml cylinder so that its end is several inches up the tube as shown in the diagram.

3. Connect the other end of the 3/8" ID tube to the barbed fitting on the Buchner flask.
   a. Wet the barbed fitting before connecting to ensure a better seal.

4. Record the number of tick marks seen on the 3/8" tube in between the water-level of the 2000 ml beaker, and the minimum location of the tube where it begins to curve upwards into the 500 ml cylinder.
   a. This distance represents the total amount of water that will be displaced by gas in the tube before any bubbles reach the 500 ml cylinder. Recording and accounting for this volume will allow for more accurate measurements.

5. Connect tube from output of syringe into the input of the cork.
   a. Place flow adjustment valve on the tube and ensure that it is set to "open."

6. Place a BB in the Buchner flask and seal the flask with the cork
   a. Wet the cork before pushing it in to ensure a better seal

7. Use the syringe to push 5ml of water into the flask, turn the flow adjustment valve to "closed" when done.

8. Immediately after injecting water into the flask, use a stopwatch or clock to begin recording measurements of the gas flow out of the flask. Gas should begin to flow down the 3/8" tube and begin to bubble up into the 500 ml cylinder.
   a. Measurements of the h2 production should be taken by recording the water level in the pipe or cylinder to within 2.5ml every 15 seconds. These should be taken until the reaction is believed to be complete.
      i. The reaction should be considered complete when no observable change in gas level was observed after 1 minute.

9. Once the reaction is believed to be complete, open the flow valve and inject an additional 5ml of water into the flask. This ensures that any underacted aluminum can come into contact with the excess water. Close the flow valve when complete.

10. A final gas measurement should be recorded after the water level of the cylinder is again observed to have remained unchanged for at least 1 minute.

11. Now that the reaction is complete, the flask should be placed in a bath of cool water and let sit for several minutes.
    a. When placing the flask in the bath it is best to agitate the flask and water for faster cooling.

12. The water level in the 3/8" tube should be seen receding as the flask cools and the volume of gas in the flask + tube system decreases. Record the number of tick marks that the water level has receded once the flask is considered fully cooled.
    a. Flask is considered fully cooled when the water level can no longer be seen receding, this can take several minutes.
    b. This measurement accounts for the effect of increased temperature on the system and allows the tester to account for any observed increase in volume that may have been due to increased temperature rather than the actual production of additional gas.

Note on Cleaning: All beakers should be cleaned with a mix of water and dilute HCl. They should then rinsed and dried thoroughly before being used.

8.3 SOP for Fuel Production Using a Bath Method

Procedure:

1. Create a eutectic mix of 20% Indium 80% Gallium (% measurements are by mass)
   a. See notes below on making a eutectic mix
2. Measure out a desired weight of aluminum to be treated
3. Pipette the Ga/In eutectic into a beaker
   a. The mass of this mixture should be ~5x the weight of the Aluminum that will be treated
   b. The eutectic will stick to the walls of the beaker. Pipetting is done rather than pouring, in order to try to avoid having the eutectic lost onto the beaker walls.
   c. Beaker should be narrow enough that eutectic fills the entire bottom
4. Preheat the eutectic on a hotplate set to 175 °C for 20-25min. Wait until metal is ~120 °C.
   a. Hot plate temperature may need to be increased to achieve this eutectic temperature, depending on specific tray used.
5. Pour Aluminum into the eutectic and spread it all out so that no aluminum pieces are stacked on top of each other
6. Leave Aluminum sitting in eutectic for 1.5-2 hours, stirring approximately every 30min using a spatula tool
   a. Stirring may not be necessary for porous materials. Even for BBs, they should only be pressed down into the eutectic and not actually turned over. This is because too much exposure can lead to excessive corrosion of the material.
7. Use spatula or other tool to pick the aluminum fuel out of the eutectic bath and put them into a plastic 60ml vial
8. Centrifuge vial of new fuel at 5000 RMP for 30 seconds to further separate eutectic
   a. May need to centrifuge multiple times
   b. Stones or other material can be placed at the bottom of the vial to ensure that the fuel doesn't pool in the eutectic
9. Pour/push fuel out of centrifuged container into final storage jar
   a. Final fuel can be weighed to ensure the process was done correctly. A 3 gram BB should now weigh 3.1±0.05 grams due to eutectic absorption
10. Clean all beakers that contained the eutectic using muriatic acid
    a. See notes below on cleaning procedure.

Notes on eutectic, cleaning, and safety are the same as those listed in section 8.1

9. REFERENCES

[1] S. H. O. B. N. A. T. A. M. D. A. K. Abdalla M. Abdalla, "Hydrogen production, storage, transportation and key challenges with applications: A review," *Energy Conversion and Management,* vol. 165, pp. 602-627, 2018.

[2] K. M. Babak Alinejad, "A novel method for generating hydrogen by hydrolysis of highly activated aluminum nanoparticles in pure water," *International Journal of Hydrogen Energy,* vol. 34, no. 19, pp. 7934-7938, 2009.

[3] J. M. W. R. A. K. G. C. Jeffrey T. Ziebarth, "Liquid phase-enabled reaction of Al–Ga and Al–Ga–In–Sn alloys with water," *International Journal of Hydrogen Energy,* vol. 36, no. 9, pp. 5271-5279, 2011.

[4] J. Slocum, "Characterization and Science of an Aluminum Fuel Treatment Process," MASSACHUSETTS INSTITUTE OF TECHNOLOGY, 2018.

[5] U. D. o. E. F. C. T. Office, "Fuel Cells Fact Sheet," November 2015. [Online]. Available: https://www.energy.gov/sites/prod/files/2015/11/f27/fcto_fuel_cells_fact_sheet.pdf. [Accessed January 2019].

[6] T. L. Johannes Haller, "Thermodynamic concept for an efficient zero-emission combustion of hydrogen and oxygen in stationary internal combustion engines with high power density," *International Journal of Hydrogen Energy,* vol. 42, p. 27374 e27387, 2017.

[7] The Port Authority of NY and NJ, "HAZARDOUS MATERIALS Transportation Regulations," [Online]. Available: https://www.panynj.gov/truckers-resources/pdf/red-book.pdf. [Accessed January 2019].

[8] A. R. C. a. J. N. Murray Jacobson, "EXPLOSIBILITY OF METAL POWDERS," UNITED STATES DEPARTMENT OF THE INTERIOR, BUREAU OF MINES , 1964.

[9] B. Perry, "Rocketology: NASA's Space Launch System, We've Got (Rocket) Chemistry, Part 2," NASA, [Online]. Available: https://blogs.nasa.gov/Rocketology/tag/aluminum/. [Accessed January 2019].

[10] N. R. M. I. C. T. M. G. C. B. Porciúncula, "Production of hydrogen in the reaction between aluminum and water in the presence of NaOH and KOH," *Brazilian Journal of Chemical Engineering,* vol. 29, pp. 337 - 348, 2012.

[11] W. Chen, "Recycling Rates of Aluminum in the United States," *Journal of Industrial Ecology,* vol. 17, no. 6, pp. 926-938, 2013.

[12] "High-Pressure Hydrogen Tank Testing," United States Office of Energy Efficiency and Renewable Energy, [Online]. Available: https://www.energy.gov/eere/fuelcells/high-pressure-hydrogen-tank-testing. [Accessed January 2019].

[13] D. A. V. W. Vedder, "Aluminum + water reaction," *Transactions of the Faraday Society,* vol. 65, pp. 561-584, 1968.

[14] "Chemistry Learning Free Online Education Resource: Adsorption," Xamplified, 2017. [Online]. Available: http://www.chemistrylearning.com/adsorption/. [Accessed January 2019].

[15] B. WA., Deformation Processing, Addison-Wesley Educational Publishers Inc, 1972.

[16] R. G. H. R. C. HUGO, "THE KINETICS OF GALLIUM PENETRATION INTO ALUMINUM GRAIN BOUNDARIESÐIN SITU TEM OBSERVATIONS AND ATOMISTIC MODELS," *Acta Materialia,* vol. 48, pp. 1949-1957, 2000.

[17] Amazon, "Amazon: Gallium 99.99% Pure - 1,000g Kilogram," Bruntfield Goods, [Online]. Available: https://www.amazon.com/Gallium-99-99-Pure-000g-Kilogram/dp/B0151SRSPK/ref=sr_1_1?ie=UTF8&qid=1548810226&sr=8-1&keywords=gallium+1kg. [Accessed January 2019].

[18] RotoMetals, "RotoMetals: Indium 99.99% Pure 1 KG Ingot," [Online]. Available: https://www.rotometals.com/indium-99-99-pure-1-kg-ingot/. [Accessed January 2019].

[19] "Price of Scrap Metal," Capital Scrap Metal, 2017. [Online]. Available: https://www.capitalscrapmetal.com/prices/. [Accessed January 2019].

[20] L. R. M. B. M. A. S. G. T. Z. Jason Fischman, "SINDRI Aluminum-Fueled Electric Vehicle," MIT Course 2.014, 2018.

[21] B. J. Hopkins, "Stopping Self-Discharge in Metal-Air Batteries," Massachusetts Institute of Technology, 2018.

[22] Evonik Industries, "AEROSIL® – Fumed Silica Technical Overview," [Online]. Available: https://www.aerosil.com/product/aerosil/downloads/technical-overview-aerosil-fumed-silica-en.pdf. [Accessed July 2018].

[23] Evonik Industries, "Successful use of AEROSIL fumed silica in liquid systems Technical Information 1279," Evonik Industries, 2017.

[24] S. M. M. Y. H. Seila Selimovic, "Aging effects of precipitated silica in poly(dimethylsiloxane)," *Journal of Rheology,* vol. 51, pp. 325-340, 2007.

[25] N.-S. Cheng, "Effect of Concentration on Settling Velocity of Sediment Particles," *Journal of Hydraulic Engineering,* pp. 728-731, 1997.

[26] G. Elert, "Viscosity Discussion," The Physics Hypertextbook, 2019. [Online]. Available: https://physics.info/viscosity/. [Accessed January 2019].

[27] I. W.S.Dodge Oil Co., "White Oil Light SDS," Maywood, CA, 2015.

[28] E. M. a. R. P. C. Maurice Renaud, "Power-Law Fluid Flow Over a Sphere: Average Shear Rate and Drag Coeffi cient," *The Canadian Journal of Chemical Engineering,* vol. 82, pp. 1066-1070, 2004.

[29] R. P. Chhabra, Bubbles, Drops, and Particles in Non-Newtonian Fluids, Boca Raton: CRC Press, 2007.

[30] Y. N. T. V. A. Doroganov, "HIGHLY CONCENTRATED CERAMIC BINDER SUSPENSIONS BASED ON SILICON CARBIDE," *Refractories and Industrial Ceramics,* vol. 51, no. 4, pp. 302-304, 2010.

[31] "Combined Heat and Power Technology Fact Sheet Series," U.S. Department of Energy Office of Energy Efficiency and Renewable Energy, [Online]. Available: https://www.energy.gov/sites/prod/files/2016/09/f33/CHP-Steam%20Turbine.pdf. [Accessed January 2019].

[32] J. B. Heywood, Internal Combustion Engines Fundamentals, New York: McGraw-Hill Inc. , 1988.

[33] A. S. Campbell, Thermodynamic Analysis of Combustion Engines, John Wiley and Sons Inc. , 1979.

[34] Performance Trends Inc, "Cylinder Pressure," [Online]. Available: http://performancetrends.com/Definitions/Cylinder-Pressure.htm. [Accessed January 2019].

[35] R. R. W. B. J. G. A. F. N. I. M. Kuznetsov, "Laminar burning velocities of hydrogen-oxygen-steam mixtures at elevated temperatures and pressures," *Proceedings of the Combustion Institute,* vol. 33, p. 895–903, 2011.

[36] U.S. Office of Energy Efficiency and Renuable Energy, "Hydrogen Production: Natural Gas Reforming," [Online]. Available: https://www.energy.gov/eere/fuelcells/hydrogen-production-natural-gas-reforming. [Accessed January 2019].

[37] K. C. Seto, "Hydrogen Production from Aluminum-Water Reactions Subject to High Pressure and Temperature Conditions," Massachusetts Institute of Technology, 2017.

[38] "Process Engineer's Resource Page," Process Engineer's, [Online]. Available: http://www.processengineers.info/rankine.html. [Accessed January 2019].

[39] M. BRAIN, "How Steam Engines Work," HowStuffWorks, 2008. [Online]. Available:

https://science.howstuffworks.com/transport/engines-equipment/steam1.htm. [Accessed January 2019].

[40] T. Zahl, "How Does An Internal Combustion Engine Work?," CarID, May 2018. [Online]. Available: https://www.carid.com/articles/how-does-internal-combustion-engine-work.html. [Accessed January 2019].